TEXTILE RESEARCH JOURNAL

Publication of

TEXTILE RESEARCH INSTITUTE

VOLUME 30 JUNE 1960 NUMBER 6

PHYSICIST or PHYSICAL CHEMIST | **TEXTILES POLYMERS**

The laboratories of Textile Research Institute, a nonprofit organization for research, education, and publication in the field of fibrous materials, fibers, yarns, and fabrics, have an opening for a physical scientist, to conduct research on the basic geometrical, mechanical, and electrical properties of textile fibers and fiber assemblies. An advanced degree, or the equivalent proven, successful research experience, is required. Candidate must be prepared to assume the responsibility for the progress of an experimental program, with ability to prepare concise periodic reports. A background in polymer or fiber mechanics is desirable, but not essential.

Personal interviews will be arranged for qualified candidates. Résumés outlining research experience and academic training and listing publications (if any) should be sent to:

The President
Textile Research Institute
Box 625
Princeton, N. J.

TEXTILE RESEARCH JOURNAL

Volume 30 *June 1960* Number 6

Editor: **Richard K. Toner**

Production Editor: **Candida Frenking**

Advisory Board

Herbert J. Ball
Earl E. Berkley
John Boulton
C. H. Fisher
Walter J. Hamburger
Milton Harris
R. M. Hoffman
Harold P. Lundgren
Herman Mark
Edward R. Schwarz
George Switlyk
Helmut Zahn

TEXTILE RESEARCH JOURNAL, published monthly at Prince and Lemon Streets, Lancaster, Pa., is devoted to the interest of research in textile and allied industries. It is published by Textile Research Institute.

Manuscripts and communications should be sent to the Publications Department, P.O. Box 625, Princeton, N. J.

Second-class postage paid at Lancaster, Pa.

Subscription rates: $25.00 per year; additional for postage, 50 cents to Canada, $1.00 to all other countries. Single copies, $2.50 each.

Contents copyright © 1960 by Textile Research Institute. Advertising rates applied on request.

IN THIS ISSUE

Dynamic Distribution of Strain in Textile Materials Under High-Speed Impact

Part I: Experimental Methods and Preliminary Results on Single Yarns. *D. R. Petterson, G. M. Stewart, F. A. Odell, and R. C. Maheux* 411

Part II: Stress–Strain Curves from Strain-Position Distributions. *D. R. Petterson and G. M. Stewart* 422

Electrical Conduction in Keratin. *J. E. Algie, J. G. Downes, and B. H. Mackay* 432

The Analysis of Variations for Certain Physical Properties of Combed Cotton Yarns. *D. S. Hamby, W. C. Stuckey, B. Gast, and R. J. Hader* 435

Kinetic Studies of the Wool–Water System. Part I: The Influence of Water Concentration. *I. C. Watt* 443

An X-Ray Study of Acetylateted Jute. *S. C. Roy* 451

Behavior of Sample Pleated Strips of Wool Fabric in an Extensometer. Part II: Modifications Due to Pleat Curvature and Other Second Order Effects. *H. W. Holdaway* 456

Weathering and the Resulting Chemical Changes in Some South African Merino Wools. *D. F. Louw* 462

LETTER TO THE EDITOR

Acid Hydrolysis of Chemically Modified Celluloses. *E. H. Daruwalla, P. J. Kangle, and G. M. Nabar* 469

Book Review 471

REPRINT REQUESTS SHOULD BE DIRECTED TO THE AUTHORS
SEE ARTICLES FOR ADDRESSES

TEST FOR **STATIC** *WITH*

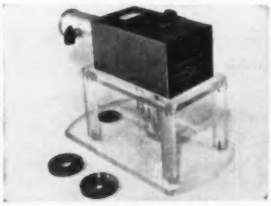

Model CS-66

The ELECTROSTATIC VOLTMETER (CS-66) was developed by the Institute of Textile Technology to detect and measure electrostatic charges on moving or stationary equipment or materials.

The ELECTRICAL RESISTANCE TESTER (CS-51) has been developed for measurement of electrical resistance of fabrics, fibers, film and other materials to determine the static propensities of the materials.

FOLDERS AND PRICE UPON REQUEST

Model CS-51

CUSTOM SCIENTIFIC INSTRUMENTS, Inc.

541 Devon St. Kearny, N.J.

JUNE 1960
VOL. 30 NO. 6

TEXTILE RESEARCH JOURNAL

Dynamic Distribution of Strain in Textile Materials Under High-Speed Impact

Part I: Experimental Methods and Preliminary Results on Single Yarns

D. R. Petterson,[1] G. M. Stewart, F. A. Odell,[2] and R. C. Maheux[3]

Biophysics Division, U. S. Army Chemical Warfare Laboratories, Army Chemical Center, Maryland

Introduction

The basic objective of this series of investigations is a study of the dynamics of energy absorption in materials used for personnel body armour. To present a useful statement of the dynamic requirements of a body armour material, the various modes of energy absorption must be determined. These evaluations must be related to the basic textile fiber material, the structure of the yarn, and the interaction of yarn behavior in a complex multilayer woven fabric mass. To determine the behavior of such materials to the impact of a high-speed projectile (fragment simulator), it was necessary to develop high-speed techniques for direct observation of the impact.

Historically, this investigation was initiated by the development of a new and complex weave for body armour materials by the Canadian Directorate of Interservice Development. Evaluation of this material in 1954, together with the standard 2×2 basket weave used in the U. S. Army nylon body-armour vest, established no significant difference on a weight-for-weight basis. These results, including a preliminary study of the maximum transient deformation, have been previously reported [11].

Studies by high-speed cinematography of the deformation of the back of the armour led to a decision to analyze the motions on a microsecond time scale. It was hoped that study of individual frames of a high-speed camera record would allow measurements of the deceleration of the projectile. In the first experiments, an 8-mm. Fastex Ciné Camera (approximately 15,000 frames/sec.) was used. The plane of the film was perpendicular to the plane of the armour panel or target strips. The camera was focused at the vertical plane determined by the path of the impacting projectile so that the field of view showed the back of the armour (the side opposite impact) during transient deformation. During the critical time, a light flashing on the edge of the film inside the camera provided millisecond markings to determine accurately the speed of the film and thus the time interval between consecutive frames.

It was shown that a transverse pyramid formed

[1] Present address: Research Division, Chicopee Manufacturing Corporation, Milltown, New Jersey.

[2] Present address: Army Medical Research Laboratories, Fort Knox, Kentucky.

[3] Present address: International Business Machines, Toronto, Ontario, Canada.

during the early stage of the transient deformation. This pyramid changed into a somewhat spherical shape at a later time. There is no method of determining from such pictures whether or not the first ply impacted by the projectile was conforming exactly to the shape of the last ply. Thus, any computation as to the kinetic energy transfer from the projectile to the fabric would be somewhat speculative.

To provide a more comprehensive understanding of the decelerating mechanism, it was decided to impact single layers of nylon cloth at a striking velocity slightly below the penetration velocity of this material. Such impacts were recorded by the photographic microflash technique to be described. This procedure, the results obtained, and the technical limitations have previously been discussed [12]. Limited as these results were, they indicated that approximately 40% of the initial energy of the bullet was absorbed by the transversely displaced portion of the fabric in motion. This would indicate that there are other modes of energy absorption of considerable importance in the fabric. The more important of these might be considered as (1) strain energy in the yarns of the fabric pyramid in transverse motion, (2) longitudinal kinetic energy in the fabric moving perpendicularly toward the path of the projectile, (3) strain energy in the yarns of the fabric outside the fabric pyramid in transverse motion, and (4) energy in the form of heat as would result from fiber, yarn, or projectile friction.

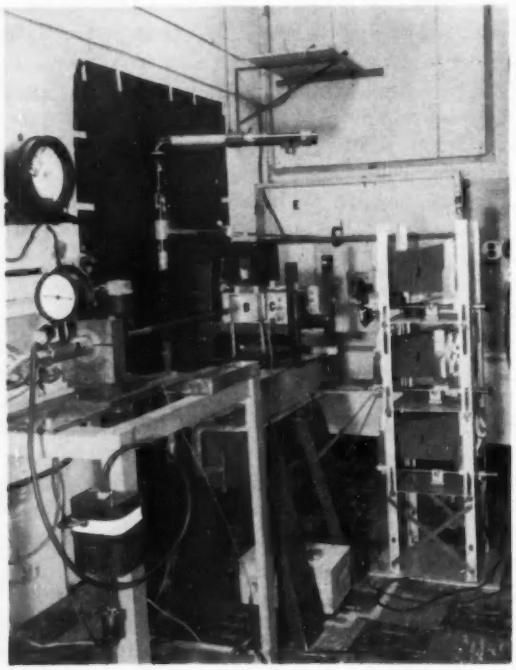

Fig. 1. Experimental range.

While this listing is quite arbitrary, it does seem to offer a common point of departure for further experimentation. Knowledge of the majority of these modes of energy absorption requires information concerning the local strain in the yarns of the fabric and some relationship between the stress and strain in both yarns and fabric under this extreme dynamic loading. There is no available information on the behavior of nylon at the rates of straining produced by these high-speed impacts. The work covered by the literature does not describe satisfactorily the relationships between stress, time, and strain at these rates and under these experimental conditions.

Experimental Methods

The ballistic research range of the body armour group was originally constructed to determine the ballistic limit of various forms of material under consideration for body armour, and for the study of various projectiles. The experimental range as modified for the ballistic impact of yarns is indicated in Figure 1. A helium gun (A) is shown mounted in position, although helium and powder propulsion systems are used interchangeably, depending upon the missile velocity desired.[4] A muzzle blast deflector (B) protects the two velocity-measuring screens (C, D). The yarn (E) is shown mounted in the upper yarn clamp (F) and lower adjustable yarn clamp (G). A photographic light source (H) illuminates the yarn, and the photographs are taken by three cameras (J) mounted vertically on a camera stand in a plane perpendicular to the line of fire of the missile.

The projectile velocity is determined by accurately measuring the time elapsed for the projectile to travel an accurately-known distance. The projectile, upon passing through and breaking the printed grid on the first of two velocity screens, starts a counter chronograph; the projectile's passage through the second screen stops the counter. To prevent the chronograph from being "excited," or triggered, by spurious noise, the chronographs are desensitized [5].

[4] A more complete description of the helium gun is given in a previous report [18].

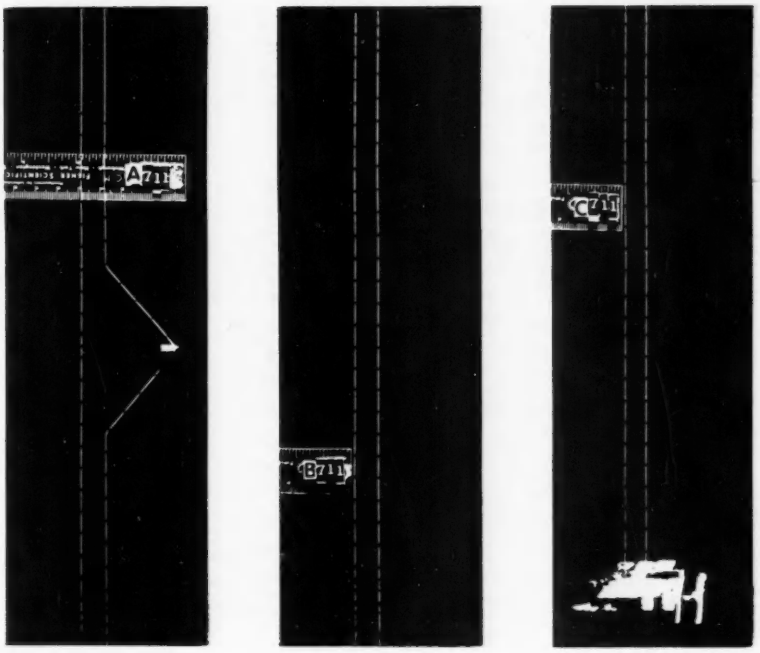

Fig. 2. Impacted yarn, 120 cm.

To obtain a photograph of the deformation of the yarn or fabric, a light source must be triggered at a predetermined time. This is accomplished by an interval generator, whose delayed output pulse sets off a microflash unit.

Because of the inherent errors in the system and the desired accurate timing of the projectile, a separate means of determining the time of the flash was used as a check. This is accomplished by a photo pickup circuit operating to stop a chronograph previously started by rupture of the second screen.

Such instrumentation gives an extremely accurate ballistic range capable of measuring velocities to less than 0.2% error and times of impact to ± 2 μsec.

Experimental Preparation of Yarn

To observe the progress of the strain wave down the yarn, marks were placed upon the yarn. This was accomplished by modifying a typewriter to produce a narrow carbon "tick mark" covering an average width of 0.025 cm. and spaced 0.2, 0.6, or 1 cm. apart. Instron tensile tests on the unticked and ticked yarns showed no damage to the yarn. The yarn is ticked and mounted for firing under roughly 1% of its breaking load, and without any change in its original twist.

The first yarn tests were conducted with a yarn 20 cm. in length, impacted near the center. Analysis of the results on such yarns showed that, because of the short length, the strain pattern quickly became very complex, with reflection of the strain wave at the clamps. Since it was felt unlikely that a boundary condition of full clamping would occur in the actual use of the body armour, a 120-cm. yarn length was chosen to allow strain studies *without reflection*.

In photographing an impacted 120-cm. yarn, three cameras mounted one above the other were positioned so as to obtain coverage of the yarn from 20 cm. above the intended point of impact to the bottom clamp with overlapping areas of the yarn in the view of adjacent cameras. Figure 2 shows three typical photographs of the control (before firing) and of the impacted yarn. Photograph A shows the control yarn at left and the impacted yarn at the right with Photographs B and C showing the continuation of the yarn to the bottom clamp. The control yarn and ruler are photographed prior to firing and the camera backs shifted slightly to displace the image of the impacted yarn.

Experimental Measurements of Strain

Negatives as described above are mounted on a Wilder microprojector, which by transmitted light

throws an enlarged image of a portion of the negative on a ground glass screen. The negative is placed between two glass plates on a table attached rigidly to the moving split-nut of a micrometer screw. By mounting the negative and negative holder on the table, a linear translation of the negative is produced with respect to a vertical index line on the ground glass. As each negative contains a centimeter scale originally placed in the plane of the yarn at the line of fire when the control picture was taken, the readings of the micrometer screw can be converted to actual centimeters on the yarn. By reference to the schematic diagram of an impacted yarn, Figure 3, the Wilder microprojector is used to determine the transverse displacement (TD) equal to SS′; the transverse wave positions (TW) equal to A′S and B′S, and the distance from the line of fire to the tick mark on the control corresponding to the first measurable tick mark on the impacted yarn. The standard procedure is to measure consecutively down the length of the control and the impacted yarn twice, using each reading of a tick mark as the end of one segment and the beginning of its adjacent segment. This gives two lengths of the control segment and two lengths of the impacted segment, both of which are averaged.

The strain for a particular segment is then plotted against the position of the center of the control segment along the yarn or as the original distance of the segment center from the line of fire. The intersection of zero strain with the distance axis determines the distance that the strain wave has traveled during the time after impact, and the quotient of these two yields the strain wave velocity C. This procedure provides an inertialess method for determining the strain wave velocity. Dividing the displacement of the transverse wave points from the line of fire by the time after impact determines the transverse wave velocity, U, expressed in laboratory coordinates.

The major errors involved in the determination of the elongation of a particular segment depend upon the ease with which the center of a tick mark can be determined. The marks vary in width from 0.15

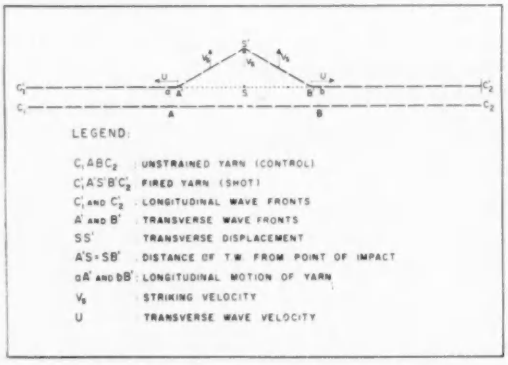
LEGEND:
C_1ABC_2 : UNSTRAINED YARN (CONTROL)
$C_1A'S'B'C_2'$ FIRED YARN (SHOT)
C_1' AND C_2' : LONGITUDINAL WAVE FRONTS
A' AND B' : TRANSVERSE WAVE FRONTS
SS' : TRANSVERSE DISPLACEMENT
A'S = SB' : DISTANCE OF T.W. FROM POINT OF IMPACT
aA' AND bB' : LONGITUDINAL MOTION OF YARN
V_0 : STRIKING VELOCITY
U : TRANSVERSE WAVE VELOCITY

Fig. 3. Schematic diagram of impacted yarn.

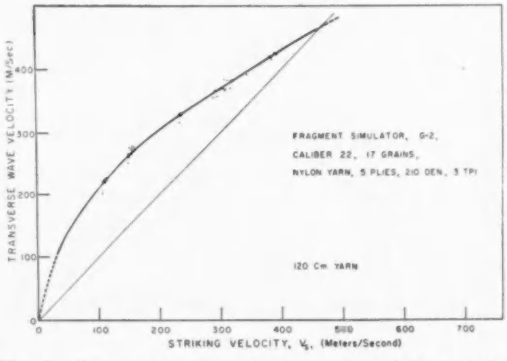
TRANSVERSE WAVE VELOCITY (M/Sec)
STRIKING VELOCITY, V_0, (Meters/Second)
FRAGMENT SIMULATOR, G-2,
CALIBER 22, 17 GRAINS,
NYLON YARN, 5 PLIES, 210 DEN., 3 TPI
120 Cm YARN

Fig. 4. Transverse wave velocity versus striking velocity.

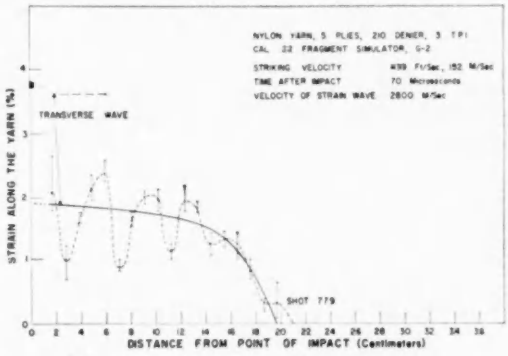
NYLON YARN, 5 PLIES, 210 DENIER, 3 TPI
CAL. 22 FRAGMENT SIMULATOR, G-2
STRIKING VELOCITY 839 Ft/Sec, 152 M/Sec
TIME AFTER IMPACT 70 Microseconds
VELOCITY OF STRAIN WAVE 2800 M/Sec
TRANSVERSE WAVE
STRAIN ALONG THE YARN (%)
SHOT 779
DISTANCE FROM POINT OF IMPACT (Centimeters)

Fig. 5. Strain versus position along yarn.

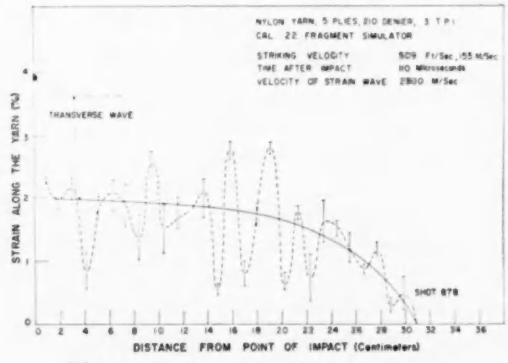
NYLON YARN, 5 PLIES, 210 DENIER, 3 TPI
CAL. 22 FRAGMENT SIMULATOR
STRIKING VELOCITY 909 Ft/Sec, 155 M/Sec
TIME AFTER IMPACT 110 Microseconds
VELOCITY OF STRAIN WAVE 2800 M/Sec
TRANSVERSE WAVE
STRAIN ALONG THE YARN (%)
SHOT 878
DISTANCE FROM POINT OF IMPACT (Centimeters)

Fig. 6. Strain versus position along yarn.

mm. to 0.50 mm., and an experienced operator can determine the position of the center of a tick mark within 1/10 of its width. For segments 1 cm. in length, this error in elongation is approximately ±0.5% strain. A more complete discussion of instrumentation and measurement errors is contained in a previous report [19]. The yarn used in nearly all of these experiments has been Type 300 nylon yarn of 1080 den., consisting of 5 plies of 210 den. with 3.0 turns/in. The impacting projectile in all cases has been the U. S. Army Ordnance Fragment Simulator Caliber 0.22.

Experimental Results

The velocity of the transverse wave was observed to be constant prior to reflection of the strain wave for a given striking velocity. The velocity of the transverse wave for a series of striking velocities is presented in Figure 4. The equation best fitting the experimental data is the parabola $U^2 = 460V$. At striking velocities greater than 460 m./sec. (1400 ft./sec.), experimental determination of the transverse wave velocity becomes difficult, since the yarn ruptures before any significant development of the transverse wave has taken place.

Strain Distributions

Figures 5, 6, and 7 give typical curves of the strain distribution versus position along the yarn for three different times after impact at striking velocities of approximately 500 ft./sec. It is apparent that the front of the strain wave is somewhat attenuated with increasing time and that the level of strain in the vicinity of the projectile remains constant. Although some variation in the velocity of the strain wave front is apparent, there does not seem to be any consistent order with time after impact. Each point on the curve represents the average of 4 to 16 measurements of elongation, and where bars are shown they represent the highest and lowest measured strains for that segment.[5] The smooth curve was obtained from the raw data by the moving average method (five segments). A pictorial diagram of the configuration of the fired yarn shows the position of the transverse wave point on the unstrained yarn. The difference in position of the transverse wave on the strained yarn and the unstrained yarn represents the displacement of the longitudinal portion of the yarn towards the line of fire. The "variations" in the strain distribution have been extensively examined and will be discussed separately.

Figure 8 shows a composite of four curves at 500 ft./sec. and indicates more graphically the apparent plateau of strain in the vicinity of the projectile and the change in shape of the distribution and the attenuation of the slope of the strain wave front with increasing time. It is apparent from these and the following curves that the hypothesis of Hookean behavior is incorrect at high rates of straining and moderate strains. Figures 9, 10, and 11 give composites of "smoothed" strain distributions at different times after impact for the impact velocity levels of 750, 1000, and 1250 ft./sec.

[5] The highest measured elongation was obtained by dividing the largest measurement for the shot yarn segment by the smallest measurement for the control segment. The lowest measured elongation was obtained by dividing the smallest measurement for the shot yarn segment by the largest measurement for the control segment.

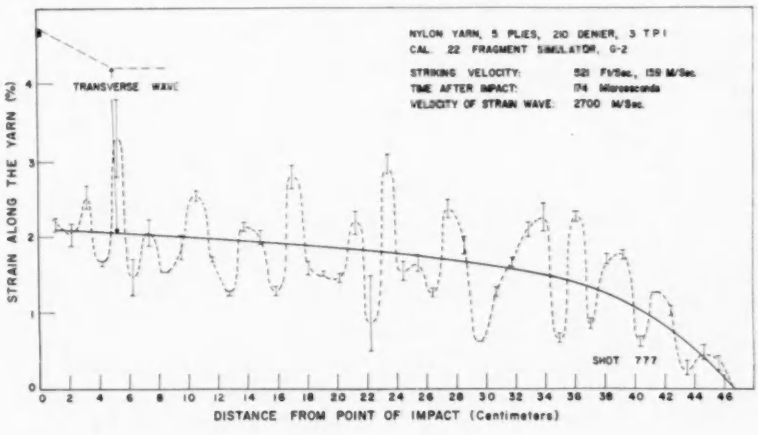
NYLON YARN, 5 PLIES, 210 DENIER, 3 TPI
CAL. .22 FRAGMENT SIMULATOR, G-2
STRIKING VELOCITY: 521 Ft/Sec., 159 M/Sec.
TIME AFTER IMPACT: 174 Microseconds
VELOCITY OF STRAIN WAVE: 2700 M/Sec.
TRANSVERSE WAVE
SHOT 777
STRAIN ALONG THE YARN (%)
0
1
2
3
4
0 2 4 6 8 10 12 14 16 18 20 22 24 26 28 30 32 34 36 38 40 42 44 46
DISTANCE FROM POINT OF IMPACT (Centimeters)

Fig. 7. Strain versus position along yarn.

A small amount of data has been obtained at the velocity range 1500–1700 ft./sec. The times to rupture are so short that no adequate representation of the strain distribution can be given; however, the strain appears to decrease more linearly with distance and the maximum strain is in the order of 14%.

The transverse critical velocity of nylon yarn, Type 300, has been verified experimentally as 1900 ft./sec. The transverse critical velocity is defined for this study as the velocity at which the yarn ruptures within 10 μsec.

Variations in the Strain Distributions

It is readily apparent in all of the curves that the data obtained for the strain distributions do not present a smooth curve.[6] Careful study of all the graphs gives evidence of some form of oscillating behavior in which neither the period nor amplitude appears constant. The existence of "variations," as these deviations have been termed, has been an important stumbling block to more rapid publication of this work. The authors recognize that this subject is by no means closed; for if these variations are accepted as real, they add enormous complications to any theoretical treatment of transient strain distributions within textile materials. The following description of the experiments undertaken is very brief; the reader is referred to a previous report [14].

As observed in Figures 5 through 7, where the maximum and minimum elongations are given for each segment, it appears that the variations are larger than the error which could occur in measuring.

[6] Only three distributions are shown. Approximately 75 strain-position distributions have been measured and plotted; in all but a very few, the variations in strain present are larger than the experimental error.

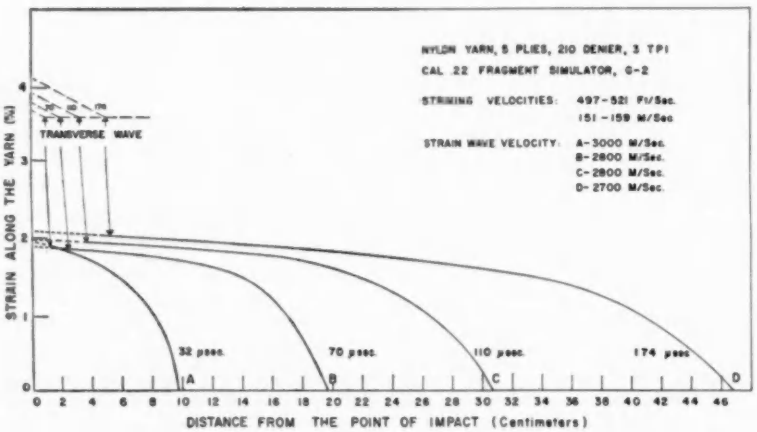

Fig. 8. Strain versus position along yarn.

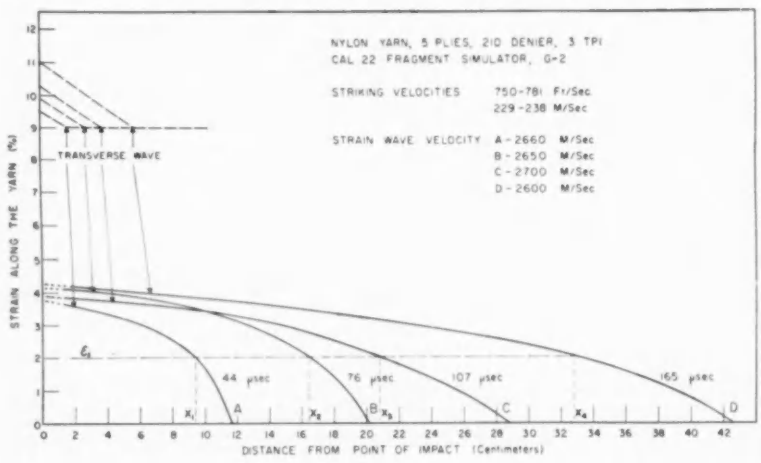

Fig. 9. Strain versus position along yarn.

Subsequent remeasurement of the negatives by different operators on different measuring devices (including one equipped with a densitometer [7]) produced excellent duplication of the results. This system of repetition led to as many as 10 separate and distinct measurements of elongation made on one negative, with the conclusion that the observed variations were not the result of the measuring device or operator error.

As the experimental techniques improved, the yarn was marked every 2 mm. in order to determine the frequency of variations in the strain distribution. The result of such an impact is presented in Figure 12, where the apparent amplitude and frequency of the strain variations have increased considerably. As the length of a segment decreases, the relative error in the measurement procedure increases, and thus the inaccuracy surrounding each elongation point for 2-mm. segments is approximately $\pm 2\frac{1}{2}\%$ strain. Still, the variations are larger than the observational error.

Measurements have been made for a number of

[7] In the Spectroscopy Section, Atomic and Radiation Physics Division, N.B.S.

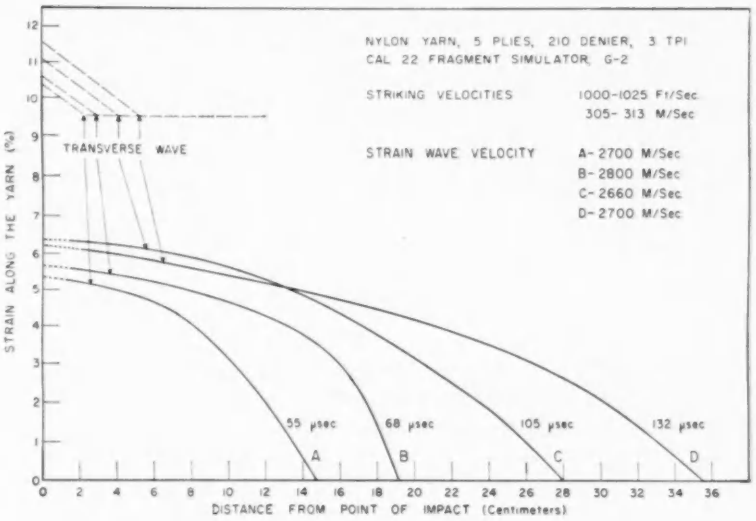

Fig. 10. Strain versus position along yarn.

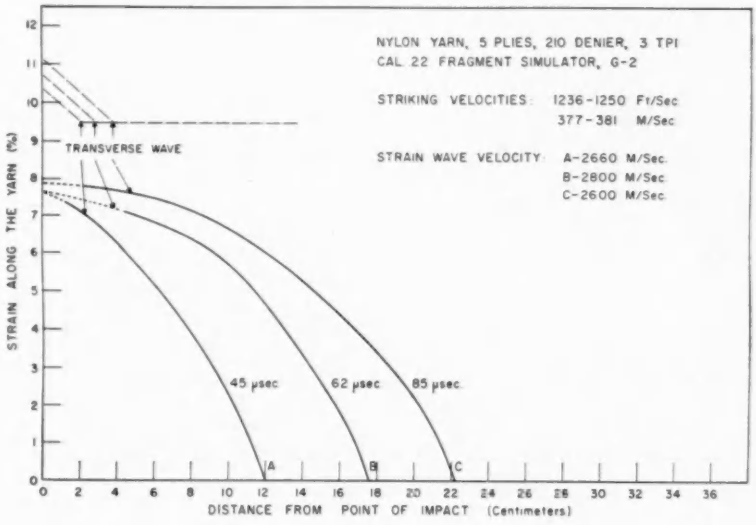

Fig. 11. Strain versus position along yarn.

centimeters beyond the strain wave front, and no variations larger than the error were detected between segments of the control and of the fired yarn. Shots were fired with a caliber .22 lead projectile and a caliber .22 fragment simulator tipped with rubber, without any effect on the variations. The possible apparent rotation of the yarn due to its twist and subsequent unequal displacement of the tick marks was investigated. Statistical analysis of static elongation measurements taken every 90° around the yarn axis showed that there was no significant difference between strain measurements from segment to

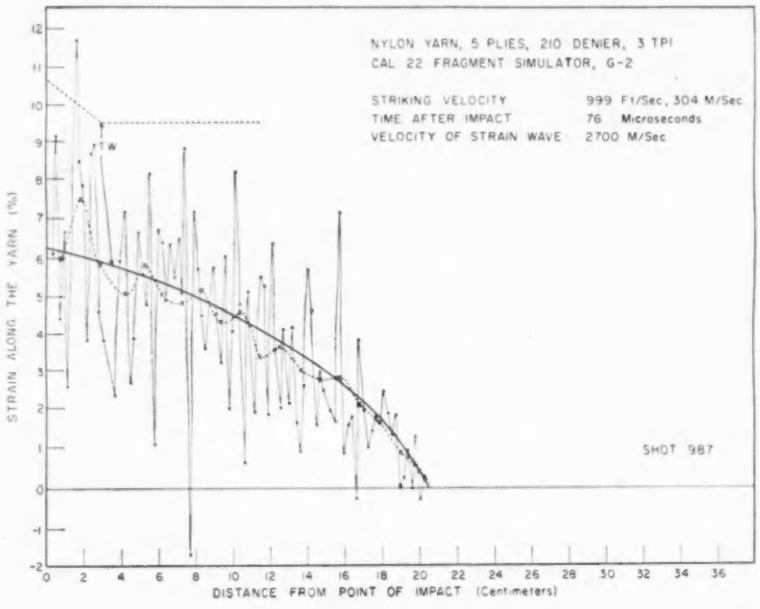
NYLON YARN, 5 PLIES, 210 DENIER, 3 TPI
CAL .22 FRAGMENT SIMULATOR, G-2
STRIKING VELOCITY 999 Ft/Sec, 304 M/Sec
TIME AFTER IMPACT 76 Microseconds
VELOCITY OF STRAIN WAVE 2700 M/Sec
Tw
SHOT 987
STRAIN ALONG THE YARN (%)
DISTANCE FROM POINT OF IMPACT (Centimeters)

Fig. 12. Strain versus position along yarn.

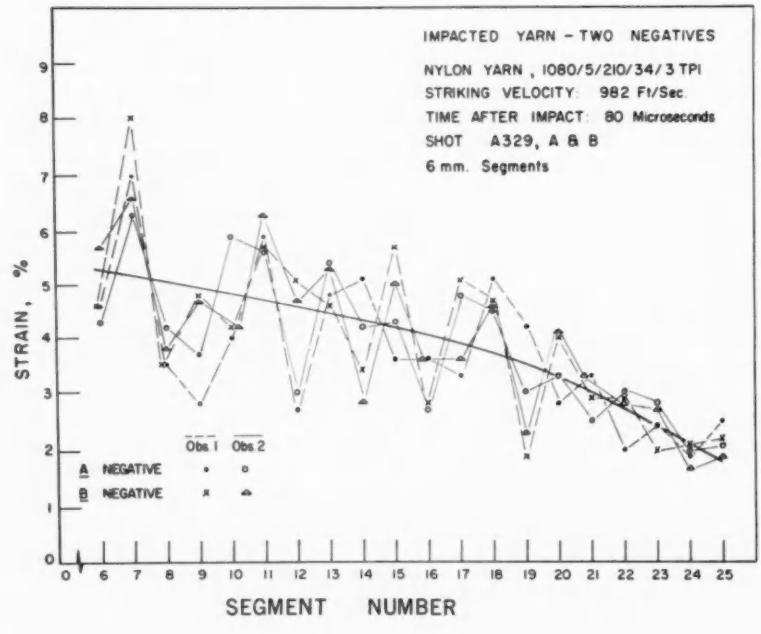

Fig. 13. Strain versus segment number, impact test.

segment along the yarn. This was true for both 5-ply and 1-ply yarns and for 1-cm. and 2-mm. segment lengths.

To consider possible photographic error, two cameras were placed 110° apart to photograph, from the same microflash output, a portion of the yarn just below the transverse wave point; 1-ply, marked with 2-mm. segments, and 5-ply, having 2-mm. and 6-mm. segments, were tested. The statistical results of these negatives and those for the static case are included in Table I. Statistical analysis showed a significant difference between strain measurements, segment to segment, but no significant difference between observers or negatives, as exemplified by Figure 13.

Thus even though the impacted yarn was viewed at different angles, photographed through different camera systems, and the strain measured by different observers, the same variations were present and proved statistically significant, segment to segment. Investigators in other fields have reported, without explanation, the existence of similar high-frequency variations in experiments on the transverse impact of steel beams [4] and the longitudinal impact of steel columns [8]. The investigators conclude that there appear to be equivalent high-frequency variations of strain superimposed upon the outward-moving transient strain distribution.

Discussion

Some explanation of the term "rate of straining" as related to the velocity of impact is necessary. As long as the velocity of impact is sufficiently slow (10 m./sec.), such that the local strain along the specimen closely approximates the average strain, the general term "rate of straining" has significance.

TABLE I. Analysis of Variance—Static and Impact Tests, Nylon Yarn, Type 300

Description of test	Source	Analysis of variance: Sum of squares	Degrees of freedom	Mean squares	*F* Test	$\hat{\sigma}$(*)
Static—210/34/0.6 turns/in. 2-mm. segments S-19	Total	52.64	79	—		
	Segments	10.38	19	0.55		
	Angles	0.06	3	0.02		
	Remainder	42.20	57	0.74		0.86
Static—1080/5/210/34/3 turns/in. 2-mm. segments S-16	Total	168.66	79	—		
	Segments	28.02	19	1.47		
	Angles	4.93	3	1.64		
	Remainder	135.71	57	2.38		1.54
Shot—one negative—210/34/0.6/3 turns/in. 2-mm. segments A-306	Total	97.40	53	—		
	Segments	69.15	17	4.07	4.90†	
	Observers	0.04	2	0.02		
	Remainder	28.21	34	0.83		0.91
1080/5/210/34/3 turns/in. 2-mm. segments 987	Total	506.04	62	—		
	Segments	421.61	20	21.08	9.99†	
	Observers	0.14	2	0.07		
	Remainder	84.29	40	2.11		1.45
Shot—two negatives—210/34/3 turns/in.‡ 2-mm. segments A-370	Total	351.68	79	—		
	Segments	166.44	19	8.76	2.75†	
	Observers	0.04	1	0.04		
	Negatives	0.48	1	0.48		
	Remainder	184.72	58	3.18		1.78
1080/5/210/34/3 turns/in. 6-mm. segments A-329	Total	72.98	79	—		
	Segments	45.15	19	2.38	5.05†	
	Observers	0.03	1	0.03		
	Negatives	0.65	1	0.65		
	Remainder	27.15	58	0.47		0.69

* Estimated standard deviation of experimental error.
† Significant at 1% level.
‡ Negatives of very poor quality, used to test worst possible case of negatives and observer error.

However, when the magnitude of the strain pulse becomes larger, the local rate of straining becomes independent of the specimen length and more dependent on the form of the strain wave front. Thus, in the experiments described here, the local rate of straining approaches infinity at the instant of impact and continually decreases for segments farther from the point of impact. The term "nominal rate of straining" used in this work is related to the concept of maximum strain attained in a specimen during an arbitrary time of 10 μsec. Thus, at a transverse impact of 500 ft./sec., the "nominal rate of straining" is 2% strain in 10 μsec. or 2×10^5 %/sec. The time period of 10 μsec. is the same as that used in connection with the transverse critical velocity.

Several impact studies on yarns and wires have been reported in the literature. Since the impact velocities reported are much lower than those used in this study, any comparisons must be made with caution. However, two phases of work have sufficient literature background to warrant their mention.

Studies on the effects of wave propagation on strains and breaking loads started with J. Hopkinson [7] and B. Hopkinson [6]; their work was summarized by G. I. Taylor [21]. Later, Taylor [22] and von Kármán [23] independently developed the concept of the plastic strain wave, to predict the impact behavior in plastic materials where the dynamic modulus continually decreased and approached zero in the plastic region. They were able to derive a theoretical transient strain distribution prior to reflection. The theory was verified in part by Duwez [3], although his measurements were made on the residual plastic strain in copper wire, complicated by the method of unloading the stress in the specimen. A concave upward strain-position curve was obtained for plastic materials by the analysis of von Kármán. The measured strain-position distributions obtained for nylon are concave downward. The significance of this curvature in the transient strain distribution is discussed in the second part of this study [13].

A second area covered in the literature is that of experiments at lower impact velocities with theories assuming Hookean behavior. Schiefer [10, 20] measured the displacement of a load on one end of a yarn impacted longitudinally at the other end. With impact velocities up to 300 ft./sec., and by use of the average strain in the specimen, his experiments gave a mean rate of straining of 4000%/sec. The implicit assumption was that the strain traveled with constant velocity and constant amplitude and was totally reflected. Schiefer [15] reported the strain wave velocity for nylon as 2200 m./sec. This value is considerably lower than the value reported here and in experiments on the dynamic modulus [1, 2, 9]. Smith [16] has presented an analysis of the form of the reflected strain wave assuming Hookean behavior for the longitudinal case, similar to the technique of Hopkinson. Smith has also reported his analysis of the transverse impact behavior of textile yarns, again using the reflected small strain pulse and Hookean response [17]. Studies similar to those reported here were sponsored by the Navy at Fabric Research Laboratories. The unclassified portions will be discussed in a subsequent paper.

The assumption of Hookean behavior in view of the data presented in this study presents a serious limitation on the interpretation of textile materials. This is particularly true since textile fiber materials generally have nonlinear stress–strain response and are quite sensitive to changes in rates of straining. One immediate experimental difficulty is whether the strain wave velocity of the reflected wave is equal to the original strain wave velocity (C) as the strain in the specimen increases. If the material is Hookean in behavior, the velocities of reflected strain pulses will be equal. If the material is not Hookean in behavior, these strain wave velocities at various strain levels will not be equal, and analysis of the reflection of the strain pulse becomes extremely difficult. This raises serious doubt concerning the use of the average strain in the specimens in lieu of the local strain at the point of application of the stress. It would appear that the use of the reflected strain technique for determining impact performance must be carefully substantiated by measurements of the local strain wave velocity at various levels of strain or accurate determination of the strain-position relationship for reflected waves.

Conclusions

The experimental data have presented accurate transient strain-position distributions for textile materials at very high rates of straining. The experimental techniques have made possible the inertialess determination of:

1. The strain wave front velocity (which for nylon is constant at all impact velocities, thus is a property of the material).

2. The transverse wave front velocity which is directly related to the impact velocity and, for nylon, has a constant value for any given striking velocity prior to arrival of the reflected strain wave.

3. The transient strain-position distributions in the yarn prior to reflections of the strain wave front.

The experimental data indicate the strain-position distribution form for nylon changes with increasing time after impact (for a given striking velocity). The strain wave front becomes more attenuated but the level of strain at the vicinity of the projectile remains constant. The form of the strain-position distribution changes with different striking velocities, departing more and more from the square wave form with increasing striking velocity and increasing strains in the material. The distributions indicate that the assumption of Hookean behavior in nylon is not valid at these high rates of straining.

Effort will be made in the next part of this study to explain the significance of the experimental results, with mention of the published theories. The presence of variations in the strain-position distribution has been noted and extensively examined. To the authors' satisfaction, they are real, although their origin has not been explained.

Literature Cited

1. Ballou, J. W. and Smith, J. C., TEXTILE RESEARCH **14**, 282–292 (1944).
2. Chaikin, N. and Chamberlain, N. H., *J. Textile Inst.* **46**, T25–T62 (1955).
3. Duwez, P. E., "Preliminary Experiments on the Propagation of Plastic Deformation," OSRD Report 380, 1942, NDRC Report No. A33 (1942).
4. Goland, M., Dickersham, P. D., and Dengler, M. A., *J. Appl. Mech.* **22**, 1–7 (1955).
5. Grossman, D., "Description of Ballistic Velocity Instrumentation System in Use at the Bio-Physics Division," CWLR 2081 (1956).
6. Hopkinson, B., *Proc. Roy. Soc.* **74**, A498 (1905).
7. Hopkinson, J., *Phil. Trans. Roy. Soc.* **213**, A437 (1944).
8. Kraffts, S. M., *Proc. Soc. Exp. Stress Anal.* **22**, 173–179 (1955).
9. Lyons, W. J. and Prettyman, J. B., *J. Appl. Phys.* 473–480 (1948).
10. McCrackin, F. L., Schiefer, H. F., Smith, J. C., and Stone, W. K., *J. Research Nat. Bur. Standards* **54**, 277–280 (1954).
11. Maheux, R. C. and Stewart, G. M., "A Comparative Ballistic Study of the Standard U. S. Vest, M-1952-A and of the Canadian Armour Vest, X53," Medical Laboratories Research Report 300, Army Chemical Center, Md. (1954).
12. Maheux, R. C., Stewart, G. M., Petterson, D. R., and Odell, F. A., "Dynamics of Body Armour Materials Under High Speed Impact, Part I, Transient Deformation, Rate of Deformation, and Energy Absorption in Single and Multi-Layer Armour Panels," Chemical Warfare Laboratories Report (CWLR) 2141, Army Chemical Center, Md. (1957).
13. Petterson, D. R. and Stewart, G. M., TEXTILE RESEARCH JOURNAL **30**, 422–431 (1960).
14. Petterson, D. R., Stewart, G. M., Maheux, R. C., and Odell, F. A., "Dynamics of Body Armour Materials Under High Speed Impact, Part III: Dynamics Strain-Position Distributions of Nylon Yarn Impacted Transversely," CWLR 2161 (1957).
15. Schiefer, H. F. et al., "Critical Velocity and Stress-Strain Properties of Organic Materials at Very High Rates of Straining," NBS Report 9A115, OQMG Project No. 7-80-05-001 (1954).
16. Smith, J. C., McCrackin, F. L., and Schiefer, H. F., *J. Research Nat. Bur. Standards* **55**, 19–28 (1955).
17. Smith, J. C., McCrackin, F. L., Schiefer, H. F., Stone, W. K., and Towne, K. M., *J. Research Nat. Bur. Standards* **57**, 83–89 (1956); **60**, 5, 517–534 (1958).
18. Stewart, G. M., "A Helium Gun for Propelling Various Shaped and Weighed Missiles," CWLR 2076 (1956).
19. Stewart, G. M., Petterson, D. R., and Hamburger, T., "Dynamics of Body Armour Materials Under High Speed Impact, Part II: Single and Triple Microflash Instrumentation for Single Yarn Studies," CWLR 2142 (1957).
20. Stone, W. K., Schiefer, H. F., and Fox, G., *J. Research Nat. Bur. Standards* **54**, 269–275 (1955).
21. Taylor, G. I., "The Testing of Materials at High Rates of Loading," James Forrest Lecture (1946).
22. Taylor, G. I., "The Plastic Wave in a Wire Extended by an Impact Load," British Official Report R. C. 329 (1942).
23. von Kármán, T., "On the Propagation of Plastic Deformation in Solids," OSRD Report No. 365, 1942, NDRC Report No. A. 29 (1942).

Part II: Stress-Strain Curves from Strain-Position Distributions

D. R. Petterson and G. M. Stewart

Introduction

Previous studies of body-armour materials indicated that significant improvements required a fundamental understanding of the dynamic behavior of the yarns making up the cloth [9, 14, 16, 26]. A study of the dynamics of energy absorption under transverse impact was initiated and certain phases of the work have been reported.

Part I [14, 16] provided a description of the range and the electronic photographic and yarn-preparation equipment [14, 26], described the procedures for measuring the photographs and determining the elongation as a function of position from the point of impact [14, 16], and detailed the transient strain-position distributions before reflection in nylon yarns impacted transversely. The results indicate that the strain-position distributions are not of "square wave" form associated with Hookian behavior and that they are dependent upon the time after impact and the impacting velocity. This earlier paper also gave a brief discussion of previous impact studies although at much lower rates of straining.

Employing these data on instantaneous local strain distributions, this paper presents a preliminary mathematical treatment of the experimental data in an effort to determine a dynamic stress–strain relationship in textile yarns as the time to break approaches zero.

Strain vs. Strain-Velocity Distributions

Measurements of the type previously reported [14, 16] give local strain (elongation) vs. the distance from the point of impact prior to any reflection. Data were reported for several times after impact and for a number of striking velocities. Figure 1 represents several smooth strain distributions for a given striking velocity at different times after impact.[1] With longer times, the slope at the strain-wave front decreases, while the level of strain in the vicinity of the projectile remains approximately constant.

Consider a line of uniform strain, such as ϵ_i in Figure 1. The distance of the locus of this strain (ϵ_i) from the line of fire is indicated X_1, X_2, X_3, and X_4. These distances, divided by their appropriate times after impact, show the velocity of the locus of this strain, e_i, to be a constant. Thus a transient strain of a particular value in a yarn can be characterized as a function of the velocity of the locus of that strain, x/t, yielding one functional relationship for each striking velocity.[2]

[1] The authors have concluded previously that the "variations" in local strain about the average value are real [14, 16]. However, they feel that basic information can be gained by considering the "smooth" curves, as in this paper.

[2] Although this concept was proposed by von Kármán [30], doubt exists concerning the physical significance of a "strain velocity" for various levels of strain. Physically, it

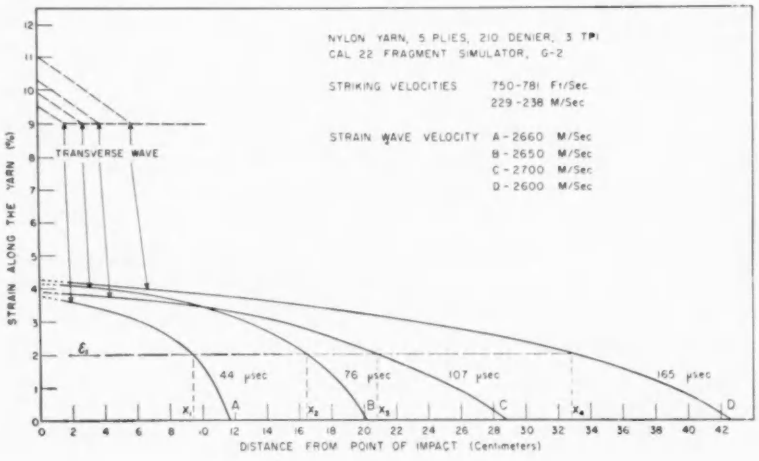

Fig. 1. Strain versus position along yarn; smooth strain distributions at four times after impact.

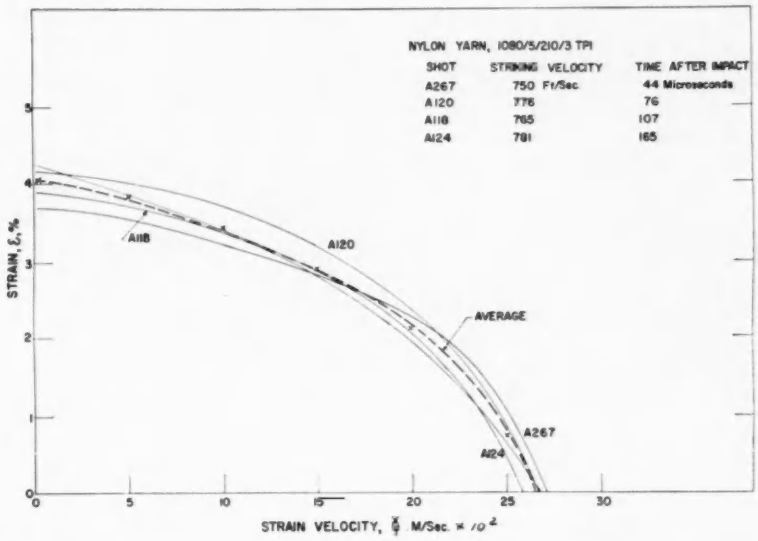

Fig. 2. Strain versus strain velocity, x/t, for one striking velocity.

The data replotted in Figure 2 as strain versus x/t (strain velocity) show that the curves coincide sufficiently to suggest one functional relationship. In Figure 2, the strains in the vicinity of the projectile have been extrapolated to the line of fire as smooth curves, and these maximum values of strain do not appear to change significantly in any consistent order with various times after impact. The variation of the strain-wave velocity, C (where C is defined as the limiting value of x/t as ϵ approaches zero) is due primarily to the selection of the proper smooth curve intersecting the position axis. The values of C at various impact velocities are averaged to obtain a mean value of the strain-wave velocity, which for both Type 300 and Type 700 nylon appears to be the same (2700 m./sec.). The dashed curve in Figure 2 indicates the average of the four curves.

Figure 3 is a plot of strain versus strain velocity for various striking velocities, where the average curves at each velocity level have been uniformly expanded or contracted to place the wave front at the mean strain-wave velocity C. Each of the four lower curves represents the average of a number of shots and is identified by its average striking velocity. The small circles indicate the velocity of the front of the transverse wave. It is apparent that while the strain versus strain-velocity distribution at a given striking velocity is independent of the time after impact, the distributions are not independent of

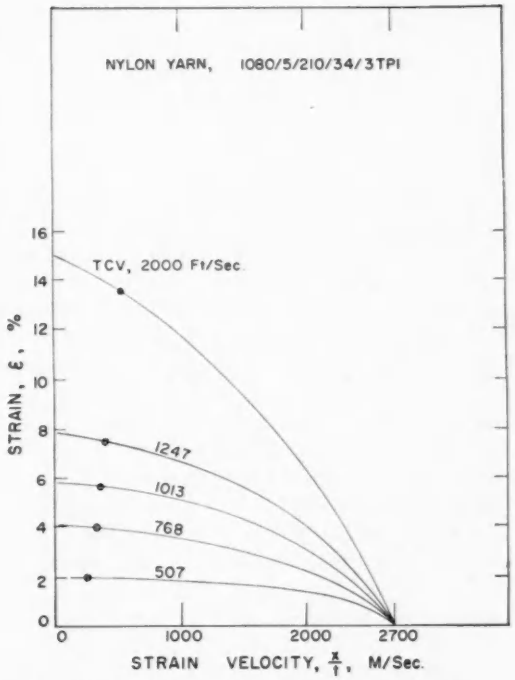

Fig. 3. Strain versus strain velocity, x/t, for four striking velocities.

would be more nearly correct to characterize the strain at a particular position and time by a strain-time distribution, but no equivalent data are available at present. Experimental techniques are under development for determination of strain-position-time relationships and will be reported later.

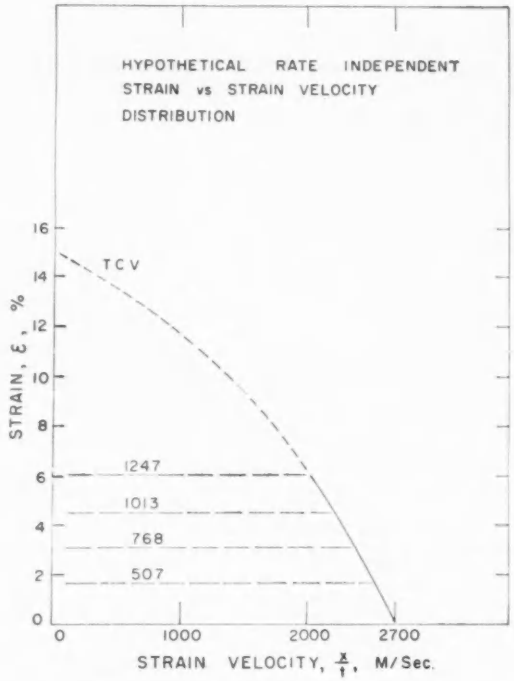

Fig. 4. Strain velocity, x/t, m./sec.

the striking velocity and thus are not independent of the speed of the test.

If the material acted independently of rate effects, the locus of a particular strain, ϵ_i, would have one and only one velocity of propagation, and a curve of strain versus strain velocity would be as shown in Figure 4. The heavy line in Figure 4 would then be that portion of the strain versus strain-velocity distribution up to the highest striking velocity for which data could be obtained. A complete curve would continue to the strain axis, the intersection giving "immediate rupture strain." Such a curve, marked TCV in Figure 4, would be generated by a striking velocity high enough to bring the strain in the vicinity of the projectile to "immediate rupture strain," thus causing instantaneous failure of the yarn.

A similar curve should exist for the time-dependent case, as shown in Figure 3 and labeled TCV. Neither curve can be obtained experimentally since, when the "rupture strain" is reached, the yarn fails and no strain distribution can be measured.

The average strain, $\bar{\epsilon}$, can be calculated for a given striking velocity, since it is dependent only upon the striking velocity, V_s, the velocity of the transverse

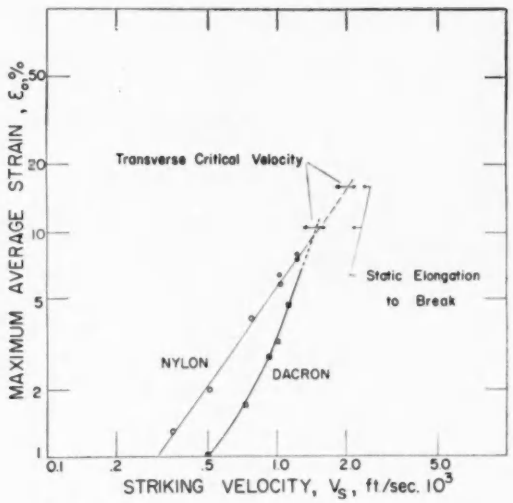

Fig. 5. Maximum strain near the projectile versus striking velocity.

wave, U, and the strain-wave velocity, C, as related by

$$\bar{\epsilon} = \frac{\sqrt{U^2 + V_s^2} - U}{C} \qquad (1)$$

In the time-independent case, Figure 4, the strain values in the plateau behind the strain front are those necessary for continuity of the yarn.

Since only transient phenomena prior to reflection are considered, low striking velocities give maximum strains less than the breaking strain of the material, and it would be possible to produce a stress–strain curve only up to the particular maximum strain associated with that striking velocity. To develop an entire stress–strain curve, the strain versus strain-velocity distribution must be known at a velocity necessary to produce an immediate rupture strain. This velocity, the Transverse Critical Velocity, is the impact velocity at which the material fails at or within 10 μsec. after impact.[3] The Transverse Critical Velocity is determined experimentally by firing a number of shots at the yarn over a range of velocities near the TCV and plotting time to rupture versus striking velocity. In the case of nylon yarn (Type 300), the TCV is 1,900 ft./sec., $\pm$50 ft./sec. This gives a "nominal rate of straining" of 1.5×10^6%/

[3] In theory, the Transverse Critical Velocity (TCV) would be that velocity at which the yarn fails instantaneously. Experimental difficulties prohibit such determinations and thus the practical definition above has been adopted.

sec., defined as the maximum strain attained (15%) divided by the critical time of 10 μsec.

To determine the form of the strain versus strain-velocity curve at the TCV, a relationship must be established between the strain, ϵ, and the strain velocity, x/t, for various striking velocities, V_s. This has been done empirically, yielding an equation of modified exponential form

$$\epsilon = \frac{\epsilon_0}{1 - \exp^{-k}} [1 - \exp^{-k(1-x/Ct)}] \qquad (2)$$

where ϵ is the strain in percent at a particular value of x/t, ϵ_0 is the maximum strain at the projectile, k is a dimensionless curve-fitting constant, x/t is the strain velocity, and C the strain-wave velocity in m./sec. The value of ϵ_0 is determined experimentally, and the proper value of k to fit a given strain–strain-velocity distribution determined empirically. The crosses along the heavy curve in Figure 2 indicate fitted points. By determination of the relationship between ϵ_0 and V_s, and the curve-fitting constant k versus V_s, specific values of ϵ_0 and k can be predicted at the Transverse Critical Velocity.

Figure 5 is a plot of the maximum strain ϵ_0 versus the striking velocity, V_s, both plotted as $\log_{10}$. This relationship is a straight line for nylon, and gives a rupture strain of 15–16% at the TCV. Figure 6 is a plot of k versus V_s, again both $\log_{10}$. The relationship for nylon is again a straight line and, at the TCV, k is 1.6. These values of k and ϵ_0, together with the strain-wave velocity, C, permit prediction of the strain versus strain-velocity distribution at the TCV; see Figure 3.

Theoretical Development

The following theoretical development follows closely that given by von Kármán [30]. While von Kármán's solution for plastic materials has two solutions, the solution obtained here with the use of Equation 2 is univalued, as shown later in Equation 7. The authors do not claim that this development treats all of the factors involved in a transverse impact. However, we did hold two pieces of information which we felt were unique. The first was the knowledge of accurate instantaneous strain vs. strain-velocity distributions at high impact speeds, and the second was the ability to predict the strain vs. strain-velocity distribution at the Transverse Critical Velocity. It was this information which led us to attempt the development of a dynamic stress–strain curve for these materials based upon the simplest nonelastic theory—that of von Kármán and Taylor.

Consider that the unbalance of force on an element, dx, is equal only to the force of acceleration on that element. Then the differential equation of Laplace in one dimension is

$$\rho \frac{\partial^2 u}{\partial t^2} dx = \frac{\partial \sigma}{\partial \epsilon} \frac{\partial e}{\partial x} dx \qquad (3)$$

where u represents the displacement of a particle, x the position of a particle from the point of impact in Lagrangian coordinates, and ρ the density in grams per cubic centimeter. Since $\epsilon = \partial u/\partial x$

$$\rho \frac{\partial^2 u}{\partial t^2} = \frac{\partial \sigma}{\partial \epsilon} \frac{\partial^2 u}{\partial x^2} \qquad (4)$$

A simple solution of this equation can be made if stress is assumed to be a single-valued function of the strain, ϵ, and independent of the rate of strain. Thus

$$\frac{\partial \sigma}{\partial \epsilon} = \frac{d\sigma}{d\epsilon} = E_i$$

and (5)

$$\frac{\partial^2 u}{\partial t^2} = \frac{E_i}{\rho} \frac{\partial^2 u}{\partial x^2}$$

With our empirical expression for strain, integration of Equation 2 yields

$$u = \frac{\epsilon_0}{1 - \exp^{-k}} \left\{ \frac{Ct}{k} [1 - \exp^{-k(1-x/Ct)}] - t\left(C - \frac{x}{t}\right) \right\} \qquad (6)$$

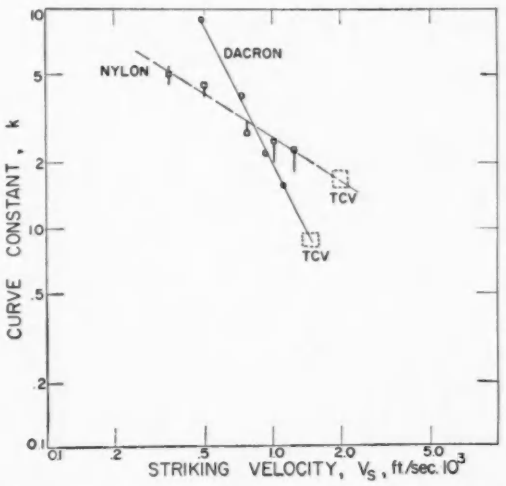

Fig. 6. Curve fitting constant, k, versus striking velocity.

Substitution of partial derivatives into Equation 5 yields

$$E_i = \rho \left(\frac{x}{t}\right)_i^2 \qquad (7)$$

Thus, the instantaneous modulus, E_i, is equal to the density times the strain velocity of that particular strain squared. The strain velocities of the various strain levels of Figure 3 are converted to instantaneous moduli. These moduli, when plotted versus strain and the area graphically integrated, give stress–strain relationships. In Figure 7, the stress–strain curves have been computed for the four experimental velocity levels at which strain versus strain-velocity distributions have been determined. The heavy curve labeled TCV is the predicted dynamic stress–strain relationship of nylon at the Transverse Critical Velocity, determined from Equations 2 and 7 with the extrapolated values of ϵ_0 and k. A portion of a static curve obtained on an Instron tester at 40%/min. is included as reference.

As pointed out before, it is impossible at lower velocity levels to determine the complete form of the stress–strain curve for the material without strain wave reflections, since the maximum strain at 500 ft./sec. is in the order of 2% and the material will not fail in a reasonable time without multiple reflections of the strain wave. This method presents a theoretical form of a dynamic stress–strain curve of nylon at the TCV, or at a "nominal rate of straining" of 1.54×10^6%/sec.

The circles on the TCV curve in Figure 7 indicate the maximum stress and strain which would have been obtained were the material rate-independent. The stress levels are the same for the various striking velocities, but larger maximum strains are observed in the strain rate-dependent case.

The maximum stress developed dynamically by this technique is considerably lower than the breaking stress in the static case. The elongation to break does not decrease significantly under dynamic conditions. These conclusions are in opposition to those previously stated by other observers [10, 21], who with high-speed tests have predicted that the breaking stress will increase while the breaking strain decreases with the increasing rates of loading. The highest *average rate of straining* (maximum strain divided by time to rupture) involved in these pre-

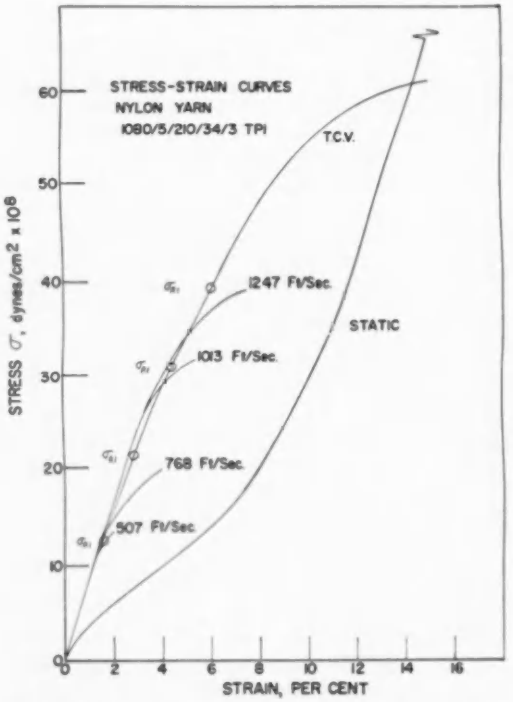

Fig. 7. Dynamic stress–strain relationship for nylon.

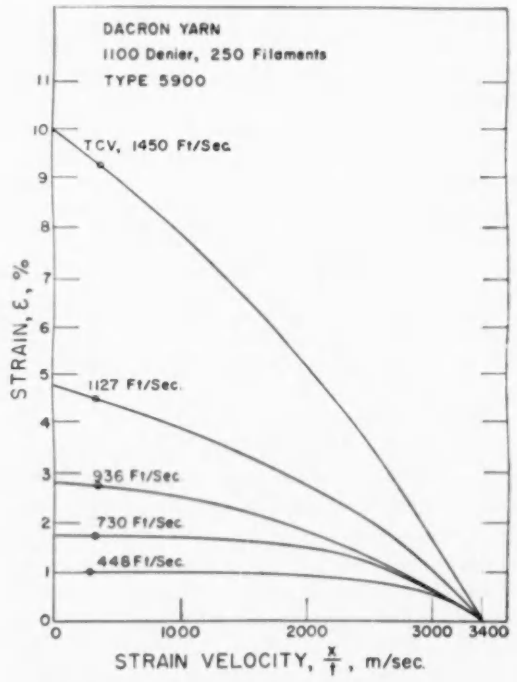

Fig. 8. Strain versus strain velocity for Dacron.

vious tests is in the order of 4000%/sec., and the dynamic data presented here are in the order of 10^5–10^6%/sec.

A check on the stress in the yarn at the transverse wave point can be made by consideration of conservation of momentum. Several investigators have solved this problem [4, 20], and one form gives the tension as

$$T = m \frac{U^2 + V_s^2}{1 + \epsilon} \tag{8}$$

where m is the mass per unit length, U the transverse wave velocity, V_s the striking velocity, and ϵ the strain at the transverse wave front. For the TCV of nylon, this gives the tension at the transverse wave as 64×10^8 dynes/sq. cm., which is in close agreement with the 61×10^8 dynes/sq. cm. given by the dynamic stress–strain curve.

By use of the same procedure, a dynamic stress–strain curve has been developed for Dacron,[4] Type 5900. Figure 8 gives the experimental curves of strain versus strain velocity for four striking velocities. The experimental TCV for Dacron is 1450 ft./sec. ±50 ft./sec. The relationship for k versus V_s, Figure 6, yields a value of 0.9 for k at the TCV. The relationship for ϵ_0 versus V_s, Figure 5, becomes linear when plotted semilogarithmically, and ϵ_0 equals 10.5% at the TCV. The strain versus strain-velocity curve for Dacron can then be computed at the Transverse Critical Velocity. Following the same procedure as for nylon yields the dynamic stress–strain curve for Dacron, Figure 9. Only the stress–strain curve at the TCV has been plotted; both the static and dynamic curves for nylon have been included for comparison. Again the dynamic breaking stress has decreased, but the dynamic breaking strain has remained approximately constant.

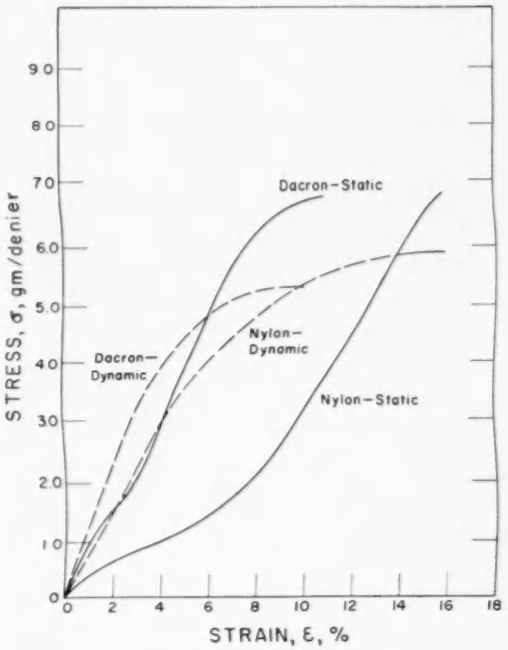

Fig. 9. Dynamic stress–strain relationship for nylon and Dacron.

Discussion of Method

Early studies on wave propagation have assumed that all strains traveled with the same velocity, or that the strain–strain velocity distribution was rectangular. Von Kármán [30] and others [18, 28] proposed that for a material which exhibited plastic deformation, for example ductile copper wire, two waves could exist: one, elastic, corresponding to the initial modulus of the material and a second, much slower, plastic wave corresponding to the slope of the stress–strain curve in the plastic region. He predicted from the *static* curve of ductile copper wire that this distribution of strain would appear as Curve B in Figure 10A. This was later confirmed [3], although the measurements were made on the *residual* plastic strain.

Several types of strain versus strain-velocity distributions might be expected. Curve A in Figure 10A represents the "square-wave" hypothesis. Curve C corresponds to the results found in nylon, and Curve D is a linearly decreasing function. These are plotted with the same strain-wave velocity and with equal areas, i.e., equal average strain, implying approximately the same striking velocity (the Transverse Wave Velocity U will not be constant). Figure 10B then shows the form of the stress–strain curves which would give rise to these particular strain versus strain-velocity distributions. The square-wave distribution A would result from a perfectly Hookian material where the modulus is constant. Curve C, the distribution for nylon, would be obtained from a gently curving relationship C for stress versus strain. A ductile material of the von Kármán type would have a stress–strain curve showing a plastic region, B. The straight-line relation-

[4] Du Pont trademark.

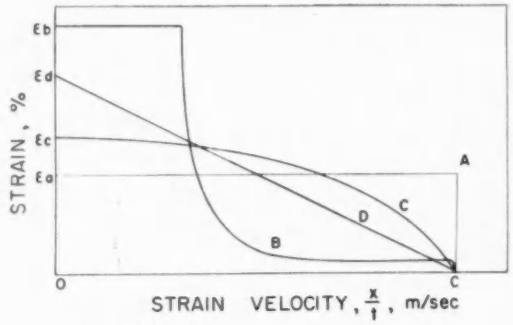

Fig. 10A. Strain versus strain velocity.

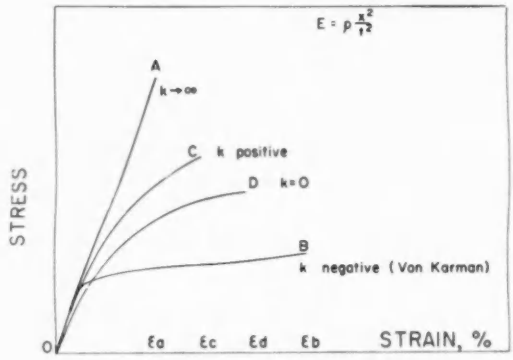

Fig. 10B. Dynamic stress–strain.

ship, D, would result in a cubic equation relating stress and strain.

The square-wave case, A, requires that k approach positive infinity. For the strain versus strain-velocity straight line, D, k approaches zero. All materials which lie between A and D have positive k values. Materials which show plasticity, B, have negative k values.

It is interesting to note that preliminary tests on Orlon,[4] which has a static stress-strain curve having a relatively sharp yield point (similar to B in Figure 10), have given strain versus strain-velocity distributions of the von Kármán type. The handling of the data for such materials has not been fully resolved, and further work on materials of this type has been deferred for the present time. In cases where k is positive, a dynamic stress–strain curve can be determined for those materials whose strain versus strain-velocity distributions lie above the straight line D and approach the square wave in form.

Figure 11A shows strain versus strain-velocity curves for nylon and Dacron at the transverse critical velocity and two curves for hypothetical or theoretical materials. Curve A represents a material approaching "square-wave" form with a k of approximately 5. Theoretical B in Figure 11A might arise from the modulus versus strain relationship indicated in Figure 11B and the stress–strain curve in Figure 12, under the assumptions of quasi-plastic shock waves as investigated by White [31] and Lee [6]. The procedure utilized here for determining stress as a function of strain is satisfactory only if the modulus is a continually decreasing function of strain. If the stress–strain relationship is not convex towards increasing stress, the strain versus strain-velocity curve becomes a function of shock-wave phenomena. It might prove possible to determine the form of the strain versus strain-velocity distribution and the modulus versus strain relationship from a dynamic stress–strain curve such as Theoretical B in Figure 12, but the reverse may not be true.

This places a limitation upon the method described unless there is assurance that the modulus versus stress–strain relationship is monotonically decreasing. Since nylon, in static tests, does not fall in this category, it is questionable whether the dynamic

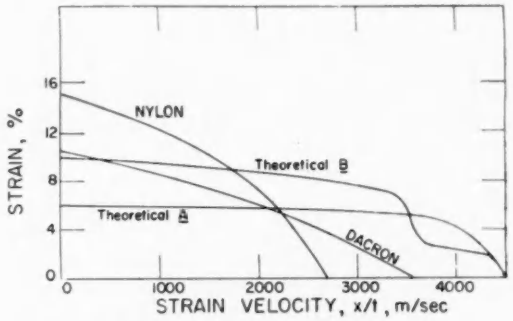

Fig. 11A. Strain versus strain velocity.

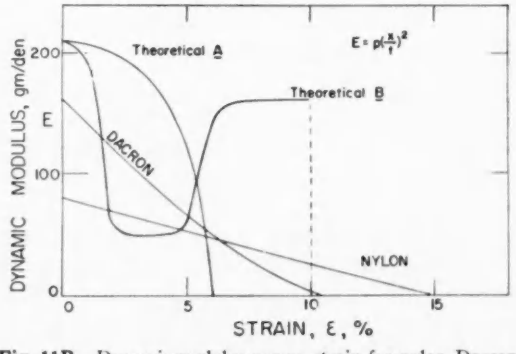

Fig. 11B. Dynamic modulus versus strain for nylon, Dacron, and two theoretical materials.

stress–strain curve obtained for nylon is any more than an approximation. This is an important question for future theoretical treatment; i.e., to develop a procedure for handling the case where the slope of the stress–strain curve does not uniformly decrease with increasing strain.

The procedures described are not limited to transverse impact, since an expression for particle displacement can be obtained. Assume the impact of the yarn to be longitudinal, that is, along the axis of the yarn, where the position x of a particle is measured from the point of impact. Then the partial derivative of Equation 6 with respect to time evaluated at $x/t = 0$ will give the equivalent longitudinal impact velocity

$$V_L = \left(\frac{\partial u}{\partial t}\right)_{x=0} = \epsilon_0 C \left[\frac{1}{1 - \exp^{-k}} - \frac{1}{k}\right] \quad (9)$$

When $\epsilon_0 = 15\%$, indicated as the rupture strain for nylon by the Transverse Critical Velocity, the longitudinal critical velocity is 245 m./sec., which agrees well with the value of 228 m./sec. given by Schiefer [19].

Equation 2 can also be used to predict the strain–time distributions at particular positions from the point of impact. The small amount of experimental data obtained to date indicates good prediction of these distributions. An experimental procedure for obtaining strain–position–time distributions on the single yarn is being improved and will be the subject of a separate report. Information of this type should answer a number of questions concerning the behavior of the material and perhaps suggest the appropriate mechanical model for a general mathematical solution to this problem. This in turn may provide a physical explanation for the curve-fitting constant, k, which has proved so valuable in the empirical handling of the data.

General Discussion

The method described in this report presents a procedure for determining a dynamic stress–strain curve for textile yarns at maximum rates of straining on minimum breaking times. It is based on the ability to predict the strain–strain velocity distribution at the TCV, whether the material is or is not rate-dependent.

Unfortunately, the method does not provide a means for determining an equivalent stress–strain curve to rupture at velocities of impact less than the TCV or at rates of straining intermediate between previous data and these ballistic rates.

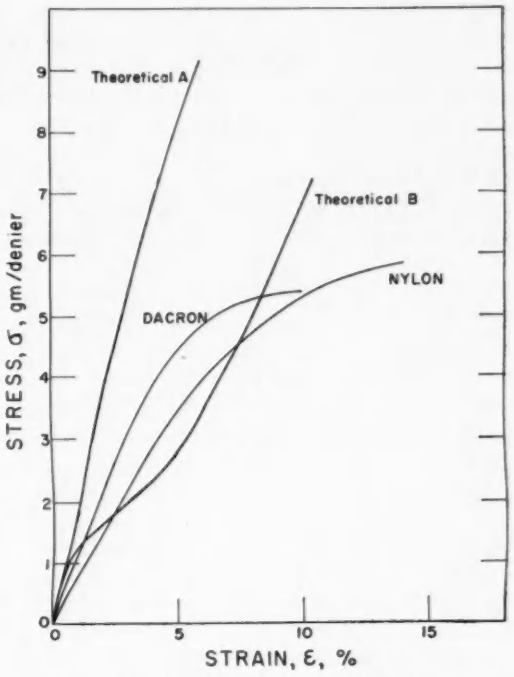

Fig. 12. Dynamic stress–strain relationship for nylon, Dacron, and two theoretical materials.

Experimental investigations at high impact velocities are incomplete. The majority of published work in this field has been limited to small strains, to reflected waves, or to theoretical considerations. The published experimental investigations dealing with strains up to the breaking strain are of three types and will be discussed separately.

The first of these methods, by Schiefer et al. [8, 22, 27], measured the acceleration of a load on the end of the yarn impacted longitudinally on the other end at impact velocities up to 250 ft./sec. By determining the force at the end of the specimen (by double graphical integration of the displacement curve) and the average strain in the specimen, he was able to plot stress–strain relationships to rupture at an average rate of straining of 4000%/sec. Certain experimental limitations, together with severe analytical problems, caused abandonment of this approach.

In continuing this work, Smith et al. [23, 24, 25] have determined the stress–strain relationship for yarns impacted transversely at their midpoint.

Changes in the velocity of the transverse wave front upon reflections of both the strain wave front and the transverse wave front allow calculations of tension by methods similar to Equation 8. The strain at the transverse wave front is taken as the average strain in the specimen. They report that, for average rates of straining of 5000%/sec., the breaking stress increases slightly and the breaking elongation decreases slightly, conclusions similar to those reached by Meredith [10].

The work by Schiefer and Smith, carried out concurrently with this study, although published previously, provides the best available technique for characterization of a dynamic stress–strain curve at low impact speeds. However, the method appears limited to low velocities of impact, since the strain pulses must remain small to permit the use of "square-wave" analysis and the average strain for local strain.

Fabric Research Laboratories have conducted investigations similar to those reported in Part I. The work was sponsored by the Navy, and their reports are classified. However, certain portions of the work were reported at The Fiber Society meeting in September 1956. While their investigations on this particular subject were not extensive, the same general conclusions of lowered dynamic rupture stress and equivalent rupture strain were reached.

At present, a large gap exists in our information between rates of straining of 10^3 and 10^6 %/sec. Further, the two testing techniques are not the same, and do not give the same strain–time increment history. Perhaps more serious is the fact that neither method corresponds to the two standard techniques for measuring static stress–strain response: constant rate of straining or constant rate of loading. A device for producing constant rate of straining in longitudinal impact requires constant acceleration, not constant velocity. In addition, the test must be run to completion prior to strain-wave reflection.

Some mention should be made of the limitations and assumptions of this technique. Yarn structure has been assumed of small importance in the analysis compared to the major variables. The problems of yarn bending at the transverse wave and possible coupling effects between longitudinal and transverse motion have been handled by using the analytical method only up to the transverse wave front. Obviously, this is not a complete answer, but it appears to be a practical one.

This same restriction also eliminates consideration of the air drag on the yarn. The effect of air drag at velocities less than the TCV is quite real, as shown by Morgan [11]. At the TCV, the length of yarn in transverse motion is so small that the drag-induced tension has been ignored. However, it is quite possible that air drag, together with shear at the projectile, explains yarn ruptures at short times after impact (20–40 sec.) for velocities considerably below the TCV. Stress relaxation and continued constant stress are also possible explanations. This phase of the problem is quite complex, and has not been considered.

Mention should be made of the large number of theoretical studies published. Unfortunately most solutions have been in terms of stresses related to various other parameters. The experimental method discussed gives strains related to different parameters. The authors have not been free to attempt a comparison in either direction to provide either a theoretical justification for their conclusion or an experimental verification of any of a number of theories. The studies are noted briefly for purpose of general reference.

Taylor [29] and Lee [7] have considered the transverse-impact problem, as has Huth [1]. Craggs [2] has discussed the problem for plastic-elastic strings with reflections. Ringleb [17] has considered oblique impacts. Lee and Kantner [5] have considered wave propagation in elastic and Maxwell materials. Zverev [32] considered the impact of a semi-infinite bar of a Voigt material. Morrison [12, 13] has expanded this work to three- and four-parameter models of viscoelastic materials.

Conclusions

A technique has been presented for obtaining a dynamic stress–strain relationship for textile yarns at rates of straining approaching 10^6 %/sec. The procedure, while lengthy, provides the only available information at these rates. A semi-empirical analysis has been used, with certain assumptions as to impact behavior. The plastic wave analysis of von Kármán has proven useful in this technique. Results have been given for nylon and Dacron yarns and predictions made about the probable behavior of other textile materials.

Certain parameters of textile materials appear to contribute to higher transverse critical velocities, and thus, it is hoped, to a higher ballistic protection value

for body armour. Of first importance is a high initial modulus, or strain-wave velocity, insuring maximum involvement of material in the same time interval after impact. A high k value is important, such that the ratio of the maximum strain near the projectile ϵ_0 and the average strain in the yarn $\bar{\epsilon}$ approaches 1.

A high value of k dictates small curvature of the stress–strain curve and, with the practical limitation of available tensile rupture stress, tends to exclude those materials with large breaking strains. Thus, curves such as theoretical B in Figure 12 would prove of value since they would possess high moduli at relatively large strains. A reversal in the stress–strain curve might prove necessary in obtaining a good ballistic material.

Several other materials are under study and will be reported later. The analysis presented has been related superficially to the performance of the yarn in a panel for body-armour use. Additional work is in progress on the importance of the Transverse Critical Velocity in the prediction of the ballistic protection of body-armour materials from individual yarn tests.

Literature Cited

1. Cole, J. D., Dougherty, C. B., and Huth, J. H., *J. Appl. Mech.* **20**, 519–522 (1953).
2. Craggs, J. W., *J. Mech. Phys. Solids* **2**, 286 (1954).
3. Duwez, P. E., OSRD Report 380 (1942); NDCR Report No. A33.
4. Lee, E. H., Report to Fabric Research Laboratories (October 1949).
5. Lee, E. H. and Kanter, I., *J. Appl. Phys.* **24**, 1115–1122 (1953).
6. Lee, E. H. and Tupper, S. J., Paper No. 53–A–28, ASME, Applied Mechanics Division; Annual Meeting (1953).
7. Lee, E. H., private communication (1954).
8. McCrackin, F. L., Schiefer, H. F., Smith, J. C., and Stone, W. K., *J. Research Nat. Bur. Standards* **54**, 227–280 (1955); TEXTILE RESEARCH JOURNAL **25**, 529 (1955).
9. Maheux, R. C., Stewart, G. M., Petterson, D. R., and Odell, F. A., Chemical Warfare Laboratories Report 2141 (1957).
10. Meredith, R., *J. Textile Inst.* **45**, T30 (1954).
11. Morgan, H. M., unpublished data, Fabric Research Laboratories (1956).
12. Morrison, J. A., Picatinny Arsenal Contract NORD 11496, Brown University PA–TR–5/17 (1953).
13. Morrison, J. A., Picatinny Arsenal Contract NORD 11496, Brown University PA–TR–6 (1953).
14. Petterson, D. R., Stewart, G. M., Maheux, R. C., and Odell, F. A., Chemical Warfare Laboratories Report 2161 (1957).
15. Petterson, D. R. and Stewart, G. M., Chemical Warfare Laboratories Report 2184 (1957).
16. Petterson, D. R., Stewart, G. M., Odell, F. A., and Maheux, R. C., TEXTILE RESEARCH JOURNAL **30**, 411–421 (1960).
17. Ringleb, F. O., *J. Appl. Mech.* **24**, 417 (1957).
18. Rachmatulim, Kh. A., *Pvikl. Mat. i Mech.* **9**, 91 (1945).
19. Schiefer, H. F., National Bureau of Standards Report 2928, OQMG Project No. 92–06–05 (1953).
20. Schiefer, H. F. et al., NBS Report 9A115, OQMG Project No. 7–80–05–001 (1954).
21. Schiefer, H. F. et al., National Bureau of Standards Report 4403, OQMG Project No. 7–80–05–001 (1955).
22. Smith, J. C., McCrackin, F. L., and Schiefer, H. F., *J. Research Nat. Bur. Standards* **55**, 19–28 (1955); TEXTILE RESEARCH JOURNAL **25**, 701 (1955).
23. Smith, J. C., McCrackin, F. L., Schiefer, H. F., Stone, W. K., and Towne, K. M., *J. Research Nat. Bur. Standards* **57**, 83–89 (1956); TEXTILE RESEARCH JOURNAL **26**, 821 (1956).
24. Smith, J. C., McCrackin, F. L., and Schiefer, H. F., *J. Research Nat. Bur. Standards* **60**, 517–534 (1958).
25. Smith, J. C., McCrackin, F. L., and Schiefer, H. F., *J. Textile Inst.* **50**, T55–68 (1959).
26. Stewart, G. M., Petterson, D. R., and Hamburger, T., Chemical Warfare Laboratories Report 2142 (1957).
27. Stone, W. K., Schiefer, H. F., and Fox, K., *J. Research Nat. Bur. Standards* **54**, 269–276 (1955); TEXTILE RESEARCH JOURNAL **25**, 520 (1955).
28. Taylor, G. I., British Official Report R. C. 329 (1942).
29. Taylor, G. I., unpublished data (1942).
30. von Kármán, T., OSRD Report 365 (1952); NDRC A29 (1949).
31. White, M. P. and Griffis, L., *J. Appl. Mech., Trans. ASME* **70**, 256 (1948).
32. Zverev, I. N., *Pvikl. Mat. i Mech.* **15**, 295–302 (1950); Brown University Translation A11–T12/16.

Manuscript received December 9, 1957.

Electrical Conduction in Keratin

J. E. Algie, J. G. Downes, and B. H. Mackay

C.S.I.R.O. Wool Research Laboratories, Division of Textile Physics, Ryde, N.S.W., Australia

Abstract

The increase in electrical conductivity of keratin fibers after the application of an abrupt change of the relative humidity from $0 \rightarrow 90\%$ RH has been examined as a function of time. A comparison of these results with regain vs. time, for the same experimental conditions, indicates that the water inside a fiber is not initially in a state which facilitates conduction. It is proposed that the slow rise of conductivity is due to the formation of a hydrogen bonded network which allows the passage of protons under the influence of the applied electric field.

Introduction

It has been shown by all those who have worked on the electrical conduction of keratin that the moisture content or regain is of paramount importance. Marsh and Earp [11] made the observation that the conductivity attains an equilibrium value several days after the equilibrium regain has been reached. They also reported hour-to-hour fluctuations in resistance which they attributed to some internal process of readjustment within the fiber affecting the distribution of water. Sharman, Hersh, and Montgomery [13] found that the conductivity of nylon increased with conditioning time even though the regain was constant.

This paper presents the results of a series of experiments designed to investigate the above effects in keratin fibers.

Experimental Procedure

The single fibers used in the experiments were obtained from pen-grown Corriedale or pen-grown Merino wool. The diameters of the fibers, measured microscopically in distilled water, were 50μ for the Corriedale and 22μ for the Merino. All fibers were cleaned by several changes of cold petroleum ether and ethyl alcohol, then many changes of tin-distilled water. The ash content after the cleaning treatment was $\approx 0.01\%$ for the Corriedale and $\approx 0.002\%$ for the Merino fibers. Resistance measurements were made by use of an apparatus which has already been described [1], consisting of an electrometer attached to a potentiometric recorder. The fiber was contained in a small enclosure which could be rapidly coupled into a system circulating air at 0% RH or into a similar system circulating air at 90% RH. The whole apparatus was maintained at 35° C. $\pm$ 0.02° by an air thermostat placed in a temperature-controlled room. The regain of a small bundle of similar fibers was measured by Watt [14] by suspending them from a quartz spring. In both regain and resistance experiments an abrupt change from $0 \rightarrow 90\%$ RH was made in the atmosphere surrounding the fiber.

In order to achieve a low enough value of electrical resistance, the length of the 50-μ diameter fibers was 2 mm., while in the case of the 22-μ diameter fibers, 4 fibers 2 mm. long spaced approximately 3 mm. apart were used.

A voltage of 67.5 volts was applied to the fibers continuously while the resistance was changing rapidly, but for the later periods of the experiment the voltage was applied only when a reading was being taken, since it was found that, although the fiber resistance was ohmic (Figure 1), changes in the

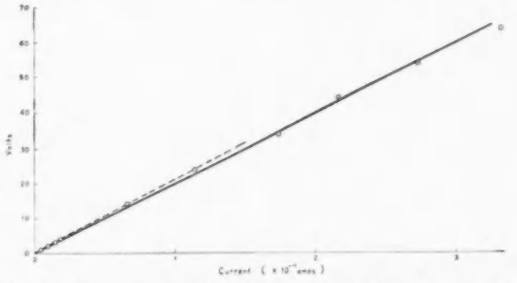

Fig. 1. Current vs. voltage for a Corriedale fiber at 90% RH, 20° C.

resistance (Figure 2) occurred if the voltage was applied for a sufficiently long time. A similar time dependence has been observed by Hearle [8].

The standard resistors used in the experiments were either $10^{11}\Omega$ or $10^{12}\Omega$ and the electrodes were made of brass.

Results and Discussion

When an abrupt increase is made in the relative humidity of the atmosphere surrounding a wool fiber, our results (Figure 3) show that the increase of conductivity is a very slow process in relation to the increase of regain. In Figure 4 a comparison is made between the regain vs. time curves as obtained by a weighing experiment and the *equivalent* regain vs. time curves calculated from the results in Figure 3 and King and Medley's data for conductance vs. regain.

At 10 min. after the relative humidity change has been made the equilibrium regain has been reached, while the conductivity is still a decade from its equilibrium value.

A similar slow build-up process which occurs at the same rate as the conductivity increase has been observed by Mackay and Downes [10] in the increase in rigidity of a Merino wool fiber following a rapid large change of relative humidity.

Feughelman [7] has proposed that the build-up of rigidity is due to the formation of interchain hydrogen bonds via water molecules, the water molecules eventually becoming associated in an icelike state. Such a network would facilitate conduction by translation of protons along hydrogen bonds by a similar mechanism to that put forward by Bjerrum [5] for conductivity in ice.

There is not sufficient data available at present for a decision to be made about what is occurring in the later period of the conductivity build-up, i.e. the period from 100 min. onwards. The rigidity build-up process has been observed only for a period of 100 min., so we can not obtain corroborative evidence for hydrogen-bond formation from the rigidity experiments for times in excess of 100 min. Consequently it is possible that another mechanism may account for the later stages of conductivity increase, e.g. a redistribution of water within the fiber as

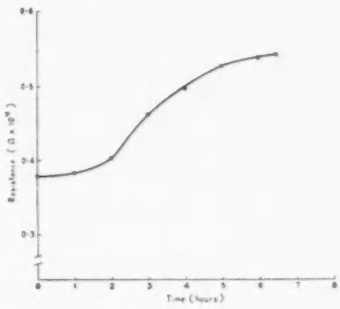

Fig. 2. Resistance changes with time after applying 67.5 volts. Merino fiber conditioned for 7 days at 90% RH, 20° C.

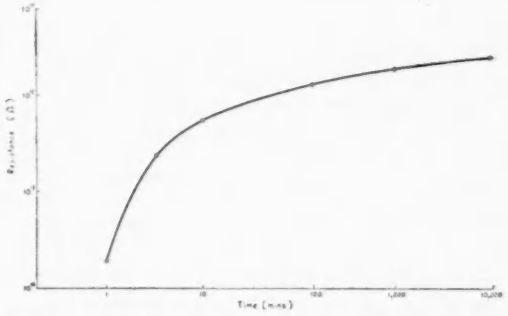

Fig. 3. Log resistance vs. log time for Merino fiber after step change from 0 → 90% RH at 35° C.

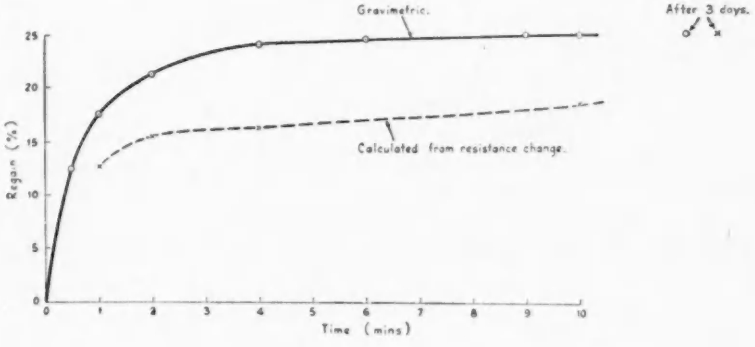

Fig. 4. Comparison between: (dashed line) regain vs. time calculated from the resistance changes similar to Figure 3, and (full line) regain vs. time determined by gravimetric methods. Both for Merino fiber after step change from 0 → 90% RH at 35° C.

suggested by Sharman, Hersh, and Montgomery [13] for the nylon–water system. It has been proposed by Feughelman [6] that keratin exists in two phases and that a redistribution of water can occur between these two phases. This redistribution could produce the observed slow increase in conductivity.

Baxter [4] has suggested that the wool–water system is a semiconductor in which the water is in an oriented state unlike liquid water. He claimed that the conduction was by movement of electrons and that the activation energy of the conduction process was similar to that of conduction in ice.

King and Medley [9], however, have shown that the conduction of electricity in keratin is ionic, although the activation energy of conduction is far greater than that for electrolytic conduction in salt–water solutions. Furthermore, they found that sufficient hydrogen was given off when a current was passed through a keratin slab to account for 96% of the current which had flowed.

According to King and Medley the ionic conduction is caused by the dissociation of salts which are present as impurities. Baker and Yager [3], however, suggested that for polyamides the conduction process was ionic due to the movement of a charged atom, probably hydrogen, and Riehl [12] has recently proposed that conduction in gelatin–water systems is due to proton movement.

Our results are in agreement with this latter concept; i.e., that the wool–water system is a protonic semiconductor.

The only alternatives to protonic conductivity are ionic conductivity through the movement of impurity ions or electronic semiconduction.

Our results indicate that, even at 90% RH, ionic conductivity of the type which occurs in solutions of electrolytes can not form a major part of the conductivity process, since a few minutes after the change in relative humidity is made we have a situation in which the keratin fiber has its equilibrium regain but does not have its equilibrium conduction. One would expect that initially the water would be in a less associated state, hence more able to act as an electrolyte for electrolytic conduction.

Electronic semiconduction in keratin at high regains was not supported by the work of King and Medley. Also, Algie and Haly [2] have shown that ultraviolet light had no observable effect on the conductivity of a wool fiber at 90% RH and 20° C. provided that isothermal conditions were obtained. The activation energy of conduction at 90% RH is such that photons of ultraviolet light should have sufficient energy to release electrons from the keratin, if it were an electronic semiconductor.

We can only conclude, therefore, that the conduction process for the wool–water system is protonic and dependent upon whether the water is in an associated or unassociated state.

Conclusions

We have suggested from our results and discussion that the wool–water system is a protonic semiconductor and that it is very probable that a hydrogen-bonded network has to be formed before conduction can take place.

Ionic conduction of the electrolytic type has been shown to be a minor factor in the conductivity of clean wool fibers even for regains near saturation.

Acknowledgments

The authors are indebted to R. Rabbidge for the construction of equipment and for carrying out some of the electrical experiments.

Literature Cited

1. Algie, J. E., TEXTILE RESEARCH JOURNAL **29**, 2 (1959).
2. Algie, J. E. and Haly, R. (letter to TEXTILE RESEARCH JOURNAL, scheduled for August).
3. Baker, W. O. and Yager, W. A., *J. Am. Chem. Soc.* **64**, 2176 (1942).
4. Baxter, S., *Trans. Faraday Soc.* **39**, 207 (1943).
5. Bjerrum, N., *Dan. Mat. Fys. Medd.* **27**, 1 (1951).
6. Feughelman, M., TEXTILE RESEARCH JOURNAL **29**, 223 (1959).
7. Feughelman, M., *J. Appl. Poly. Sci.* **2**, 189 (1959).
8. Hearle, J. W. S., *J. Textile Inst.* **44**, T117 (1953).
9. King, G. and Medley, J. A., *J. Colloid. Sci.* **4**, 1 (1949).
10. Mackay, B. H. and Downes, J. G., *J. Appl. Poly. Sci.* **2**, 32 (1959).
11. Marsh, M. C. and Earp, K., *Trans. Faraday Soc.* **29**, 173 (1933).
12. Riehl, N., *Kolloid. Z.* **151**, 66 (1957).
13. Sharman, E. P., Hersh, S. P., and Montgomery, D. J., TEXTILE RESEARCH JOURNAL **23**, 793 (1953).
14. Watt, I., private communication.

Manuscript received January 4, 1960.

The Analysis of Variations for Certain Physical Properties of Combed Cotton Yarns[1]

D. S. Hamby, W. C. Stuckey, B. Gast

School of Textiles, North Carolina State College, Raleigh, North Carolina

and R. J. Hader

Institute of Statistics, North Carolina State College, Raleigh, North Carolina

Introduction

For a number of years the faculty and staff of the School of Textiles at N. C. State College have been asked by the industry to test different textile materials and to comment on the resulting quality levels. A good portion of these requests involved yarn, and a search of the literature did not reveal any suitable references to such material. The information was not available because some particular references pertained only to a specific topic or because the advance in testing techniques has developed at such a rate that the literature is not complete on some subjects.

Since this type of information was not available in suitable form, it was decided to conduct a study designed to give information as to the levels of the quality measurements normally used in evaluating yarns.

Although every effort was made to collect samples that were representative of the combed yarn industry, no claims are made by the authors that the results represent standards as such for the variables that have been measured.

Materials Studied

Sixty-one combed yarns, ranging in count from 16/1 to 120/1, were sampled from 32 different mills. For each yarn number 25 spinning bobbins were selected at random. In this first study no effort was made to separate between-side, between-frame, and between-shift variation.

The mills that participated were selected according to their reputation in the trade. Some mills considered to be producing the best yarn in the industry were selected and others considered to be producing some of the lowest quality were also selected. Most of the mills, however, were in the so-called average quality class.

Experimental Procedure

Table I summarizes by type of test the number of bobbins, k, and the number of measurements per bobbin, n, for each yarn.

For skein strength measurements, 120-yd. skeins were broken on a 150–300 lb. capacity Scott Model J tester. All single-end strength measurements were

TABLE I. Average Values for Results of Analysis of Variation of Combed Cotton Yarns

Yarn property	k	n	Average* CV_0	CV_b	CV_w	CV_r	CV_{fd}	Dev.
Skein strength, lb.	25	4	6.0	5.0	3.8	3.6		
Single end strength, g.	10	20					10.8	
Yarn number, English system	25	4	2.7	2.2	1.6	1.5		2.4
Twist, turns/in.	25	4	5.0	3.1	4.4	4.4		
Uniformity, % U	10	1						

k = Number of bobbins tested for each of the 61 combed yarns
n = Number of tests per bobbin
CV_0 = Percent coefficient of over-all variation
CV_b = Percent coefficient of variation between packages
CV_w = Percent coefficient of variation within packages
CV_r = Percent coefficient of variation (Range Method)
CV_{fd} = Percent coefficient of variation (Frequency Distribution Method)
Dev. = Percent deviation from specified number

* Each value for skein strength, yarn number, and twist represents 6100 measurements. Each value for single end strength represents 12,200 individual measurements.

[1] Presented at the Textile Division Conference of the American Society for Quality Control, Clemson, S. C., February 1960.

made on the Uster Dynamometer with a speed setting of 5.

The yarn number was measured on an Alfred Suter Direct Numbering Balance using the skeins from strength determinations.

The Uster Mean Linear Integrator was used in conjunction with a Uster Model B Evenness Tester to measure the percent linear deviation.

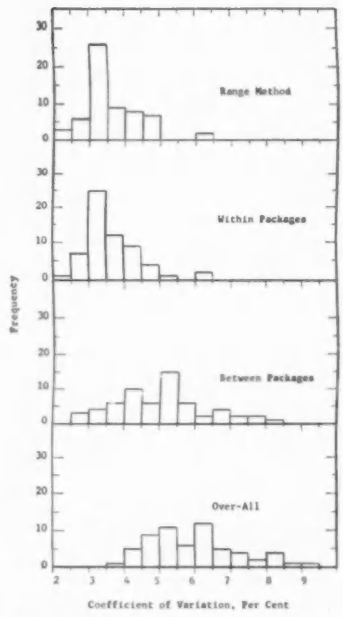

Fig. 1. Coefficients of variation for skein strength of combed cotton yarns.

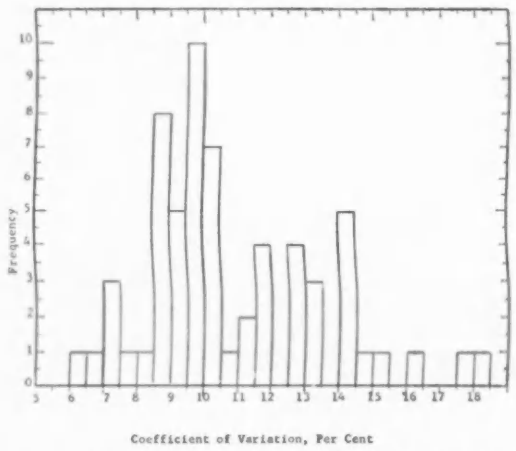

Fig. 2. Coefficient of variation for single end strength of combed cotton yarns.

The 10-in. untwist-twist method was used to determine the twist per inch using the twist tester manufactured by the U. S. Testing Company.

Data Analysis

The main portion of the data analysis consisted of application of the analysis of variance technique to study the "between bobbin" and "within bobbin" variation for each of the three properties: yarn number, skein strength, and twist. A separate analysis of variance was performed on each of these properties for each of the 61 different yarns. In each case there were 25 bobbins and 4 tests per bobbin. The general form of the analysis of variance is as follows.

Source of variation	Degrees of freedom	Sum of squares	Mean square	Expected mean square
Between bobbins	24	$4\sum_i (\bar{x}_i - \bar{\bar{x}})^2$	M_b	$\sigma_w^2 + 4\sigma_b^2$
Within bobbins	75	$\sum_i \sum_j (x_{ij} - \bar{x}_i)^2$	M_w	σ_w^2
Total	99	$\sum \sum (x_{ij} - \bar{\bar{x}})^2$		

In this analysis the total variation around the grand sum of square deviations from the bobbin means, $\sum \sum (x_{ij} - \bar{\bar{x}})^2$, is broken up into two parts, the first based on differences of bobbin means from

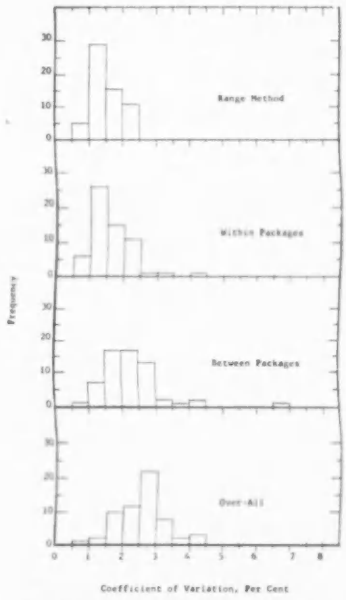

Fig. 3. Coefficients of variation for yarn number of combed cotton yarns.

the grand mean, $4 \sum (\bar{x}_i - \bar{\bar{x}})^2$, and the second a pooling of the within bobbin means, $\sum_i \sum_j (x_{ij} - \bar{x}_i)^2$.

These sums of squares are then divided by their respective degrees of freedom to yield the mean squares M_b and M_w. By statistical theory it may be shown that the expected or average value of these two mean squares are $\sigma_w^2 + 4\sigma_b^2$ and σ_w^2 respectively. The symbol σ_w represents the standard deviation of the "within bobbin" component of variation and σ_b represents the standard deviation of the "between bobbin" component. Once M_b and M_w have been calculated numerically, the values of σ_b^2 and σ_w^2 are readily found by solving the equations

$$M_b = \sigma_w^2 + 4\sigma_b^2$$
$$M_w = \sigma_w^2$$

For purposes of presentation of results all values of σ_w and σ_b were converted to coefficients of variation by dividing by the mean, $\bar{\bar{x}}$, and multiplying by 100. It was also of interest to combine the two components of variation into an over-all coefficient of variation which is found from the relation

$$CV_0^2 = CV_w^2 + CV_b^2$$

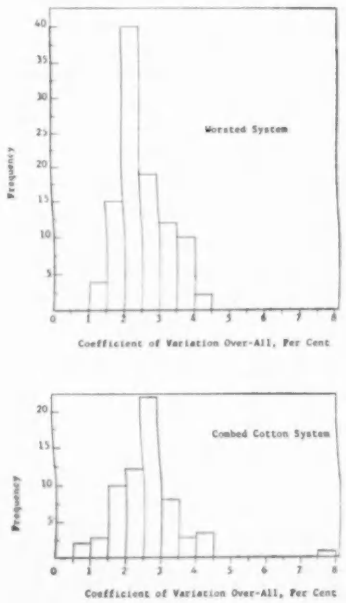

Fig. 4. Comparison of over-all coefficient of variation for yarns spun on the cotton and worsted systems. (Data for worsted system yarn courtesy of G. M. Bornet, Ontario Research Foundation, Toronto, Canada.)

These are illustrated by an example shown under Sample Calculations.

The "within bobbin" variance may more conveniently be estimated by the range method using

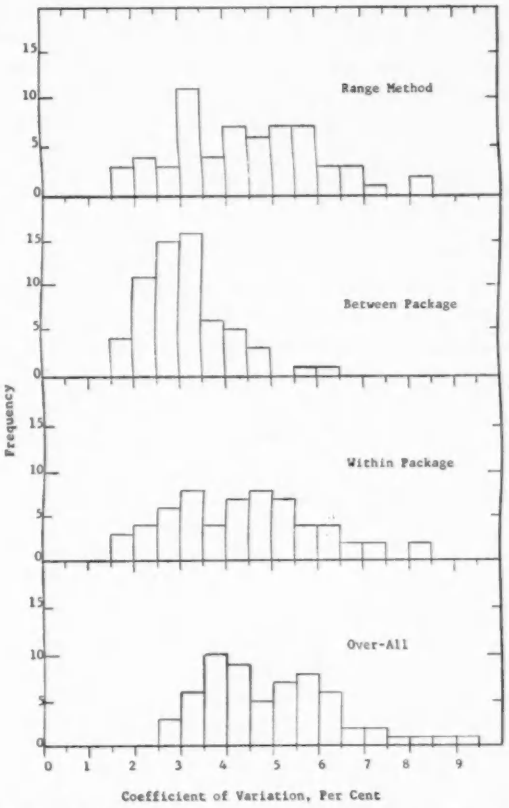

Fig. 5. Distribution of coefficients of variation for twist in combed cotton yarns.

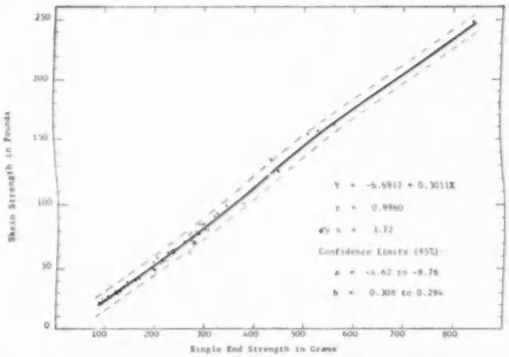

Fig. 6. Relationship between skein strength and single end strength of combed cotton yarns.

$\sigma = \bar{R}/d_2$, where $\bar{R}$ is the average "within bobbin" difference between largest and smallest values and d_2 is conversion constant dependent on the number of tests within each bobbin.[2] For four tests, $d_2 = 2.059$.

The various coefficients of variation were subjected to further study consisting of frequency distributions for each type and of attempts to correlate the various types with each other and also with additional variables such as, for example, the CV_0 for skein strength vs. the coefficient of variation for single-end tests. This will be discussed in more detail in the next section.

Results and Discussion

The difference in level (significant) for the coefficients of variations for over-all, between package and within package for skein strength are obvious in Figure 1. The over-all coefficient of variation (CV_0) averaged 6.0% and included the within-bobbin, between-spindles, between-sides, and between-frames variation. The between-package variation (CV_b) averaged 5% which, as would be expected, was slightly less than the over-all. The within-package variation (CV_w) averaged 3.8%. Since the range method of calculating the standard deviation is commonly used in quality control work, this method was also used in addition to the standard analysis of variance technique. As seen in Figure 1, as well as other figures, the coefficient of variation based on the range method (CV_r) is in close agreement with the CV_w. Although the calculations were not made in this study, the over-all coefficient of variation may also be estimated from ranges. This method is explained by Enrick [4] and has been in use for a number of years.

Figure 2 shows the distribution and level for the coefficient of variation (CV_{fd}) of the single-end strength. These values were calculated from the frequency distribution as accumulated on the Uster Dynamometer. Each entry represents the distribution of 20 measurements each for 10 bobbins.

The variation in yarn number is shown in Figure 3. The CV_0 averaged 2.7% and with the exception of one yarn ranged from 0.5% to 4.5%. The CV_b averaged 2.2% and the CV_w averaged 1.6%. As was the case with the skein strength, the CV_r and CV_w were in close agreement. Each measurement entered in this figure represents 4 measurements each from 25 bobbins.

A comparison is shown in Figure 4 between over-all coefficients of variation for the combed cotton yarns used in this study and for worsted yarns. The details of the worsted yarn study were presented by Bornet [3]; a comparison of the two types of yarns

[2] ASTM Manual on Quality Control of Materials, Table B2.

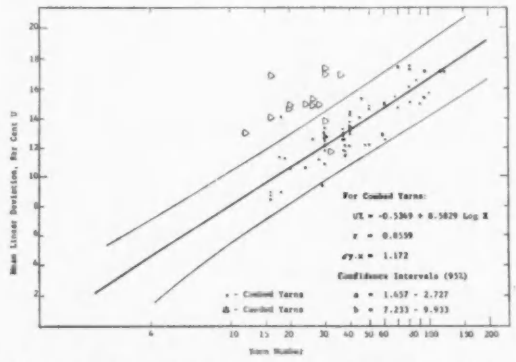

Fig. 7. Relationship between yarn number and mean linear deviation as measured by the Uster integrator.

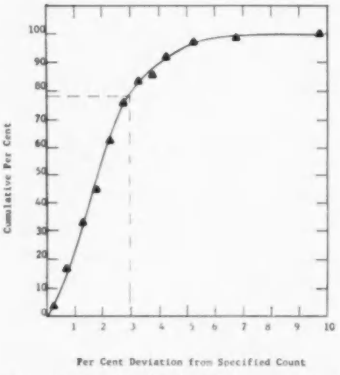

Fig. 8. Cumulative distribution for per cent deviation of yarn number from specified count of combed cotton yarns. A tolerance of 3% is specified by ASTM.

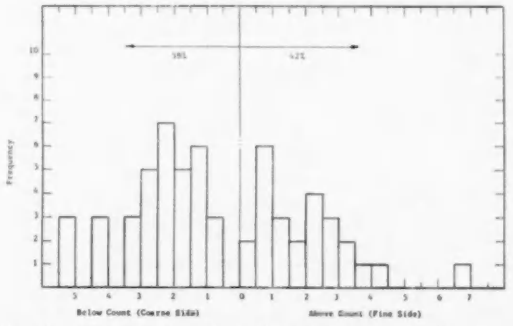

Fig. 9. Percent deviation of actual yarn number from specified number for combed cotton yarns.

shows a remarkable degree of similarity in this particular property.

Since the original study of yarn number variation was not designed to permit a complete analysis of the variation in yarn number and strength, subsequent studies [1, 7] were made to determine the magnitude of the influence of spindles, sides, and frames. A summary of these studies is shown in Table II. It is interesting to note the close agreement between yarn number and strength when comparing the sources of variation. Beckwith [2] reported that 32% of the variation was within cones and 68% between cones. The results of this study confirm these findings.

TABLE II. Sources of Variations in Yarn Number and Skein Strength for Combed Cotton Yarns

Source	Percent of total variation	
	Yarn number	Skein strength
Within bobbin	33	34
Between bobbin	44	47
Between sides of spinning frames	10	5
Between frames	13	14

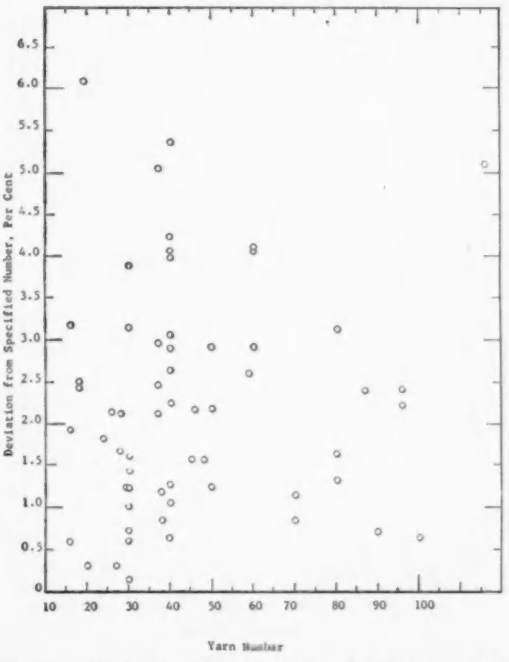

Fig. 10. Relationship of yarn number variation and specified number for combed cotton yarns.

In view of the interrelationship of certain physical properties of yarns, the basic data from this study were further analyzed in an effort to determine the degree of some of these relationships. Figure 6 shows the correlation between skein strength and single-end strength. This, as well as subsequent data, shows excellent correlation ($r = 0.996$) between these two properties. The equation $Y = -6.6917 + 0.3011X$ is for X in units of grams. For X in pounds the equation becomes $Y = -6.6917 + 136.58X$.

The relationship between the Mean Linear Deviation, Percent U, as measured by the Uster Linear Integrator, and the logarithm of the yarn number proved to be most interesting. As shown in Figure 7, there is a distinct difference between the combed and carded yarn. Only one combed yarn exceeded the limits on the high side and only two carded yarns entered the combed yarn area. Subsequent combed yarn data not shown on the chart fell between the two limits. A comparison between these limits and

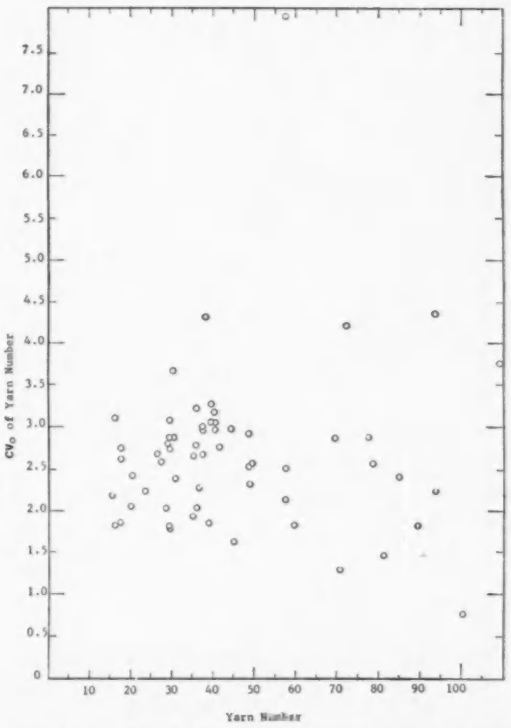

Fig. 11. Relationship between the coefficient of over-all variation for yarn number and the specified yarn number for combed cotton yarns.

the Uster Standards will show the limits in this figure to be somewhat lower than the Uster Standards.

Figure 8 is a cumulative frequency distribution showing that slightly less than 80% of the mills tested were within the American Society for Testing Materials tolerance of 3%. Figure 9 shows the distribution above and below target number.

There appears to be no relationship between yarn number and percent deviation from specified count or yarn number and CV_o for yarn number. Coefficients of correlation were not calculated; however, no trends are apparent by examination of Figures 10 and 11.

There is some correlation ($r = 0.83$) between the coefficient of variation for single-end strength (CV_{fd}) and the Mean Linear Deviation, Percent U. This plot is shown in Figure 12.

No statistical analysis was made of the data in Figure 13; however, by visual examination it is obvious that there is no trend or pattern between CV_o of skein strength and CV_{fd} for single-end strength.

Figure 14 shows that there is fair to poor correlation for over-all coefficients of variation for yarn number and skein strength; Figure 15 shows fair to poor correlation for CV_w for yarn number and CV_w for skein strength.

The CV_{fd} for single-end strength and the CV_o for turns per inch exhibited very poor correlation ($r = 0.38$).

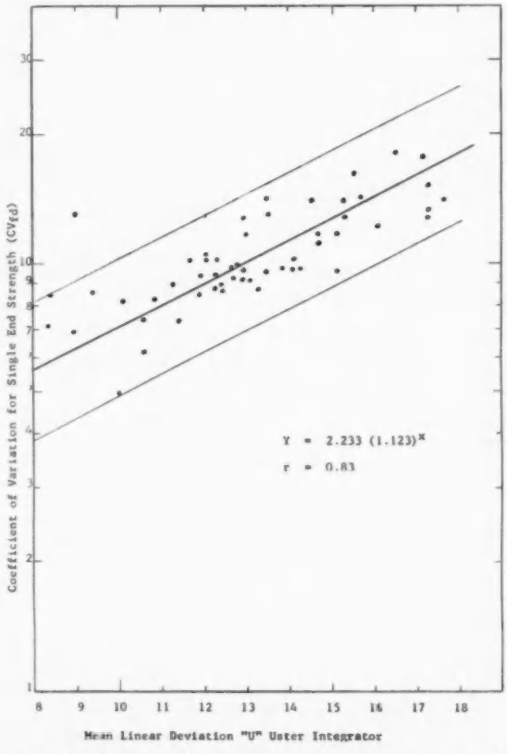

Fig. 12. Relationship between percent mean linear deviation and coefficient of variation for single end strength of combed cotton yarn.

Practical Applications of Results

In order to illustrate the practical application of the results and conclusions of this study, suppose that the quality control program for a mill develops the following information: for skein strength a CV_o of 6.54% and a CV_w of 3.37%; for yarn number a CV_o of 2.70%, a CV_w of 1.29%, and a deviation from specified count of 2.15%. By examination of Table I, the value 6.54 is found to be higher than the average of 6.0; also inspection of the bottom diagram in Figure 1 shows the value 6.54 is in the upper portion of the diagram. This means that if this yarn is to be considered as an average to good quality yarn, this variation should be reduced. The CV_w of 3.37% is better than average. Since the variation between bobbins is high or worse than average, effort should be directed toward reducing the variation in strength from bobbin to bobbin.

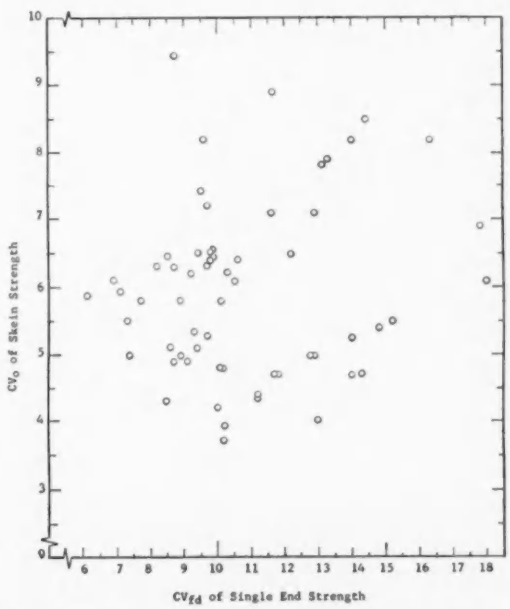

Fig. 13. Relationship between coefficients of variation for skein and single end strengths.

The percent deviation of the yarn number from the nominal or specified count of 2.15% is below the average of 2.4%, as shown in Table I, and also is below the 3% specified by the American Society for Testing Materials. The CV_0 of 2.70% is the same as the average shown in Table I. The CV_w of 1.29% is below the average of 1.6% and the CV_b of 2.46% is higher than the average value of 2.2%.

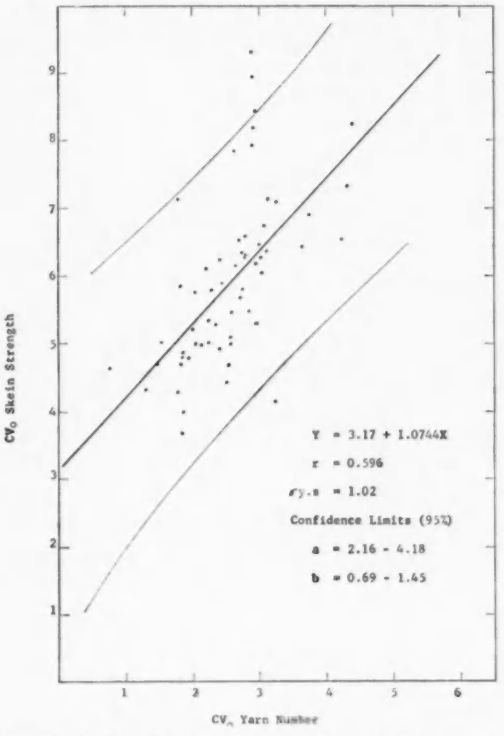

Fig. 14. Relationship between over-all coefficient of variation for skein strength and yarn number.

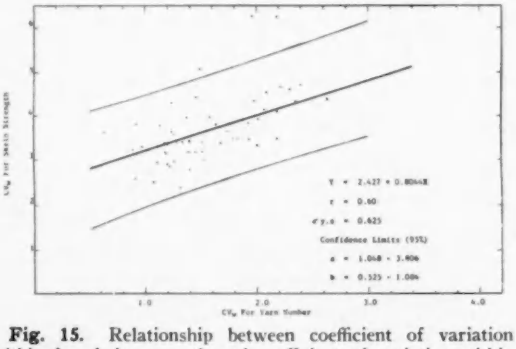

Fig. 15. Relationship between coefficient of variation within for skein strength and coefficient of variation within for yarn number.

It should be remembered when using this type of analysis and interpretation that the coefficient of variation will vary to some extent as the result of sampling variation. If there is a doubtful case as to the significance of the level of a variable, further statistical tests should be made on the data before any definite decision is made.

Sample Calculations

The conclusions and body of this report have been written in such a manner as to facilitate easy interpretation and use by management and other supervisory personnel. For the readers that are interested in the statistical techniques used in the analysis of the data, the following sample calculations are presented.

Total variance[3] $= \sum(X - \bar{\bar{X}})^2 = 20600.6$

Variance within bobbins[3] $= \sum(X_i - \bar{X}_i)^2 = 6750.0$

[3] See Table III.

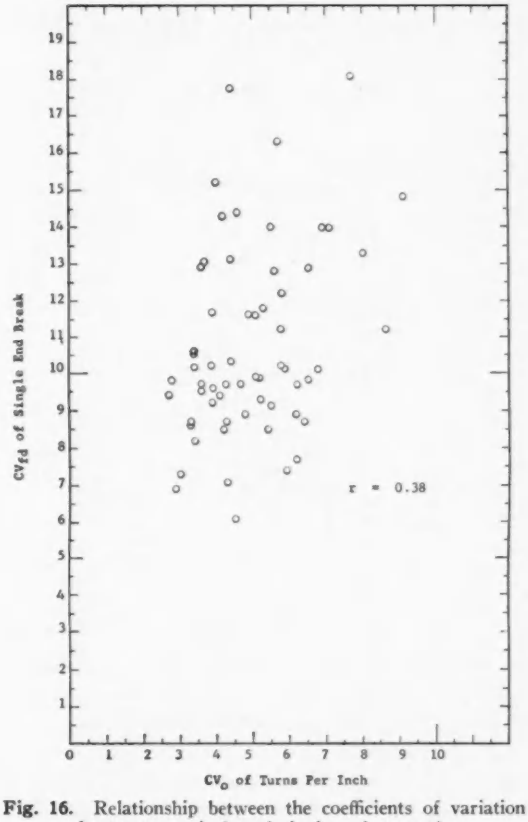

Fig. 16. Relationship between the coefficients of variation for turns per inch and single end strength.

Variance between bobbins[3]

$$= N\sum(\bar{X}_i - \bar{\bar{X}})^2 = 4(3462.6) = 13{,}850$$

	Sum of squares	Degrees of freedom	Mean squares
Within bobbins	6750.0	75	$90.0 = \sigma_w^2$
Between bobbins	13850.0	24	$577.1 = \sigma_w^2 + n\sigma_b^2$
Total	20600.0	99	

$$\sigma_w^2 + 4\sigma_b^2 = 577.1$$

$$\sigma_w^2 = 90.0$$

$$\sigma_b^2 = \frac{577.1 - 90}{4} = 121.78$$

$$CV_w = \sqrt{\frac{90}{248.4}} \times 100 = 3.81\%$$

$$CV_b = \sqrt{\frac{121.78}{248.4}} \times 100 = 4.42\%$$

$$CV_0 = \sqrt{\frac{90 + 121.78}{248.4}} \times 100 = 5.84$$

$$90 + 121.78 = 211.78$$

$$\frac{90}{211.78} \times 100 = 42\%\ V_w$$

$$\frac{121.78}{211.78} \times 100 = 57\%\ V_b$$

$$\sigma = \frac{\bar{R}}{d_2} = \frac{15.32}{2.059} = 7.44$$

$$CV_r = \frac{7.44}{248.4} \times 100 = 3.0\%$$

TABLE III. Skein Strength

Cone No.	Skein strength, X	$X - \bar{\bar{X}}$	$(X - \bar{\bar{X}})^2$	$X_i - \bar{X}_i$	$(X_i - \bar{X}_i)^2$	$\bar{X}_i - \bar{\bar{X}}$	$(\bar{X}_i - \bar{\bar{X}})^2$	R
1	248	0.4	.16	7.3	53.29			
	256	7.6	57.76	0.7	.49			
	261	12.6	158.76	5.7	32.49			
	256	7.6	57.76	0.7	.49			13
Σ	1021							
$\bar{X}_i$	255.3					6.9	47.61	
2	242	6.4	40.96	3.5	12.25			
	252	3.6	12.96	6.5	42.25			
	238	10.4	108.16	7.5	56.25			
	250	1.6	2.56	4.5	20.25			12
Σ	982							
$\bar{X}_i$	245.5					2.9	8.41	
	.	.	.	.	.	.	.	.
	.	.	.	.	.	.	.	.
	.	.	.	.	.	.	.	.
24	239	9.4	88.36	3.8	14.44			
	250	1.6	2.56	7.2	51.84			
	242	6.4	40.96	0.8	.64			
	240	8.4	70.56	2.8	7.84			11
Σ	971							
$\bar{X}_i$	242.8					5.6	31.36	
25	249	0.6	.36	1.5	2.25			
	249	0.6	.36	1.5	2.25			
	240	8.4	70.56	7.5	56.25			
	252	3.6	12.96	4.5	20.25			12
Σ	990							
$\bar{X}_i$	247.5					0.9	0.81	
Sum	24844		20600.6		6750.0		3462.6	383
Avg. $\bar{\bar{X}}$	248.44							15.32

Acknowledgments

The authors are indebted to Dr. A. H. Grandage of the Department of Experimental Statistics at North Carolina State College for his cooperation and advice in the analysis of the test data. Professor E. B. Grover, Head of the Department of Fiber and Yarn Technology, School of Textiles, N. C. State College, was most helpful during the course of this study with numerous suggestions and advice. Hassan Makhlouf, Ahmed Baz, Mahmoud Ibrahim, and Nabil Costandy, graduate students of the School of Textiles, contributed to the study by performing special calculations during the preparation of the final report.

Literature Cited

1. Baz, Ahmed, "Design of Sampling Plans for Skein Strength of Yarn Based on the Analysis of Variations," Thesis for Master of Science Degree, School of Textiles, N. C. State College, Raleigh, North Carolina (1959).
2. Beckwith, O. P., *Textile Inds.* **122**, 104–106 (1958).
3. Bornet, George M., *Textile Quality Control Papers* **5**, 39–72 (1958).
4. Enrick, N. L., "Quality Control Through Statistical Methods," Paulton, England, Modern Publishing Company (1954).
5. Grover, E. B. and Hamby, D. S., "Handbook for Textile Testing and Quality Control," N. C. State College (1958).
6. Hader, R. J., "Introduction to Statistics for Engineers," N. C. State College (1957).
7. Ibrahim, Mahmoud, "Design of Sampling Plans for Yarn Number Measurements Based on the Analysis of Variations," Thesis for Master of Science Degree, School of Textiles, N. C. State College, Raleigh, North Carolina (1959).

Manuscript received December 21, 1959.

Kinetic Studies of the Wool–Water System

Part I: The Influence of Water Concentration

I. C. Watt

C.S.I.R.O. Wool Research Laboratories, Division of Textile Physics, Ryde, N.S.W., Australia

Abstract

Studies have been made of the sorption of water by wool fibers, after changes of the external water vapor pressure, by following the weight changes of the fibers. The sorption kinetics are dependent on the size of the concentration change and the initial regain of the wool. For low regains, 0–2.5%, sorption is Fickian with a concentration-dependent diffusion coefficient. At 35° C. and zero regain the diffusion coefficient $D_0 = 1.0 \times 10^{-10}$ cm.²/sec. and the activation energy of diffusion is > 11 kcal./mole. For concentrations above 2.5% regain, a portion of the water vapor uptake on absorption occurs by a non-Fickian mechanism; the relative contributions of the Fickian and non-Fickian mechanisms to the total uptake vary with the initial regain.

Introduction

Despite the many excellent studies which have been made of the wool–water system, it was felt that a more detailed kinetic study was required. Since the publication by King and Cassie [12] in 1940 of their results showing the importance of temperature changes of the fiber surroundings on the subsequent sorption behavior, it has been evident that the study of water vapor sorption must be made in the absence of temperature effects in order to yield information on the structure of wool fibers.

Haly and Roberts [9] placed the fibers to be studied in an air stream in order to keep the temperature and humidity of the air at the fiber surface constant. However, the accuracy of this method permitted its use only for large changes of relative humidity. A second method, devised by Downes and Mackay [6, 7], measured, by a vibroscope tech-

nique, the change in the mass of a single fiber due to sorption. The relative humidity around the fiber was again controlled by air of the desired humidity flowing past the fiber. These studies showed that the conclusion reached by King and Cassie [12] that 15 sec. would be the maximum time required to attain equilibrium within a fiber at 20° C. was invalid, even for the most rapid sorption steps with Merino fibers.

The present studies are entirely on the kinetics of water sorption into wool carried out in such a manner so as to minimize the complicating effects of the heat of absorption so ably studied by King and Cassie [12] and others. In addition, as discussed by Barkas [2] for gels in general and more recently by Downes and Mackay [7] for wool, the relative importance of water diffusion and stress relaxation in the fiber as they affect the sorption process is further elucidated.

The absorption or desorption of a penetrant by a sorbent material has been termed integral sorption by Prager [20] and Kokes, Long, and Hoard [13] when the change of penetrant concentration at the boundaries of the sorbent is large. In order to obtain more accurate kinetic data in polymer–penetrant systems in which the coefficient of diffusion was concentration-dependent, Kokes, Long, and Hoard developed the technique of interval sorption. That is, the sorbent was equilibrated with penetrant and the concentration of the penetrant at the surface of the polymer changed by a small discrete step to the chosen final concentration. For a small change of penetrant concentration, the diffusion coefficient can be considered constant over the whole concentration range.

In view of the dependence of sorption behavior on penetrant concentration observed in this work for integral sorption steps in the wool–water system, it was considered advantageous to study the sorption behavior for small changes of water concentration over the entire concentration range. It has been established that only where the initial and final water concentrations are less than 2.5% regain is the uptake of water entirely a diffusion mechanism. The diffusion coefficients within this concentration region are given at various temperatures.

Experimental

Apparatus and Procedure

Measurements of regain changes were carried out on widely teased-out wool samples by use of a McBain-Bakr sorption balance consisting of a calibrated quartz spiral spring suspended inside a sorption chamber. Connected to the chamber were a wide bore differential mercury manometer and a large reservoir of 11 l. capacity. The apparatus was enclosed in an efficient air thermostat, the temperature of which was controlled to ±0.01° C. The whole apparatus could be evacuated to less than 10^{-3} mm. Hg through a liquid air trap. The water vapor pressure in the sorption chamber was changed as desired by opening the connecting tap to the reservoir, which was sufficiently large that vapor pressure change due to absorption or desorption from the wool was negligible.

Quartz springs of sensitivity of the order of 5 mm./mg. and cathetometers reading to 0.005 mm. were used, enabling weight changes of 0.001 mg. to be measured. Hence with wool samples as small as 10 mg., regain changes of 0.01% could be detected. Corriedale wool was taken from a fleece which has been used a great deal in this laboratory because of the uniformity of the fibers. The average dry diameter was 37μ. The wool was cleaned by several washings with cold petroleum ether followed by thorough rinsings with distilled water. The pH of the final rinse water was unaltered after standing in contact with the wool for several hours.

Heat of Wetting

Wool samples of widely separated fibers were used to minimize the effect of local temperature rise due to heat of absorption. Indeed, a calculation of this effect showed that, for the Corriedale fibers used and the dimensions of the wool sample and the sorption chamber, the rise in surface temperature could not be greater than 0.13° C. even for the largest relative humidity change of 0–100%. It was shown by experiment that only if the distance between the fibers was decreased by a factor of 10 could a slower rate of water uptake be observed on changing the relative humidity from 0 to 100%.

Direct measurements of the temperature inside the sorption vessel were made with a copper–constantan thermocouple. (These experiments have been reported by Nordon and Watt [18].) An initial rise of temperature within the sorption chamber was observed on admitting water vapor to the evacuated chamber even in the absence of wool, due to compression of the water vapor. The rise in temperature of 3° C. was almost immediate and the heat loss very rapid, so that the temperature returned to

within 0.1° C. of the equilibrium value within 2 sec. for large changes of relative humidity. For smaller changes of relative humidity, the effect was much reduced.

No evidence was found of a rise of temperature within a wool bundle due to the evolution of heat during absorption. That is, the fiber surroundings remained at the equilibrium temperature. Therefore it is assumed that any temperature effects are too small to affect the sorption behavior significantly and that the bundle of fibers would record the same sorption behavior as a single fiber or a thin film under the same conditions.

Results

Integral Sorption with High Humidities

The largest integral sorption step which can be applied in the wool–water system is achieved by changing the boundary concentrations of water between zero vapor pressure and saturation vapor pressure. In Figure 1, Curve A, the absorption of water is shown as a function of $(\text{time})^{\frac{1}{2}}$ when vacuum-dried wool is exposed rapidly to a saturated vapor pressure of water at 35° C. Curve B shows the corresponding desorption of water from wool when the water vapor pressure surrounding the wool is rapidly reduced to zero. The units of $(\text{time})^{\frac{1}{2}}$ were chosen for the abscissa in order to show more clearly deviations from Fickian diffusion behavior.

It will be noticed that there is an inflection in the absorption curve and that the initial rate of desorption is much faster than the initial rate of absorption. However, the time to dry the wool to the equilibrium dry weight is much greater than the time required to reach saturation equilibrium. The inflection in the absorption curve has not been previously reported for the wool–water system, and Haly and Roberts [9] claim that the uptake is linear against $(\text{time})^{\frac{1}{2}}$ until 12% regain has been absorbed. However, King [10] has reported inflections in the uptake vs. $(\text{time})^{\frac{1}{2}}$ curves of the wool–methanol and wool–ethanol systems.

Another prominent feature of the water absorption curve is that the uptake passes through a maximum of 35.4% regain before settling down to an equilibrium value of 33.6% regain. It was necessary to test whether this "overshoot" in the uptake curve was due to condensation on the wool. Therefore a series of large integral absorption steps were made from zero to high humidities but less than saturation vapor pressure. The uptake curves for four such integral absorptions at 35.0° C. are shown in Figure 2. It is apparent that the magnitude of the overshoot decreases as the final humidity of the absorption step is lowered. For a relative humidity change of 0–94.9% (Curve A) the maximum absorption was 29.1% regain and the equilibrium regain was 28.0%, showing an overshoot of 1.1% regain. For 0–90.4%

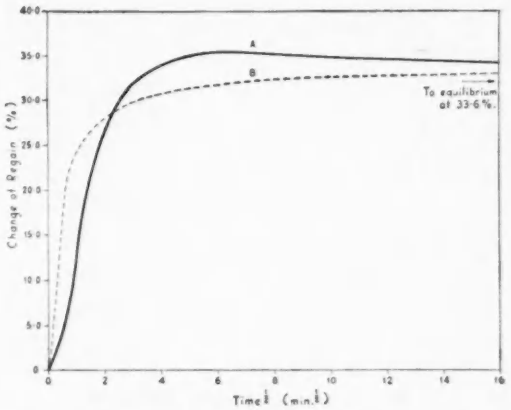

Fig. 1. Integral sorption at 35° C. Curve A: Change of regain vs. $(\text{time})^{\frac{1}{2}}$ following a relative humidity change from 0 to 100%. Curve B: Change of regain vs. $(\text{time})^{\frac{1}{2}}$ following a relative humidity change from 100% to 0%.

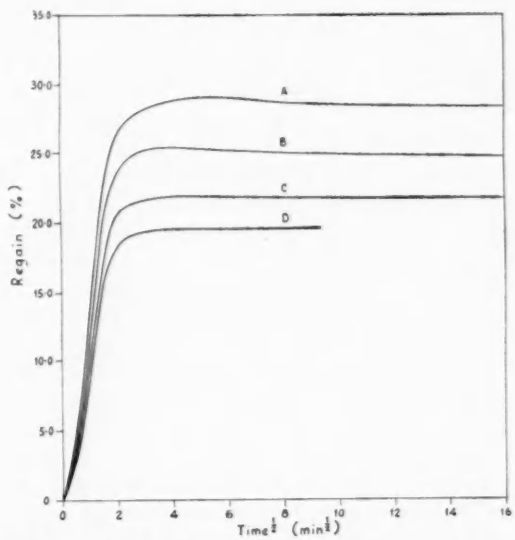

Fig. 2. Integral absorption at 35° C. Regain vs. $(\text{time})^{\frac{1}{2}}$ plots following relative humidity changes of Curve A: 0–94.9%; Curve B: 0–90.4%; Curve C: 0–85.4%; Curve D: 0–79.5%.

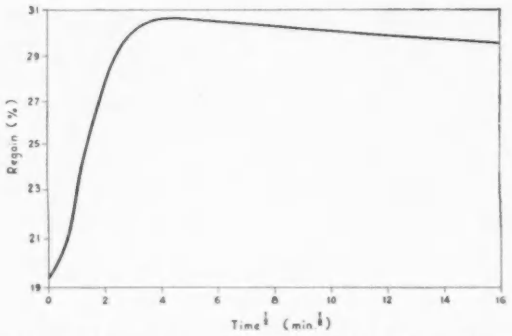

Fig. 3. Integral absorption at 35° C. Regain vs. (time)$^{\frac{1}{2}}$ following a relative humidity change from 79.4% to 94.8%. Equilibrium regain, 27.9%.

RH and 0–85.4% RH absorption steps (Curves B and C), the overshoot amounted to 0.6% regain and 0.2% regain respectively. No absorption overshoot could be detected for a relative humidity step of 0–79.5% (Curve D) or for any sorption steps in which the final water vapor concentration was less than 80% RH.

In order to test whether the appearance of an absorption overshoot was related to the magnitude of the concentration change, a wool sample which had been equilibrated with water vapor at 79.4% RH was subjected to a relative humidity of 94.8% (Figure 3). The absorption curve showed a marked inflection as a function of (time)$^{\frac{1}{2}}$ and an overshoot of the equilibrium uptake of 2.6% regain, which was much greater than the overshoot observed for a 0–94.9% RH absorption step.

Integral Sorption at Low Humidities

For integral absorption and desorption steps where the water vapor concentration is varied between dryness and progressively decreasing relative humidities, the inflection in the uptake vs. (time)$^{\frac{1}{2}}$ curve becomes less pronounced and the ratio of the initial rate of desorption to the initial rate of absorption becomes progressively less.

When the upper limit of humidity was 28.2% RH, the inflection in the absorption curve had almost disappeared, and the initial rate of desorption was nearly the same as the initial rate of absorption (Curves C and D of Figure 4). The regain change of 8.0% in the wool fibers for this relative humidity step is comparable with the regain change of 8.4% for the relative humidity step from 79.4% to 94.8% (cf. Figure 3).

Curves E and F of Figure 4 show the amount of absorption and desorption as a function of (time)$^{\frac{1}{2}}$ for the relative humidity limits of 0 and 11.0%. In each case the initial slope is linear, and the initial rate of desorption is less than the initial rate of absorption.

It is apparent from the foregoing that the kinetic behavior of sorption is dependent on the region of humidity in which the sorption step is made.

Interval Absorption

The criterion adopted for choosing the size of the concentration steps for interval sorption studies was that the form of the absorption curves would not be altered by further decreasing the size of the concentration changes. It was found that a change of concentration of not greater than 1% regain in the wool sample satisfied the above requirement for all initial regains.

Accordingly a wool sample was vacuum dried at 35° C. and taken to saturation regain with a series of 36 steps, the increase of water vapor pressure in each case being such that the equilibrium regain increment was not greater than 1%. The system was allowed to come to equilibrium after each concentration increment before proceeding with the next absorption step.

Figure 5 shows the very different shapes of the uptake curves as a function of (time)$^{\frac{1}{2}}$ obtained at five widely spaced initial regains. For simplicity only 5 of the 36 curves are shown. It can be seen that, at a low initial concentration (0.95% regain), the uptake of water is initially linear with (time)$^{\frac{1}{2}}$

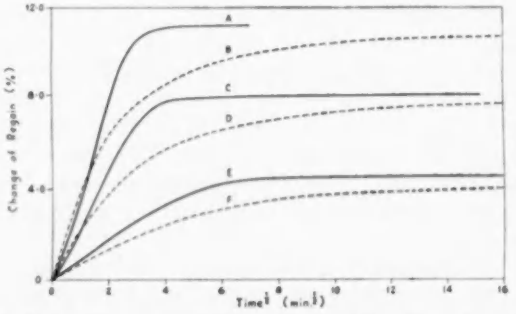

Fig. 4. Integral sorption at 35° C. Curves A, C, and E: change of regain vs. (time)$^{\frac{1}{2}}$ following relative humidity changes from 0 to 48.2%, 28.2%, and 11.0% respectively. Curves B, D, and F: change of regain vs. (time)$^{\frac{1}{2}}$ following relative humidity changes from 48.2%, 28.2%, and 11.0% respectively to 0.

(Curve A) and comes to equilibrium at 1.88% regain after (15 min.)$^{\frac{1}{2}}$.

At regains above 2.5%, the form of the interval uptake curve changed; the initial uptake of water was faster but the time to final equilibrium was longer. At higher concentrations the absorption occurred in two distinct phases, a fast initial uptake and a slow second stage. An increasing proportion of the uptake occurred in the second stage of absorption at higher initial regains and reached a maximum for an interval absorption from an initial regain of 11.59% to a final regain of 12.56% (Curve C of Figure 5). During the first stage of this absorption the uptake was 0.27% regain in 9 min. but reached final concentration equilibrium only after 5 days. The change in the form of the uptake curve with concentration is gradual and Curve B at an initial regain of 5.18% illustrates the transition from Curve A to Curve C.

At initial regains above 12.56% the proportional size of the second stage of absorption decreased, but the rate of uptake for this stage showed a decided increase (Curve D of Figure 5). For the interval step from an initial regain of 19.29%, the first stage of the uptake developed a sigmoidal shape as a function of (time)$^{\frac{1}{2}}$ and the second stage became so rapid that it was indistinguishable from the first stage. From an initial regain of 20.13%, the uptake passed through a maximum before settling to the final equilibrium value for the sorption interval. Similar absorption behavior was observed at all higher initial regains; Curve E of Figure 5 is typical of the absorption behavior observed in this high water concentration region. There is a marked similarity in the shape of this uptake curve for an interval absorption step and the uptake curve for an integral absorption step at high concentrations (cf. Figure 3). Further experiments showed that the form of the uptake curve was independent of the size of the concentration interval at high regains.

Interval Absorption at Low Water Vapor Concentrations

At a low concentration of water vapor the uptake vs. (time)$^{\frac{1}{2}}$ curve appeared linear initially; then the rate of uptake decreased. This is the form of uptake curve expected for Fickian diffusion into an infinite cylinder. Crank [4] has given mathematical solutions for the amount of penetrant entering or leaving a cylinder at any time following a change of surface concentration for a variety of conditions, providing that the diffusion is Fickian. The appropriate expression for the interval experiments of this paper is that obtained assuming that the surface concentration of water vapor was changed instantaneously to a constant value, the penetrant concentration through-

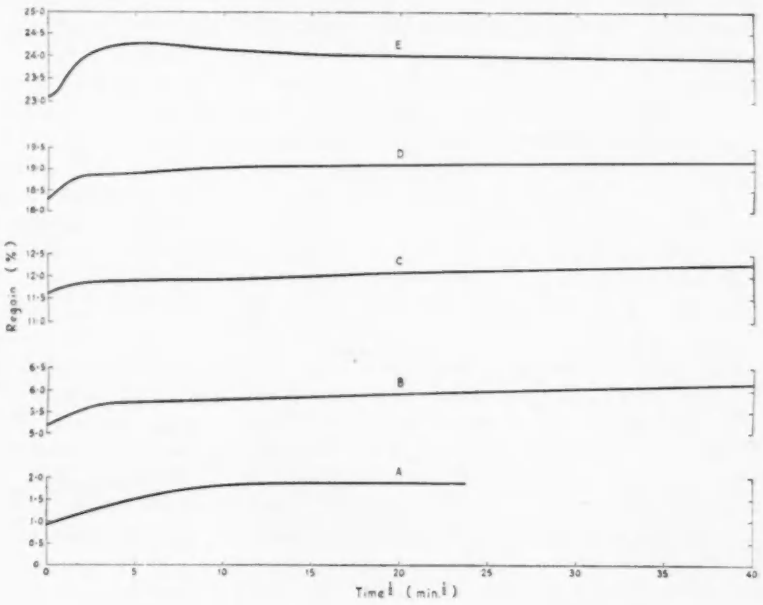

Fig. 5. Interval absorption at 35° C. Regain vs. (time)$^{\frac{1}{2}}$ plots for regain increments of <1% at various initial regains. Curve A: initial regain 0.95%; Curve B: initial regain 5.18%; Curve C: initial regain 11.59%; Curve D: initial regain 18.30%; Curve E: initial regain 23.11%. Curves B, C, D, and E are not shown to equilibrium.

TABLE I

Temperature, °C.	Concentration range, % regain	Diffusion coefficient D, cm.²/sec.
35.0	0 –0.76	1.23×10^{-10}
	0.76–1.22	1.72×10^{-10}
	1.22–1.70	2.03×10^{-10}
	1.70–2.20	2.36×10^{-10}
50.0	0 –0.78	3.10×10^{-10}
	0.78–1.31	4.14×10^{-10}
	1.31–1.69	5.13×10^{-10}
	1.69–2.37	6.03×10^{-10}
64.7	0 –0.51	5.62×10^{-10}
	0.51–0.90	6.51×10^{-10}
	0.90–1.21	7.68×10^{-10}
	1.21–2.01	9.37×10^{-10}
77.7	0 –0.72	1.03×10^{-9}
	0.72–1.10	1.36×10^{-9}
	1.10–1.76	1.64×10^{-9}

TABLE II

Temperature, °C.	Diffusion coefficient at zero regain, D_0
35.0	$1.0 \pm 0.05 \times 10^{-10}$ cm.²/sec.
50.0	$2.35 \pm 0.1 \times 10^{-10}$ cm.²/sec.
64.7	$4.7 \pm 0.2 \times 10^{-10}$ cm.²/sec.
77.7	$8.3 \pm 0.2 \times 10^{-10}$ cm.²/sec.

out the cylinder was initially uniform, and the diffusion coefficient was constant over the small concentration interval. A plot of the uptake as a function of $(\text{time})^{\frac{1}{2}}$ using the appropriate Crank's equation is in excellent agreement with Curve A of Figure 5.

The coefficients of diffusion D for the small range of concentration where the sorption mechanism appeared Fickian were calculated from the rates of absorption over small concentration intervals at four temperatures. The values obtained are given in Table I.

It can be seen that the diffusion coefficients are dependent on concentration. The values of the diffusion coefficients were plotted against the mid-value of the concentration range over which they were measured. For the concentration range of 0–2% regain the variation of D with concentration is almost linear, and it was possible to extrapolate to zero regain using the line of best fit obtained by the "method of least squares." The intercepts on the ordinate at zero regain were taken as estimates of the values of the diffusion coefficient (D_0) for each temperature (see Table II). The limits shown were derived from the standard error of the slope of the regression of diffusion coefficient on concentration.

Calculation of the activation energy of diffusion from the values of the diffusion coefficient at zero regain, D_0, gives a value >11 kcal./mole.

Discussion

The sorption kinetics of the integral experiments presented in this paper show marked dependence on the regain region over which the sorption occurs. Similarly, the kinetics of absorption observed for interval experiments varies greatly according to the initial regain of the wool fibers.

The sensitivity of the sorption behavior to the concentration of water in the fibers suggests that, for an integral step in which the difference between initial and final concentrations is large, the distribution of penetrant concentration within the fibers at any particular time would have an important bearing on the subsequent sorption behavior.

An inflection in the absorption curve as a function of $(\text{time})^{\frac{1}{2}}$ and a greater rate of desorption compared to the rate of absorption has been observed in a number of polymer–penetrant systems. It has been shown by Crank and Park [5] that no generalized form of Fick's diffusion equation is adequate to describe the whole course of the sorption. Cassie [3] demonstrated that the mechanical properties of the wool fibers are a complicating feature of the equilibrium sorption values. It is also probable that the anomalous kinetics observed are related to the complex internal structure changes.

Long, Bagley, and Wilkins [15] showed that for the anomalous cellulose acetate–acetone system there were in fact two distinct processes of sorption if the penetrant concentration was changed by small intervals. The kinetics of the first stage of sorption obeyed Fick's laws, but it was demonstrated by Long and Watt [14] that the second stage did not occur by a diffusion-controlled mechanism. Bagley and Long [1] proposed that sorption in this second stage occurred as a result of the breaking of interchain bonds which had been strained by the entry of penetrant during the first stage of sorption. Downes and Mackay [7] obtained two-stage sorption for small changes of humidity in the wool–water system and concluded that wool behaved as a polymer below its second order transition temperature, with respect to sorption of water vapor. A coupled diffusion–

relaxation mechanism has been put forward by Newns [17] as an explanation of anomalous sorption by polymers below their second order transition temperature.

The results presented in this paper show that the extent of the deviation of sorption behavior from Fickian diffusion is dependent on the concentration of water in the wool fibers. As anomalous sorption has been associated with two mechanisms of sorption, it is probable that the relative importance of each mechanism changes with the concentration of the water in the wool.

The interval absorption uptake curves fall into three categories according to the concentration of water in the wool fibers: (a) at low concentrations of water (<2.5% regain) the absorption obeys Fick's laws; (b) the appearance of a relaxation mechanism in addition to the diffusion-controlled mechanism for absorptions to a final concentration above 2.5% regain; (c) an overshoot of the equilibrium regain for absorption steps to concentrations above 20% regain.

The appearance of an overshoot of uptake for absorption to high regains is not to be expected as a result of either a diffusion or a stress relaxation mechanism. However, these observations are consistent with the idea put forward by Feughelman [8] that, following absorption to high regains, a sol–gel transformation takes place. That is, most of the weak interchain bonds are broken by the initial inrush of water but some later re-form, giving the fiber increased rigidity. This re-formation of bonds could cause the exclusion of some of the previously absorbed water. It is proposed to leave further discussion of the causes of absorption overshoots until a more detailed study has been made.

Interval absorption to a final concentration above 2.5% regain cannot be fitted by the equation given by Crank [4] for penetrant uptake due to Fickian diffusion; uptake of water vapor continues for a longer time than would be expected if the sorption were only diffusion-controlled.

For initial water concentrations in the wool higher than 15% regain, the rate of the second stage of absorption became comparable with the first-stage absorption rate. It is probable, therefore, that although the uptake curve at high regains shows no discontinuity, the mechanism of absorption is a combination of the two distinct mechanisms of absorption operative at lower concentrations, i.e., a diffusion mechanism and a stress relaxation mechanism. At high concentrations of water, the uptake curves for interval sorptions have a form similar to the integral absorption curves, and the mechanism of sorption appears to be independent of the size of the concentration interval.

Only at low regains can the rate of absorption of water into wool be termed entirely diffusion-controlled. The value of $D_0 = 1.0 \times 10^{-10}$ cm.^{2}/sec. at 35° C. for the diffusion coefficient at zero regain is a factor of 10 lower than the value of $D \approx 10^{-9}$ cm.^{2}/sec. for low regains obtained by King [10, 11] from absorption of water into horn keratin and the permeability of horn keratin to water vapor at 25° C. It is not possible to make a direct comparison of these values without knowing the absorption interval over which King made his measurements or the lowest regains at which the permeability measurements were made. However, the magnitude of the difference suggests that the coefficient of diffusion of water into wool is less than the coefficient of diffusion of water into horn keratin at low regains.

The value of more than 11 kcal./mole for the activation energy of diffusion near zero regain is higher than the values in the literature for the activation energy of diffusion at higher regains. However, it is in agreement with the finding of Watt, Kennett, and James [22] that the total energy required to remove water molecules from wool fibers increased rapidly with decreasing regain at low regains and reached a value of 15 kcal./mole near zero regain. From measurements with acetylated wool they concluded that this high energy of activation in the later stages of desorption was associated with the removal of water from hydrophilic side chains. Similarly, it is probable that the high energy of absorption at low regains indicates that the mechanism of absorption involves the attachment of water molecules to hydrophilic side chains within the wool fibers. This is in agreement with the mechanism proposed by Pierce [19] for cotton fibers and by Speakman [21] for wool fibers from analyses of the appropriate sorption isotherms. The idea that some of the water molecules are bound to hydrophilic sites has been proposed for a number of proteins from equilibrium sorption data; these mechanisms are the subject of an excellent review by McLaren and Rowen [16].

Many polymer–penetrant systems reported in the literature appear anomalous in their diffusion behavior even at low penetrant concentrations. It is

probable that it is the diffusion of the water molecules through the wool fibers to the hydrophilic side chains which follow Fickian laws. It appears that there is not sufficient strain set up in the fibers to cause additional absorption as a result of stress relaxation of the fibers, as may occur at higher regains.

Acknowledgment

I should like to thank my colleagues for their many helpful discussions during the course of this work.

Literature Cited

1. Bagley, E. and Long, F. A., *J. Am. Chem. Soc.* **77**, 2172 (1955).
2. Barkas, W. W., "Swelling Stresses in Gels," Forest Products Research Special Report No. 6, H.M.S.O. (1945).
3. Cassie, A. B. D., *Trans. Faraday Soc.* **41**, 458 (1945).
4. Crank, J., "Mathematics of Diffusion," Oxford, 66 (1956).
5. Crank, J. and Park, G. S., *Trans. Faraday Soc.* **47**, 1072 (1951).
6. Downes, J. G. and Mackay, B. H., *Proc. 1st Int. Wool Text. Res. Conf. Aust.* (1955).
7. Downes, J. G. and Mackay, B. H., *J. Polymer Sci.* **28**, 45 (1958).
8. Feughelman, M., *J. Appl. Polymer Sci.* **2**, 189 (1959).
9. Haly, A. R. and Roberts, N. F., *Proc. 1st Int. Wool Text. Res. Conf., Aust.* (1955).
10. King, G., *Trans. Faraday Soc.* **41**, 325 (1945).
11. King, G., *Trans. Faraday Soc.* **41**, 479 (1945).
12. King, G. and Cassie, A. B. D., *Trans. Faraday Soc.* **36**, 445 (1940).
13. Kokes, R. J., Long, F. A., and Hoard, J. L., *J. Chem. Phys.* **20**, 1711 (1952).
14. Long, F. A. and Watt, I. C., *J. Polymer Sci.* **21**, 554 (1956).
15. Long, F. A., Bagley, E., and Wilkins, J., *J. Chem. Phys.* **21**, 1412 (1953).
16. McLaren, A. D. and Rowen, J. W., *J. Polymer Sci.* **7**, 289 (1951).
17. Newns, A. C., *Trans. Faraday Soc.* **52**, 1533 (1956).
18. Nordon, P. and Watt, I. C., *J. Polymer Sci.* **43**, 267 (1960).
19. Pierce, F. T., *J. Textile Inst.* **20**, T133 (1929).
20. Prager, S., *J. Chem. Phys.* **19**, 537 (1951).
21. Speakman, J. B., *Trans. Faraday Soc.* **40**, 6 (1944).
22. Watt, I. C., Kennett, R. H., and James, J. F. P., TEXTILE RESEARCH JOURNAL **29**, 975 (1959).

Manuscript received November 9, 1959.

An X-Ray Study of Acetylated Jute

S. C. Roy

Indian Jute Mills Association Research Institute, Calcutta–27, India

Abstract

X-ray results for progressively acetylated jute fibers are described. The diffraction pattern of partially acetylated jute has certain features in common with that of a similarly treated pure cellulose fiber such as ramie or cotton, but the intense equatorial reflection characteristic of the acetyl cellulose appears to be absent in it. At highest acetyl content, the x-ray photograph of jute is closely similar to that of cellulose triacetate I, and the transformation to the new lattice appears as complete as in a pure cellulose fiber. The two large spacing equatorial reflections A_x and A_y show improved sharpness and intensity as well as increased spacing on the partially acetylated jute diagram but are absent in the fully substituted one. The results are discussed in the light of the structure of jute.

Introduction

The effect of acetylation on the x-ray structure of cellulose fibers has been studied by various workers [2, 3]. We leave aside the controversy [2, 3, 4] regarding the course of acetylation; the results generally indicate that when native cellulose is used as the starting material, the first acetate formed is triacetyl cellulose I. If the swelling is sufficiently great, then the structure I is transformed into II, the latter being the more stable form. With increasing acetyl content, the oblique reflections become more diffuse, while the meridian reflections remain clear and sharp; the equatorial reflections gradually disappear and new spots appear; finally, a new lattice is formed. Opinions differ [4] whether form I is to be regarded as a distorted lattice or should be given the status of a modification. According to a recent report [13], however, both the triacetates I and II are stable crystalline modifications, although the latter is the preferred structural form. The partially acetylated cellulose shows the two phases, triacetyl cellulose I and unchanged native cellulose.

In view of these results for pure cellulose fibers, an x-ray study of progressively acetylated jute seems worthwhile. Since the transformation of cellulose I to cellulose II is not complete under normal conditions of mercerization of jute [5, 9], it may be interesting to follow the transformation of jute cellulose to a new lattice during the process of acetylation. Also, an examination of the influence of the acetyl groups on the two large-spacing reflections A_x and A_y of jute [9] may lead to further elucidation. Two different views [6, 9, 10, 14] have been taken regarding the origin of these reflections. According to one, the reflections are due to the formation of reversible pseudocrystalline swelling compounds by the chain molecules in the initially noncrystalline regions through the orienting agency of water molecules, while the other regards them to originate from crystalline areas which may, of course, be in a state of imperfection.

Experimental

A good quality white jute of East Bengal origin was extracted in alcohol–benzene mixture (ratio 1:2). This is usually designated as defatted and sometimes referred to as native jute. As samples of pure cellulose fibers for comparison, commercially degummed ramie and cotton (of Egyptian origin), lightly scoured by boiling in 2% caustic soda solution, were employed. The fibers (jute, ramie, and cotton) were acetylated in glacial acetic acid medium using acetic anhydride as the acetylating agent and perchloric acid as a catalyst. The methods used for acetylation and the estimation of acetyl content were as described in a previous communication [11] from this Institute. The deacetylation of native jute was done as suggested by Bhattacherjee and Callow [1].

The x-ray patterns were taken with nickel-filtered CuK α-radiation from a demountable filament type (Raymax) tube operated at 30 kv. and 20 ma. The collimators, one 6.5 cm. long and 0.4 mm. in bore and another 5 cm. long and 0.25 mm. in bore, were made of lead glass capillary tubing. The specimen-

to-film distance was approximately 3 cm. and the exact value was calculated from the known spacing of the 020 reflection of cellulose, the latter being regarded to have remained unchanged by the treatments. All the photographs were taken at 65–70% RH and 80° F.

Results

Figures 1–10 represent the x-ray photographs of native and treated fibers; the relevant (equatorial) spacing values are given in Tables I and II, the results for cellulose triacetate II reported by Happey [2] being included in the latter. The acetyl content is expressed as follows:

$$\text{Acetyl content} = \frac{\text{Wt. of acetyl groups } (CH_3CO—)}{\text{Wt. of dry fiber}} \times 100$$

It will be seen that the diagrams for partially acetylated jute and partially acetylated pure cellulose

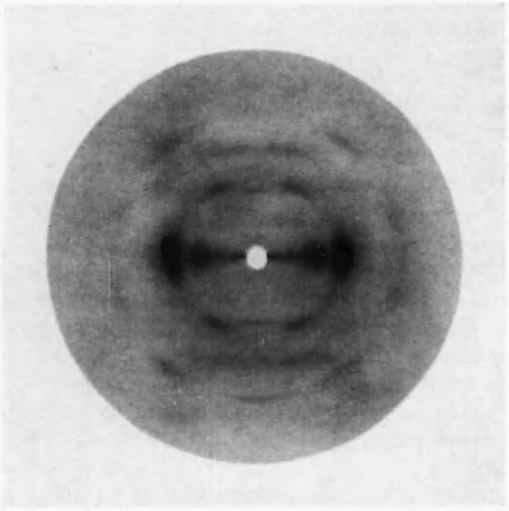

Fig. 1. X-ray photograph of native jute (AC = 4.7%).

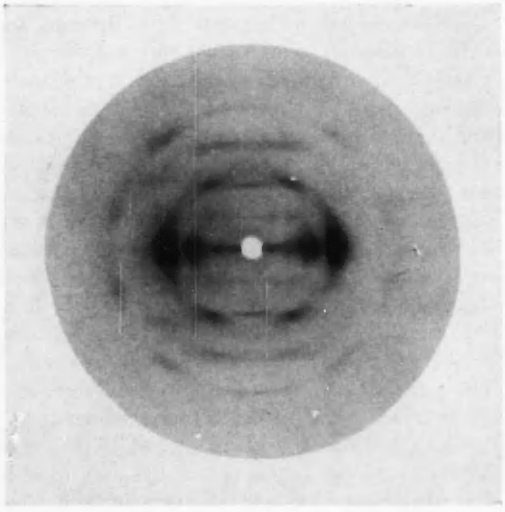

Fig. 2. Deacetylated jute (AC = 0%).

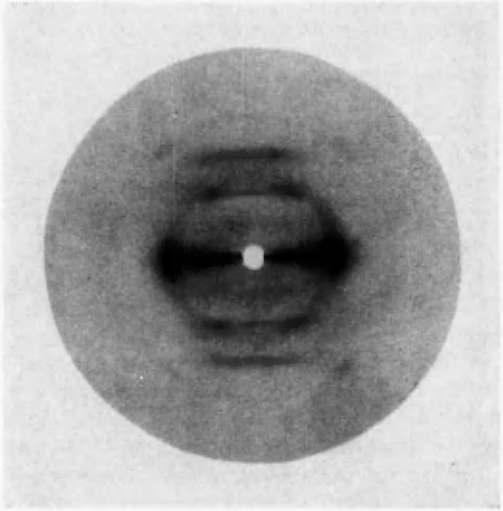

Fig. 3. Partially acetylated jute (AC = 28.4%).

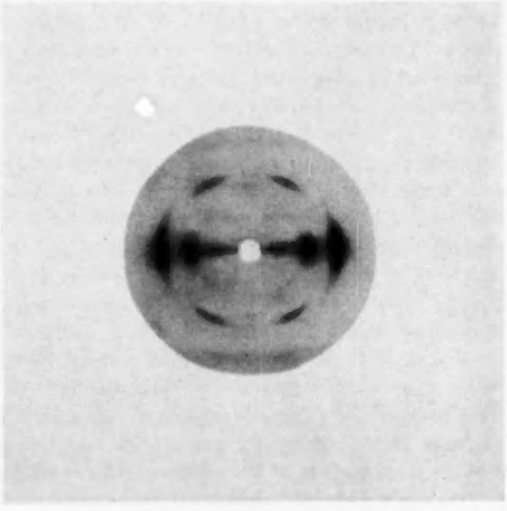

Fig. 4. Native ramie.

fibers, ramie and cotton (Figures 3, 5, and 6), have certain features in common: a diminution in intensity and increased diffuseness of the main reflections, a marked increase in sharpness and clarity of the meridian reflections, and a slight disorientation of the main diffraction arcs (this is just noticeable in jute but more prominent in ramie). On the other hand, the innermost equatorial reflection, A_c, characteristic of acetyl cellulose as found in ramie and cotton, is not observable in the jute photograph. The other special feature of the partially acetylated jute is the marked improvement in sharpness and intensity and increased spacing values of the reflections A_x and A_y (Table I and Figures 1 and 3).

At higher degrees of acetylation, particularly at maximum acetyl content (Figure 9), the changes in the x-ray pattern of jute appear to be almost similar to those reported for pure cellulose triacetate [2]. It is noted, however, that while the photograph for fully acetylated jute (Figure 9) compares fairly closely with that of cellulose triacetate I as regards the orientation and intensity of both the polar and the

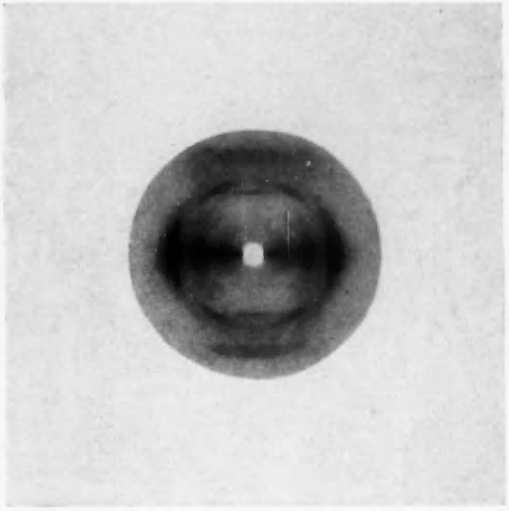

Fig. 5. Partially acetylated ramie (AC = 28.0%).

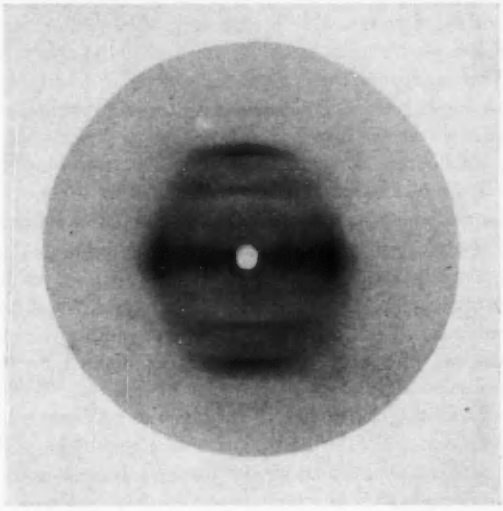

Fig. 7. Partially acetylated jute (AC = 51.1%).

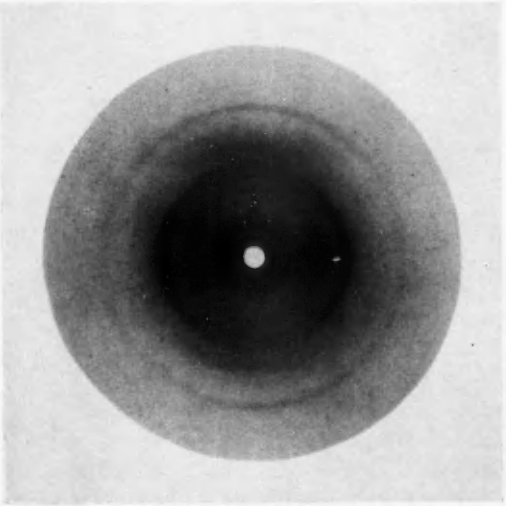

Fig. 6. Partially acetylated cotton (AC = 32.1%).

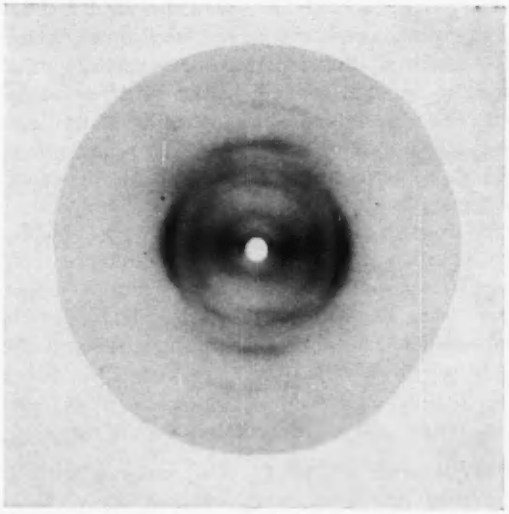

Fig. 8. Partially acetylated ramie (AC = 52.6%).

equatorial reflections, the spacing values of the equatorial reflections of jute are in agreement with those of cellulose triacetate II, reported [2] to have been obtained from highly oriented cellulose II as the starting material (Table II). In addition, the equatorial reflections of the jute diagram appear to show improved resolution when compared with the corresponding spots in the pure cellulose triacetate I photograph. This indicates that upon acetylation by a method as reported in this work, the transformation of jute cellulose I to cellulose triacetate is as complete as in a pure cellulose fiber such as ramie or flax of comparable orientation, although in view of the observation by Sprague et al. [13], particularly as regards the presence of the 8.3 Å and 6.6 Å spacings, one is not sure, until further evidence, whether the transformation in jute is to form I or II. In this connection, it may be noted that the complete transformation of jute cellulose I to cellulose triacetate is at variance with the incomplete mercerization of jute in alkali under normal conditions. Accepting that the latter is due to a restraint in the fiber structure arising from the strong linkage between lignin and cellulose [5, 9], one would presume that the same (i.e., restraint) is eliminated in the course of acetylation so as to enable the chain molecules in the crystallites to assume the required configuration. While the action of the perchloric acid (used as a catalyst in small quantity) in this regard is not known, it has been observed that jute treated in 60% perchloric acid (Merck) at room temperature (80° F.) for 10 min., washed neutral, and air-dried gives a completely mercerized diagram (Figure 10) similar to that reported for ramie [2] which obviously indicates the elimination of the restrictive influence responsible for incomplete mercerization of jute cellulose I. Furthermore, the reflections A_x and A_y, so prominent in the initial stages of acetylation of jute, are not observable in the fully substituted diagram (Figures 3 and 9). It is possible that the reflection A_y is obscured by the presence of the very strong spot A_c because of the latter's spacing value being close to it (Tables I and II), but the same is not true for A_x, which should be regarded as truly absent.

Discussion

The absence of the 11 Å spacing in partially acetylated jute is an interesting fact, but no satisfactory explanation can be given here. One possibility is that the chain molecules of jute cellulose are not equally free to undergo a configurational change as in ramie or cotton. A rigidity of the jute structure has also been suggested from the study of the kinetics of acetylation [11] and is frequently indicated by its swelling behavior [7, 8, 12]; the origin of this rigidity has often been traced to the strong association between cellulose and lignin [5, 9]. The question that the degree of acetylation considered here refers only to the amorphous regions which are

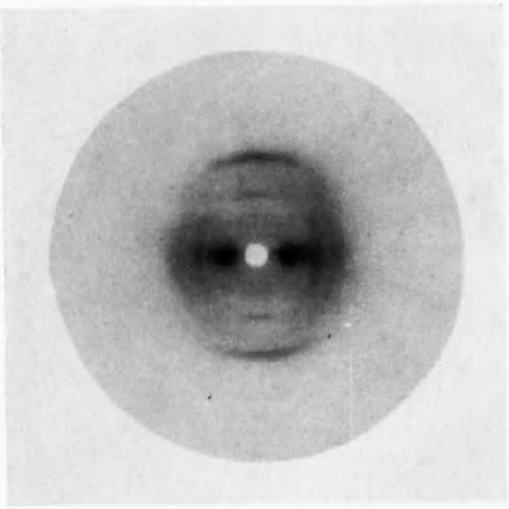

Fig. 9. Highly acetylated jute (AC = 69.5%).

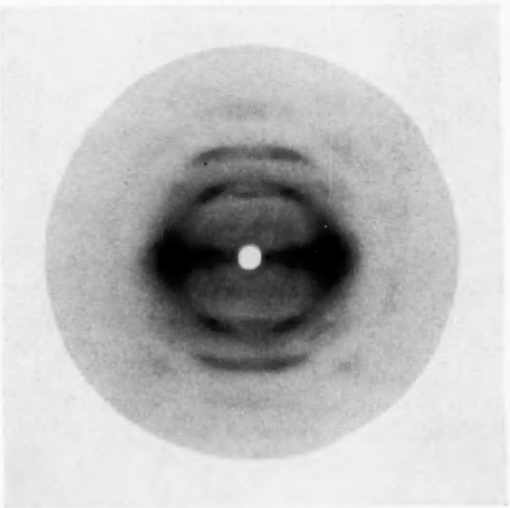

Fig. 10. Jute mercerized by treatment with 60% perchloric acid (Merck) at 26° C. for 10 min.

TABLE I. Equatorial Reflections of Native and Deacetylated Jute and Partially Acetylated Jute and Ramie

Designation	Native jute (AC = 4.7%) Spacing, Å	Intensity*	Deacetylated jute (AC = 0%) Spacing, Å	Intensity*
A_x	14.7	m	14.7	m
A_y	9.7	w	9.6	w
101	6.1	vs	6.1	vs
10$\bar{1}$	5.4	vs	5.4	vs
002	4.0	vvs	4.0	vvs

Designation	Partially acetylated jute (AC = 28.4%) Spacing, Å	Intensity*	Partially acetylated ramie (AC = 28.0%) Spacing, Å	Intensity*
A_x	15.8	ms	absent	
A_c	absent		11.1	vvs diff
A_y	10.4	m	absent	
101	7.3	s	6.0	vs
10$\bar{1}$	5.5	vs	5.3	vs
002	4.0	vvs	3.9	vvs

* Visual observation: v = very, s = strong, m = medium, w = weak, and diff = diffuse.

TABLE II. Equatorial Reflections of Fully Acetylated Jute and Crystalline Cellulose Triacetate II

Designation	Fully acetylated jute (AC = 69.5%) Spacing, Å	Intensity*	Crystalline cellulose triacetate II [2] Spacing, Å	Intensity*
A_x	absent		—	—
A_c	11.2	vvs	10.6	vvs
A_y	absent		—	—
A_4	8.3	vs	8.4	vs
A_5	6.6	vs	6.7	vs
A_6	5.4	s	5.4	diff s
A_7	4.2	ms	4.8	m
A_8	3.8	ms	4.3	m
A_9	—	—	3.4	ms diff

* Visual observation: v = very, s = strong, m = medium, w = weak, and diff = diffuse.

in excess in jute [11] does not seem to arise, since the effect on the crystalline areas is clearly indicated by the changes in both the polar arcs and the other main reflections. A smaller decrease in orientation of the equatorial reflections of jute also points to a rigid framework of the fiber. It may be stated that while we take note of the changed spacing value of the 101 reflection of (partially acetylated) jute (Table I), a further discussion of the point is not pursued in this communication.

The effect of acetylation on the reflections A_x and A_y of jute appears to be particularly interesting. Whereas an increase in the intensity and spacing of these reflections was previously observed as due to water molecules, their improved sharpness and intensity as well as enlarged spacing as found in the partially acetylated jute diagram of the present experiment (Figure 3 and Table I) are obviously to be ascribed to the acetyl radicals. It may be mentioned in this connection that acetylation of jute leads to as reduced hygroscopicity as that of ramie or cotton. One may, however, argue that the changes occurring to the reflections on partial acetylation refer to the noncrystalline regions similar to those suggested to have been produced by water molecules. In that case, it may be that a part of their intensity in native jute at ordinary humidity is due to the natural acetyl content, which is about 4–5%. No change is, however, observed in A_x and A_y following deacetylation of native jute (Figure 2 and Table I). It is, therefore, rather unlikely that the acetyl groups, either being present in the original fiber or introduced in the process of acetylation, could effect an *ad hoc* crystallization in the originally noncrystalline areas. Moreover, if the reflections A_x and A_y are assumed to belong to the originally noncrystalline areas, one should rather expect that they remain unaffected when the native cellulose transforms into the acetyl structure, provided, of course, one rules out the possibility of formation of pseudocrystallites through the agency of the acetyl radicals in a similar manner as through water molecules and their subsequent participation in the transformation to acetyl structure along with the native cellulose crystallites. On the other hand, the changes occurring to these reflections at lower degrees of acetylation and their absence in the fully acetylated diagram may be taken to indicate that they are involved in the transformation, which can apparently be explained by assuming a crystalline origin for them.

Acknowledgment

The author wishes to thank Dr. W. G. Macmillan, Research Director, Indian Jute Mills Association Research Institute, for permission to publish the results; Dr. M. K. Sen, Chief Physicist, for helpful discussion; and Mr. M. Ramaswamy, formerly of the Physics Department, for assistance in the preparation of the acetylated samples.

Literature Cited

1. Bhattacherjee, H. P. and Callow, H. J., *J. Textile Inst.* **43**, T53 (1952).
2. Happey, F., *J. Textile Inst.* **41**, T381 (1950).
3. Hess, K. and Trogus, C., *Z. Physik Chem.* **B15**, 157 (1932); *Ergebn Tech. Rontgenk* **4**, 21 (1934).
4. Meyer, K. H., "Natural and Synthetic High Polymers," edited by H. Mark, New York, Interscience Publishers, Vol. 4, 315 (1942).
5. Mukherjee, R. R. and Woods, H. J., *J. Textile Inst.* **41**, T422 (1950).
6. Mukherjee, R. R., Ph.D. Thesis, Leeds University (1949).
7. Roy, M. M. and Sen, M. K., *J. Textile Inst.* **43**, T396 (1952).
8. Roy, S. C. and Sen, M. K., *J. Textile Inst.* **50**, T640 (1959).
9. Sen, M. K. and Woods, H. J., *Biochim. Biophys. Acta* **3**, 510 (1949).
10. Sen, M. K. and Roy, S. C., *Nature* **173**, 298 (1954).
11. Sen, M. K. and Ramaswamy, M., *J. Textile Inst.* **48**, T75 (1957).
12. Sen, M. K. and Hermans, P. H., *Rec. Trav. Chim. Pays-Bas* **68**, 1079 (1949).
13. Sprague, B. S., Riley, J. L. and Noether, H. D., TEXTILE RESEARCH JOURNAL **28**, 275 (1958).
14. Warwicker, J. O., Wellard, H. J., and Woods, H. J., *Nature* **174**, 135 (1954).

Manuscript received September 1, 1959.

Behavior of Sample Pleated Strips of Wool Fabric in an Extensometer

Part II: Modifications Due to Pleat Curvature and Other Second Order Effects

H. W. Holdaway

C.S.I.R.O. Wool Research Laboratories, Division of Textile Physics, Ryde, N.S.W., Australia

Abstract

The simple theoretical model previously considered [1] was inadequate in some respects to provide a complete account of the observed elasto-mechanical behavior of a pleat when extended. Factors now included are the radius of curvature at the pleat and the variation in fabric stiffness as a function of tension. The use of additional parameters to take account of these effects permits a very good description of the observed behavior. Values of "initial pleat angle" and "initial fabric stiffness" can be determined from experimental results of longitudinal extension and lateral deflection as a function of load.

Introduction

In a previous paper, a description was given of a simple theoretical model to explain the elasto-mechanical behavior of a pleat in an extensometer. It was found experimentally that the first order behavior could be satisfactorily related to this "ideal pleated-elastica" model.

It was also noted that some departures occurred at higher load values; to a lesser extent for those pleats which had been given longer times of treatment during their formation. Qualitatively, these departures could be explained by a finite rather than infinite curvature in the immediate proximity of the pleat. In this study a mathematical analysis is made of the effect of finite pleat curvature; an allowance is made for a small variation of fabric stiffness with tension.

The application of additional terms based upon the above-mentioned analysis was found to lead to a very good representation of experimental results over the same range of tensions as employed previously [1]. By employment of some of the parameters used to fit the data by the method of least squares, estimates could be made of both the initial pleat angle[1] and initial fabric stiffness.[1]

[1] Extrapolated to zero tension.

Extension of Previous Theory to Include Second-Order Effects

The elastica model now to be employed is shown diagrammatically in Figure 1. For simplicity the diagram has been turned through 90° so that the tension P is shown acting horizontally. For convenience, gram-centimeter units are employed, as in the previous paper [1]. The essential point of departure from this earlier treatment is in no longer regarding the deflection angle γ as constant. A central section CD of the pleat proper is assumed to be bent to a radius of curvature ρ_0 under no tension. If the bending moment is assumed to be constant over CD, the latter opens to a radius of curvature ρ (a function of the tension) under the conditions illustrated in Figure 1. To simplify exposition, the radius of curvature ρ is considered to remain quite small, and as a consequence the contribution to the deflection caused by the opening out of CD itself is neglected compared with those effects which are due to the consequent variability of the pleat angle γ.

To describe the quality of a pleat satisfactorily the two parameters necessary are the initial radius of curvature ρ_0 and the initial pleat angle γ_0, both corresponding to (or extrapolated to) the zero tension condition.

The changing values of ρ may be related to the local value of bending-moment at the apex of the pleat, if the local value of fabric stiffness is known. For simplicity the local stiffness will be taken as being the same as in the remainder of the pleat. The modifications needed to include the effect of a local stiffness change are readily introduced if desired. Since, however, the resulting parameter is always associated with the parameter ρ_0, this effect may be regarded as being absorbed in the latter.

Analytical expressions based upon the ideal pleated-elastica [1] are still valid for sections AC and BD. These are, with the same equation numbers as used previously,

$$l_0 - \frac{d+e}{1+\alpha P} = 4 \operatorname{versin}\left(\frac{\gamma}{4}\right)\cdot\sqrt{\frac{S}{P}} \qquad (1)$$

and

$$Y = 2\sin\left(\frac{\gamma}{4}\right)\cdot\sqrt{\frac{S}{P}} \qquad (2)$$

An approximate allowance can be made for stretch in the arc CD, as a result of which we deduce the relationship

$$\gamma\rho = \gamma_0\rho_0(1+\alpha P) \qquad (3)$$

in which $\alpha P \ll 1$. The stretch in the fabric results in a thickness reduction and consequent reduction in stiffness. Again, some account is taken of this by writing $S = S_0(1-\beta P)$ and $\sqrt{S} = \sqrt{S_0}(1-\frac{1}{2}\beta P)$,[2] where $\beta P \ll 1$.

From the definition of fabric stiffness

$$P(h+Y) = S\left(\frac{d\psi}{ds}\right)_{C \text{ or } D} = S\left(\frac{1}{\rho_0} - \frac{1}{\rho}\right) \qquad (4)$$

and from the theory of the pleated elastica [1] it is possible to deduce the relationship

$$P(h+Y) = 2\sqrt{PS}\sin\frac{\gamma}{4} \qquad (5)$$

wherein the error of approximation is of the same order as the errors of approximation in Equations 1 and 2. These errors are negligible for practical purposes. Equations 3, 4, and 5 can be combined into the single equation

$$2\sqrt{PS}\sin\frac{\gamma}{4} = \frac{S}{\gamma_0\rho_0}\left(\gamma_0 - \frac{\gamma}{1+\alpha P}\right) \qquad (6)$$

Equation 6, apart from the relatively minor modification for variation of stiffness with tension, may be regarded as containing all the information essential to the revised version of the pleated elastica. It should be taken in conjunction with Equations 1 and 2 to determine the now unknown deflection angle γ which appears therein. Since we are not primarily concerned with evaluating γ as such, the problem may be reformulated as the elimination of γ from Equations 6, 1, and 2 to obtain two equations for e and Y.

[2] Although stiffness could be expected to vary with tension variations along the elastica, the *small* effect is allowed for by averaging in this way.

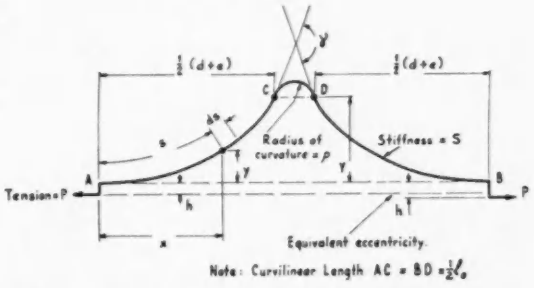

Fig. 1. Pleated-elastica model with finite pleat curvature.

Owing to the nonlinear character of Equation 6 in terms of γ, this process cannot be directly achieved. Equation 6 may, however, be linearized for a moderate range of variation of γ, which we do by introducing a new variable v defined by the equation

$$\frac{\gamma}{4} = \theta + v \tag{7}$$

where θ is a value of $\gamma/4$ at some point in a linearizing range over which v may take small positive or negative values. Equations 1, 2, and 6 may then be rewritten using first order approximants, which are valid provided v is small. The process of eliminating γ now becomes that of eliminating v in the restated Equations 1, 2, and 6. When the variation in stiffness with tension is taken in account, the relationships obtained reduce to the form (provided $\frac{1}{2}\rho_0\gamma_0 \cos\theta\sqrt{P/S} \ll 1$),

$$l_0 - \frac{d+e}{1+\alpha P} = \frac{A}{\sqrt{P}} + B\sqrt{P} - C \tag{8}$$

and

$$Y = \frac{D}{\sqrt{P}} + E\sqrt{P} - F \tag{9}$$

after neglect of small product terms which lead to expressions in P, $P^{\frac{1}{2}}$, etc. The expressions obtained for these parameters are

$$A = 4\left\{\text{vers}\,\theta + \left(\frac{\gamma_0}{4} - \theta\right)\sin\theta\right\} S_0^{\frac{1}{2}} \tag{10}$$

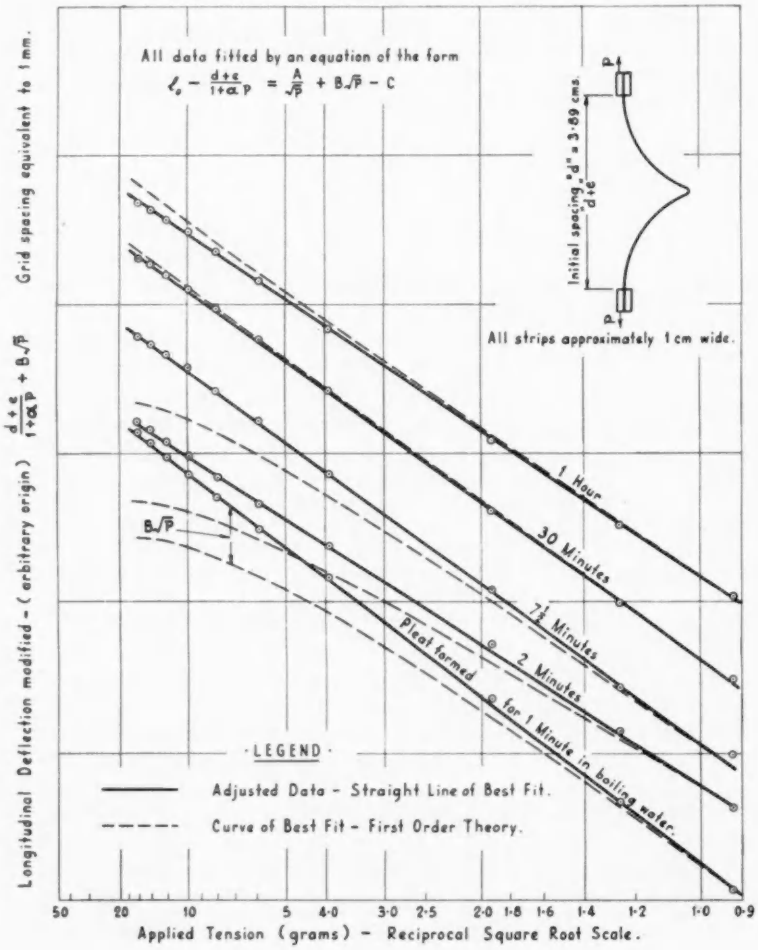
All data fitted by an equation of the form
$l_0 - \frac{d+e}{1+\alpha P} = \frac{A}{\sqrt{P}} + B\sqrt{P} - C$
Initial spacing "d" = 3·69 cms.
d+e
All strips approximately 1 cm wide.
1 Hour
30 Minutes
7½ Minutes
2 Minutes
Pleat formed for 1 Minute in boiling water.
B√P
·LEGEND·
Adjusted Data - Straight Line of Best Fit.
Curve of Best Fit - First Order Theory.
Longitudinal Deflection modified - (arbitrary origin) $\frac{d+e}{1+\alpha P} + B\sqrt{P}$
Grid spacing equivalent to 1 mm.
50 20 10 5 4·0 3·0 2·5 2·0 1·8 1·6 1·4 1·2 1·0 0·9
Applied Tension (grams) - Reciprocal Square Root Scale.

Fig. 2. Typical graphs of extension (modified by pleat curvature) plotted against $1/\sqrt{P}$. Dashed lines show the deviation from linearity of the First Order Theory.

$$B = -2\beta\left\{\text{vers}\,\theta + \left(\frac{\gamma_0}{4} - \theta\right)\sin\theta\right\} S_0^{\frac{1}{2}} + \alpha\gamma_0 \sin\theta S_0^{\frac{1}{2}} + \rho_0^2\gamma_0^2 \sin\theta\cos^2\theta \times \left\{\tan\theta + \left(\frac{\gamma_0}{4} - \theta\right)\right\} S_0^{-\frac{1}{2}} - 2\rho_0^2 \sin\theta\left\{\theta\cos 2\theta + \sin 2\theta + \left(\frac{\gamma_0}{4} - \theta\right)(3\cos 2\theta - 2\theta\sin 2\theta)\right\} S_0^{-\frac{1}{2}} \quad (11)$$

$$C = 2\rho_0\gamma_0 \sin\theta\cos\theta\left\{\tan\theta + \left(\frac{\gamma_0}{4} - \theta\right)\right\} \quad (12)$$

$$D = 2\left\{\sin\theta + \left(\frac{\gamma_0}{4} - \theta\right)\cos\theta\right\} S_0^{\frac{1}{2}} \quad (13)$$

$$E = -\beta\cos\theta\left\{\tan\theta + \left(\frac{\gamma_0}{4} - \theta\right)\right\} S_0^{\frac{1}{2}} + \tfrac{1}{2}\alpha\gamma_0\cos\theta S_0^{\frac{1}{2}} + \tfrac{1}{2}\rho_0^2\gamma_0^2\cos^3\theta \times \left\{\tan\theta + \left(\frac{\gamma_0}{4} - \theta\right)\right\} S_0^{-\frac{1}{2}} - \rho_0^2\cos\theta\left\{\theta\cos 2\theta + \sin 2\theta + \left(\frac{\gamma_0}{4} - \theta\right)(3\cos 2\theta - 2\theta\sin 2\theta)\right\} S_0^{-\frac{1}{2}} \quad (14)$$

and

$$F = \rho_0\gamma_0\cos^2\theta\left\{\tan\theta + \left(\frac{\gamma_0}{4} - \theta\right)\right\} \quad (15)$$

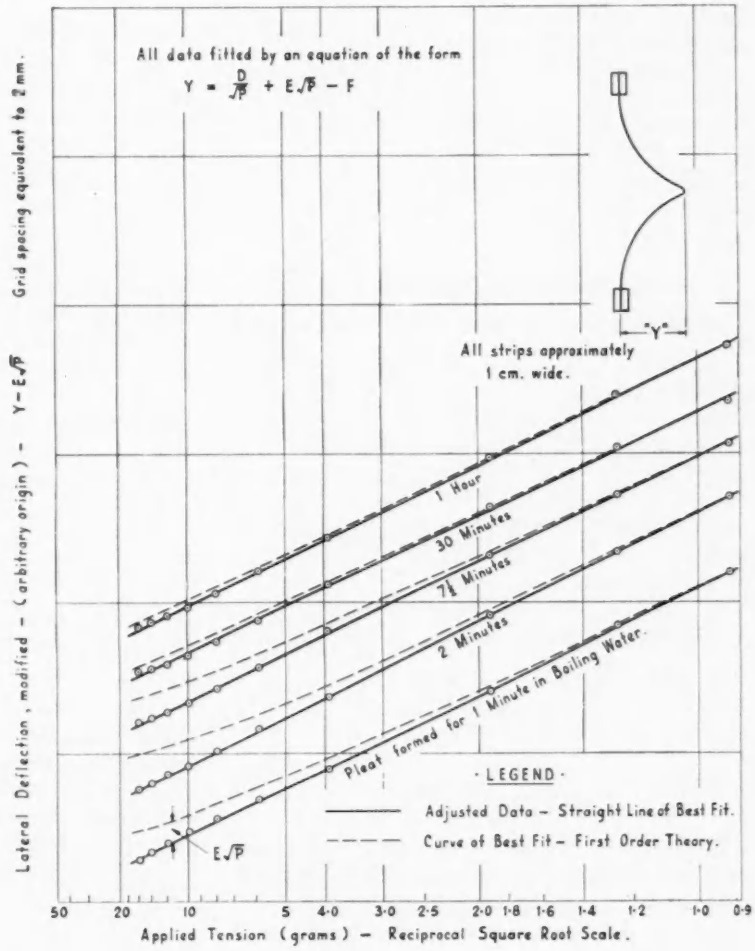
All data fitted by an equation of the form
Y = D/√P + E√P − F
Grid spacing equivalent to 2 mm.
Lateral Deflection, modified – (arbitrary origin) = Y − E√P
All strips approximately 1 cm. wide.
"Y"
1 Hour
30 Minutes
7½ Minutes
2 Minutes
Pleat formed for 1 Minute in Boiling Water.
E√P
· LEGEND ·
Adjusted Data – Straight Line of Best Fit.
Curve of Best Fit – First Order Theory.
50 20 10 5 4·0 3·0 2·5 2·0 1·8 1·6 1·4 1·2 1·0 0·9
Applied Tension (grams) – Reciprocal Square Root Scale.

Fig. 3. Typical graphs of lateral deflection (modified by pleat curvature) plotted against $1/\sqrt{P}$. Dashed lines show the deviation from linearity of the First Order Theory.

The parameters A, B, C, D, E, and F are all functions of S_0, γ_0, ρ_0, α, β, and θ. However, since the terms inside curly brackets in Equations 10 and 13 can be identified as the first two terms of a Taylor series expansion about θ, it is evident that both A and D are independent of θ to a first order in the small term $(\gamma_0/4 - \theta)$. The last term shown for B, and also for E, is a component resulting from the opening out of CD itself (ignored in the previous discussion to simplify exposition).

For any given experimental range, θ can in principle be selected so as to minimize errors resulting from linearization of Equation 6. Once this has been done the *small* terms B, C, E, and F can be regarded as constants, in fact those which permit the best possible fitting of the data by Equations 8 and 9. Because of experimental uncertainties in the absolute values of l_0 and Y, no possibility exists of attaching any particular significance to the parameters C and F. Also the general complexity of the terms for B and E prevents any significance from being attached to the value of the latter either. Thus B, C, E, and F serve a purpose only in data fitting by Equations 8 and 9, but A and D have a more fundamental significance; see Equations 16 and 17 below.

Application to Experimental Data

(Evaluation of parameters *A*, *B*, *C*, *D*, *E*, and *F*)

Equations 8 and 9 can be fitted to the experimental data by standard methods of least squares fitting. The goodness of the fit can be studied graphically in particular cases by grouping all terms except those in $P^{-\frac{1}{2}}$, the grouped expression being then plotted against $P^{-\frac{1}{2}}$. The unknown constants in Equations 8 and 9 can be regarded as combined with the parameters C and F when evaluated by the method of least squares.

If $\gamma_0/4 - \theta$ can be regarded as small (which is certainly true in the low load region), Equations 10 and 13 simplify to

$$A = 4 \operatorname{vers} \frac{\gamma_0}{4} S_0^{\frac{1}{2}} \tag{16}$$

and

$$D = 2 \sin \frac{\gamma_0}{4} S_0^{\frac{1}{2}} \tag{17}$$

There is now the advantage that A and D may be determined by maximum likelihood fitting of data extending into the higher load region where the "ideal pleated elastica model" is no longer valid. From Equations 16 and 17 we find that

$$\frac{A}{2D} = \tan \frac{\gamma_0}{8} \tag{18}$$

and

$$\frac{A^2 + 4D^2}{8A} = \sqrt{S_0} \tag{19}$$

Thus the results may be employed to make an assessment of initial pleat angle and initial fabric stiffness. It does not appear practical, however, to employ the analysis described above to make an estimate of the radius of curvature at the pleat, since the parameters B and E incorporate terms due to α and β, while terms C and F each incorporate a constant uncertainty. In any case the radius of curvature is readily measured from an optical projection of the pleat.

Analysis of Experimental Data

The extended theory outlined above has been applied to the experimental data given in a previous paper [1], in which details of fabric specifications, method, and times of pleat formation appear. Essentially all pleats were formed by folding and compressing to a standard separation between parallel (chemically inert) plates, which were inserted in boiling water for various selected times. Experimental values of longitudinal extension and lateral deflection as functions of the applied tension were based upon the "equivalent hysteresis-free" load–extension diagram described in the previous paper.

As described therein, the total jaw separation $(d + e)$ at each tension value was divided by the factor $1 + \alpha P$, where α is a stretch coefficient based upon an auxiliary experiment on an adjacent unpleated strip of the same fabric. For each experiment, values of $\frac{d + e}{1 + \alpha P}$ and Y were deduced for the one fixed set of values of the tension P. The latter procedure was found to lead to appreciable simplifications in the subsequent reduction of the data by the method of maximum likelihood. Values of A, B, D, and E and also values of γ_0 and S_0 deduced from these are set out in Table I.

Figures 2 and 3 have been plotted to correspond with Figures 8 and 9 respectively of the previous paper [1]. However, they have been modified by replacing $\frac{d + e}{1 + \alpha P}$ by $\frac{d + e}{1 + \alpha P} + B\sqrt{P}$ and Y by $Y - E\sqrt{P}$; see Equations 8 and 9.

TABLE I. Parameters Evaluated by Least Squares Fitting to Data of Equations 8 and 9

Time of formation	A, g.$^{\frac{1}{2}}$ cm.	B, g.$^{-\frac{1}{2}}$ cm.	D, g.$^{\frac{1}{2}}$ cm.	E, g.$^{-\frac{1}{2}}$ cm.	$\frac{A}{2D}=\tan\frac{\gamma_0}{8}$	γ_0, deg.	$\frac{A^2+4D^2}{8A}=\sqrt{S_0}$	S_0, g. cm^2
1 min.	.3827	.0226	.4818	.0120	.3972	173	.3511	0.123
2 min.	.3226	.0167	.4936	.0158	.3268	145	.4179	0.175
7½ min.	.3651	.0149	.4749	.0121	.3844	168	.3545	0.126
30 min.	.3618	−.0014	.4687	.0036	.3860	169	.3488	0.122
1 hr.	.3377	−.0037	.4837	.0032	.3491	154	.3886	0.151

Values obtained for the initial pleat angle γ_0 show no significant trend with time of treatment, suggesting that a final value of γ_0 is approached even for quite short times. The values deduced for fabric stiffness also show no significant trend. Variations are such as might be expected among different samples.

A reduction in curvature, hence in the value of $\rho_0\gamma_0$, might be expected to lead to a reduction in magnitude of both B and E, possibly to a reversal of sign. Such an effect would be expected to accompany an increase in the time of pleat treatment. Also, if θ is approximately 45° or a little less, E should be of the order of $\frac{1}{2}B$ if the β term is not the dominant one, e.g., in the region of smaller treatment times (see Equations 11 and 14). The results in Table I support these general contentions.

The high degree of linearity exhibited by the experimental results, as shown in Figures 2 and 3, demonstrate the remarkable effectiveness of Equations 8 and 9 for describing the elasto-mechanical behavior of these pleats in extension. In view of the small magnitude of deviations from the maximum likelihood fit, a simplified approach would be to deduce values of A and D (hence γ_0 and S_0) from manually drawn *curves* of best fit to the data plotted as in the earlier paper [1]. By selecting three points on each curve reasonably well spaced apart, three equations could be set up from which B and C could be quickly eliminated to determine A; similarly, E and F could be eliminated from another set of three equations in order to determine D.

Conclusion

A satisfactory model to represent the hysteresis-free elasto-mechanical behavior of sample pleated strips in an extensometer can be based upon an elastica consisting of a central portion of constant radius of curvature joining two straight portions tangentially (in the unloaded state). A mathematical representation of this model may be fitted by maximum likelihood procedures to the data for longitudinal extension and lateral deflection vs. tension, with only small resulting deviations. From the data thus obtained a theoretical estimate of the initial pleat angle (i.e., the deflection angle of the unloaded elastica) may be deduced, and also a measure of initial fabric stiffness. These values have the merit of being based upon pleat performance for a range of applied tensions. Further simplification is permissible with only minor loss of precision if it is desired to use the technique for routine testing of pleats.

Acknowledgment

The author wishes to acknowledge helpful discussions with Mr. I. M. Stuart of the Commonwealth Scientific and Industrial Organization, Division of Textile Physics. In particular the author is indebted to Mr. Stuart for the suggestion that the terms in Equations 11 and 14 due to opening out of the arc CD of Figure 1 are of a comparable magnitude to other terms and cannot be ignored in a complete statement of the problem.

Literature Cited

1. Holdaway, H. W., TEXTILE RESEARCH JOURNAL **30**, 296 (1960).
2. Love, A. E. H., "A Treatise on the Mathematical Theory of Elasticity," Cambridge University Press, 449 (1952).

Manuscript received November 30, 1959.

Weathering and the Resulting Chemical Changes in Some South African Merino Wools

D. F. Louw[1]

Deutsches Wollforschungsinstitut, Aachen, Germany and Laboratoire de Chemie Biologique et de la Nutrition, Université Libre de Bruxelles, Belgium

Abstract

Differences in chemical composition between root, middle, and tip sections of a number of normal crimped and of copper-deficient steely South African Merino wools have been investigated, as well as the influence of these differences on such factors as acid dye absorption, alkali solubility, and urea-bisulfite solubility. In the case of normal wools the loss in cystine and tryptophan and increase in cysteic acid reveal the extent of hydrolytic and oxidative weathering damage and explain subsequent changes in solubility and dye absorption.

The conclusion is reached that copper-deficiency retards fiber keratinization which can, however, continue during aging and weathering of steely wools on the animal's back, resulting in increased cross-linking.

Variations in amino acid content of root and tip sections of normal and steely wools have been found.

Introduction

Partly in an effort to obtain methods for evaluating the extent of weathering damage in a specific sample, total sulfur [24], cystine [30], cysteine [30, 34], tryptophan [31] and tyrosine [1, 9] have been assayed. In addition, such factors as dye absorption characteristics [7, 21, 24, 29, 32, 33], alkali [10] and acid solubility [35], and solubility in urea-bisulfite solution [14, 16, 25] have been determined by various research workers. Recently the ninhydrin test [17, 30] has been added to the impressive series of chemical and physico-chemical tests.

The main trend of these studies in the past had been to subject a specific wool sample to such treatment as ultraviolet radiation or exposure of a chosen fleece to sun and rain in order to continue the natural weathering that had already taken place on the sheep's back. In a few cases it had been shown that the extreme tips of wool fibers differed from the protected lower portions [24]; this resulted in the more or less general practice of removing approximately the tip third of the staple on the assumption that the lower two-thirds was undamaged.

Recent work at this Institute has indicated that this assumption often leads to erroneous results. We have found that in numerous cases weathering damage extends down into the middle parts of wool staples and in exceptional examples may even be detected in the root sections as well [29, 30]. It has therefore become standard practice in investigations of weathering damage to wool on the sheep's back to cut the wool staple into three or four sections: tip (T), middle (M), and root (R) or tip (T), tip-middle (TM), root-middle (RM), and root (R) and to analyze each section separately. In this way dye absorption [29], reaction with ninhydrin [17, 30], cystine and cysteine content [30], and tryptophan content [31] have been estimated, and it has been possible to establish an interrelationship of these factors as well as a correlation of these with the "quality" classification of wool appraisers.

It has now become necessary to obtain an over-all picture of actual weathering damage as can be assessed by the various methods available when applied to a fiber section (R, M, or T). This could give an indication of the interdependence of such tests and probably of their validity as measures of the extent of weathering damage. Furthermore, information on changes in the chemical constituents could throw light on the processes taking place during weathering on the sheep's back and of their relative importance.

A few samples of morphologically deviating wool,

[1] Present address: South African Wool Textile Research Institute, Grahamstown.

so-called steely wools which lack the usual well-defined crimp as a result of a trace element deficiency in the sheep's diet, have been analyzed in addition to the normal types in the hope that possible differences in behavior and/or composition may throw light on the course and effects of weathering in wool. Steely wools are known to be physically weaker [18, 19] and to contain more sulfydryl groups and fewer disulfide linkages than comparable normal wools [2, 4, 23]. The samples studied were of the copper-deficient type.

Wool Samples

The work reported here concerns an analysis and investigation of two samples, A and B, of normal good quality South African Merino wool from the (Somerset East) Karoo Area and three samples, C, D, and E, of wool from sheep from coastal belt pastures with a copper deficiency. These latter wools are steely to a greater or lesser extent. Sample C from Mossel Bay has steely roots, but normal tips; Sample D from Vredenburg on the other hand has steely tips but crimped roots; and Sample E from Darling is steely from tip to root as a result of copper deficiency in the sheep's diet throughout the total period of growth.

These five samples were cut into either three or four sections each as mentioned above and were then purified separately and treated or analyzed by the various methods described below.

Purification of Wool Sections

A wool section is rinsed twice in ether in order to remove excessive wool grease and is allowed to dry at room temperature. It is then steeped in a 0.5% nonionic detergent solution at 50° C. (liquor ratio 50:1) and left with occasional stirring for 30 min. without further heating. The excess water in the wool is pressed out, the wool rinsed with cold distilled water, and the process repeated with a 0.1% nonionic detergent solution at 40° C. (liquor ratio 30:1).

After being pressed out and rinsed, the wool section is soaked thrice for 30 min. in successive baths of cold distilled water (liquor ratio 30:1) and is then squeeze-dried between layers of filter paper and allowed to dry at room temperature after slight opening up.

Final purification is effected by Soxhlet extraction for 4 hr. each with alcohol and ether, followed by drying of the wool at room temperature. Residual vegetable matter and sand is then removed by careful teasing out; in this way satisfactory mixing of the section is also achieved. After equilibration at 65% RH and 20° C. the wool is stored in an amber-colored bottle.

Methods of Analysis and Testing

Cystine and Cysteine

The modified procedure, according to Zahn and Traumann [34], of the phosphotungstic acid method was applied.

Cysteic Acid

Diehl [6] modified the high-voltage electrophoretic estimation of cysteic acid in protein hydrolysates as developed by Zuber, Ziegler, and Zahn [37] to make it applicable in laboratories using standard equipment of ±280 volt DC. The author found that electrophoresis in the Elphor H (Bender and Hobein) for 4 hr. at 200 volts DC at a current of 12–18 mA per 6 paper strips saturated with pyridine-acetic acid buffer (pH 3.5) resulted in satisfactory separation of cysteic acid from the other acidic amino acids. By subsequent color development with ninhydrin solution, stabilization with copper nitrate reagent, and colorimetry of the eluated copper complex the quantity of cysteic acid in the wool hydrolysate could be calculated from a standard treated in exactly the same way.

Tyrosine

The method described by Fritze and Zahn [8] was applied making use of the classical Millon reaction of phenols with HNO_2 in the presence of Hg^{++}.

Tryptophan

Hydrolysis of wool at room temperature in concentrated HCl and simultaneous development of the blue color by reaction with *p*-aminobenzaldehyde were carried out as described in the original method by Mazingue, Decroix, and van Overbéke [20].

α-Amino Nitrogen

A method incorporating the modifications by Kendrick [13] and Kainz [11, 12] as applied to the van Slyke method [28] based on the reaction of α-amino acids with nitrous acid was used. Only four samples, root and tip sections (AR and AT)

of a normal wool and root and tip sections (CR and CT) of a wool with steely roots, have been analyzed in this manner.

Column Chromatographic Analysis

The rapid separation technique of Moore, Spackman, and Stein [22] was applied to wool hydrolysates for full amino acid analysis on Amberlite IR-120, while "cystine" was assayed by performic acid oxidation according to Schram, Moore, and Bigwood [26] and chromatographic separation on Dowex-2 with 0.1 *N* monochloracetic acid. In the latter case "cystine" is estimated by determining cysteic acid and corresponds to the total of cystine, cysteine, and cysteic acid present in the wool sample. An oxidation factor of 0.82 was assumed for the reaction with performic acid in view of the findings of Kimmel, Thompson, and Smith [15] for bovine serum albumin.

Hydrolysis of wool for Moore and Stein analysis was carried out by refluxing 55 mg. of purified wool of known moisture content for 22 hr. in 200 ml. of glass-distilled 6 *N* HCl. In the case of the single amino acids assayed, hydrolysates were prepared as prescribed by the authors referred to.

Acid Dye Absorption (ADA)

The slightly modified method of Elöd and Reutter [7] was applied to estimate the absorption of Crystal Ponceau Red 6R Extra from a 0.5% solution at 65° C.

Alkali Solubility (AS)

The solubility of wool in 0.1 *N* NaOH at 65° C. was determined according to the modified procedure of Harris [10].

Urea-Bisulfite Solubility (UBS)

The Lees and Elsworth method [16] for UBS prescribes a solution containing 50% urea and 3% sodium bisulfite at 65° C. A solution neutralized to pH 7 ± 0.1 was made up fresh for all determinations.

Results

The results of the various chemical analyses, solubility tests, and dye absorption are given in Table I; results of the column chromatographic analyses, corrected for losses during hydrolysis according to Corfield and Robson [5], are in Table II. All these values are calculated on the basis of 100 g. of bone-dry wool. Analytical values for the valine and cystine content of sections AR, ER, and ET (see Table II) were not estimated due to overlapping resulting from untimely changeover from buffer pH 3.25 to 4.25. Satisfactory separation is, however, attainable by a changeover immediately after the elution of cystine.

Discussion

In the case of the two normally-crimped wools (A and B) there is a marked decrease in cystine content from root to tip, especially so from middle to tip, and a slight increase in free cysteine, confirming the results of previous workers in this field. The increase in cysteic acid is quite noticeable from an almost immeasurably small quantity in the sound root sections to ±0.2% in the weathered tips.

The three samples of steely or partly steely wool (C, D, and E) also show a decrease in cystine content from root to tip, and it is to be noted that these wools contain less cystine than normal. The cysteine content of copper-deficient root sections is abnormally high, but the content of this amino acid in the tip sections is at a level only slightly above normal. The cysteic acid content of a steely root section is relatively high, while the value for the tips is about four times higher than for normal wool. Since cysteine is abundant in the so-called pre-keratinized zone of the normal wool fiber and later decreases, being transformed into cystine until the fiber emerges from the skin, the conclusion is drawn that the root sections (R) of copper-deficient steely wools are incompletely keratinized.

The process of keratinization could be catalyzed by free copper ions present in the follicle itself or in the pre-keratinized zone of the fiber. In this connection Burley [3] has claimed a higher copper content for normal than for steely wools. It is, however, also possible that the basic role played by copper is involved at another stage in the complex metabolism of the sheep. The reaction in which two molecules of cysteine are linked by oxidation to form one molecule of cystine will proceed slowly, when not catalyzed, to the extent permitted by steric relationships. A minimum or threshold value for cysteine content of a fully keratinized protein fiber can therefore be visualized. In the case of copper-deficient wool fibers emerging from the follicle, keratinization can continue under atmospheric conditions with the

TABLE I. Analyses of Sections of Wool Samples

No.	Description	Dia., μ	CySH, %	$(CyS)_2$, %	$CySO_3H$, %	Tyr, %	Try, %	α-NH_2, %	ADA, %	AS, %	UBS, %
AR	Normal	20.9	0.21	12.1	0.05	6.4	0.93	0.12	4.8	12.5	55.3
AM	Normal	20.5	0.22	12.4	0.07	6.3	0.89		4.8	12.4	57.8
AT	Normal, weathered	16.8	0.34	11.1	0.17	7.0	0.82	0.17	11.4	23.2	48.7
BR	Normal	21.8	0.21	12.4		6.0	0.97		4.9	9.7	44.7
BRM	Normal	21.8	0.21	12.4		6.2	0.90		4.6	9.4	33.1
BTM	Normal	21.2	0.22	12.3		6.1	0.85		5.0	8.3	29.1
BT	Normal, weathered	16.7	0.33	10.8		6.6	0.83		14.1	19.3	31.8
CR	Steely	20.0	1.15	11.1		6.2	0.69	0.17	13.3	33.0	34.6
CM	Partly steely	20.1	0.42	11.1		6.3	0.89		12.6	14.9	34.8
CT	Crimped, weathered	19.0	0.41	10.4		6.7	0.82	0.20	14.5	17.6	27.8
DR	Crimped	24.2	0.37	11.1		6.7	0.86		6.5	15.5	63.6
DM	Partly steely	21.6	0.49	10.3		7.0	0.69		6.8	24.2	57.6
DT	Steely, weathered	21.7	0.43	9.5		6.7	0.66		11.8	25.0	39.7
ER	Steely	18.9	1.00	10.8	0.35	6.1	0.58		8.9	28.2	34.3
EM	Steely	18.3	0.46	11.1	0.36	6.3	0.66		8.8	19.0	38.7
ET	Steely, weathered	19.5	0.35	10.0	0.90	6.1	0.66		14.6	20.0	27.3

disappearance of cysteine and formation of cystine, very appropriately illustrated by comparison of the values obtained for CR and CM and ER and EM.

Prolongation of atmospheric attack leads to destruction of cystine by oxidation and hydrolysis. This is the case during the growing period of six to twelve months on the sheep's back during which an initial sound root wool becomes a weathered tip. The decrease in cystine and the increase in cysteic acid have already been mentioned. Furthermore, the probable formation during this process of small quantities of fairly stable lanthionine has to be considered. It will be realized that the process of keratinization as visualized above for steely wools, having been continued for approximately four months after the appearance of the fiber above the skin level, has then run its full course, indicated by the low cysteine content of CM and EM, to the limits allowed by steric relationships, and a subsequent loss of cystine from middle to tip can be expected.

It should be noted that steely wool seems to be very susceptible to attack by weathering. This higher vulnerability in comparison with fully keratinized fibers is revealed in the marked increase in cysteic acid content. The more protected root-third sections of steely wools contain more cysteic acid than even badly weathered crimped tips.

In connection with actual analytical procedures, attention is drawn to the fact that methods available for cysteine assay are unsatisfactory. There is reason to believe that the actual cysteine content of a normal root wool is lower than the 0.2% to 0.3% found by the phosphotungstic acid method, values which have been confirmed by various other workers also when using other analytical procedures, and possibly closer to the 0.1% found by Zuber et al. [36] in the DNP-method. While it would perhaps, therefore, be premature to offer an explanation for the higher cysteine values found for crimped tip sections as compared with the corresponding roots, a hydrolytic process of decomposition of cystine, coupled with a steric barrier towards reoxidation of cysteine formed, could be visualized, although the formation during weathering of aldehydes also has to

TABLE II. Amino Acid Content of Sections of Normal and Copper-Deficient Wool

	Normal		Copper-deficient	
	Section AR	Section AT	Section ER	Section ET
Asp	5.9	6.2	6.0	6.1
Thr	5.8	5.2	5.7	5.6
Ser	7.9	7.8	8.3	8.2
Glu	12.5	12.1	13.0	12.6
Pro	5.0	5.4	5.1	4.6
Gly	3.8	4.6	3.9	4.0
Ala	3.2	3.3	3.1	3.3
Val		3.8		
Met	0.7	0.7	0.6	0.6
Iso-leu	3.0	3.3	3.0	2.9
Leu	6.9	7.4	7.1	7.1
Tyr	4.9	5.7	5.2	4.4
Phe	3.5	3.6	3.5	3.7
Lys	3.0	3.0	3.0	2.8
His	1.0	0.9	0.9	0.8
Arg	8.9	8.9	9.1	9.0
NH_3	1.7	1.9	1.8	2.0

be considered. These aldehydes will react along the same lines as free sulfydryl in the method used for cysteine analysis.

A discrepancy has also been detected between values for "cystine" as obtained by this method and by the column chromatographic method of Schram, Moore, and Bigwood [26]. For ER and ET the latter method yielded 10.9% and 10.1% "cystine" respectively, being cystine + cysteine + cysteic acid, in comparison with $(10.8 + 1.0 + 0.3) = 12.1\%$ and $(10.0 + 0.3 + 0.9) = 11.2\%$ respectively by the phosphotungstic acid method. This latter method is generally accepted in wool analysis, and the reasons for these differences are now being investigated. Corfield and Robson [5] have also reported the phosphotungstic acid method to give results 20% higher than their chromatographic estimation and preferred the latter because of better agreement with values for total sulfur.

The influence of weathering and of the continued keratinization of steely wool on the disulfide linkages is very noticeable in the results for alkali solubility, dye absorption, and urea-bisulfite solubility.

A decrease in cross-linking of a protein through disulfide bonds could be expected to result in an increase in alkali solubility (AS) and vice versa. This is confirmed by comparison of results for the various root and tip sections of the crimped wools. The higher cysteic acid content of the normal tip fibers is also reflected in the higher AS. The very high AS for CR and ER is especially noticeable, as well as the fact that keratinization from ER to EM has brought the AS of this fiber back to normal.

Similarly acid dye absorption (ADA) will reflect the degree of cross-linking through disulfide bonds, because these covalent bonds will restrict swelling of fibers in the aqueous solutions. Rupture of disulfide linkages increases the ADA from root to tip (see results for AR and AT and BR and BT respectively). This peculiar behavior of weathered tip sections of fibers is known to the trade as "tippy dyeing." Incomplete keratinization results in abnormally high ADA values for CR and ER, while continued keratinization returns these characteristics to normal.

Kessler and coworkers [14, 25] have explained the decrease in urea-bisulfite solubility (UBS) of wools treated with dilute alkali by assuming that disulfide exchange takes place with transformation of intrachain disulfide bonds to interchain linkages. Such a decrease in UBS is, however, also to be expected when protein-bound cystine is decomposed to lanthionine. Both reactions are favored by high pH, as would be the case in the presence of alkaline suint. It would be preferable at this stage to ascribe the 10–15% decrease from root to tip of all samples to the formation of lanthionine, which is relatively stable to bisulfite, because it is still a debatable point whether the newly formed interchain disulfide bonds (according to Kessler) are less labile towards urea-bisulfite solution than the existing or intrachain linkages. Swan [27] has recently also rejected the exchange theory and put forward the hypothesis that configurational changes in the hydrogen-bond structure of the protein, or denaturation, may be responsible for the decrease in UBS observed under these circumstances. No sufficiently accurate routine analysis to establish the conversion in wool of cystine to lanthionine is available yet to disprove the argument that this reaction could be the basis of changes in UBS.

Various other chemical components of wool keratin are attacked by oxidative, hydrolytic, and other processes involved in weathering. Thus approximately one fifth of the tryptophan present in sound crimped root wools is destroyed by atmospheric oxidation; it is believed that the decomposition products are partly responsible for yellowing of wool. Attention is drawn to the fact that values are cited in the literature for the tryptophan content of Merino wool, varying from 0.6 to 2.0%. Values of $\pm 0.9\%$ now observed correspond to those arrived at by Veldsman [31], whose finding that copper-deficient root wools contain less tryptophan than sound root fibers and approximately as much as weathered crimped wools has been confirmed.

Weathering also results in an increase in the tyrosine content of normal wools. This could be explained by the oxidation of phenylalanine according to Graham and Statham [9]

$$C_6H_5CH_2CH(NH_2)COOH \rightarrow HOC_6H_4CH_2CH(NH_2)COOH$$

or by assuming that during the growing period of the fleece, part of the cuticle layer, being relatively poor in tyrosine, is lost by rubbing off, as proposed by Zahn (private communication). Values for chromatographic and colorimetric analyses for tyrosine do not agree closely, and some uncertainty arises about the decrease in tyrosine content from ER to ET as given in Table II but not found (see Table I)

by the colorimetric method of Fritze and Zahn [8]. Column chromatographic analyses have indicated an increase in tyrosine content but no loss of phenylalanine, which could possibly point in the direction of the second explanation. It must, however, be borne in mind that the fiber sections analyzed, being taken from selected wool staples, were grown under different grazing (nutritional) conditions and therefore cannot be compared on an equal basis. Further work in this connection will be undertaken.

The nutritional differences also have to be considered in viewing the amino acid analyses given in Table II. The only appreciable differences, although they cannot be ascribed to weathering alone, are an increase in aspartic acid (5%), glycine (20%), iso-leucine (10%), leucine (7%), and tyrosine (16%) and a decrease in threonine (10%) and proline (8%) in the case of the sample of normal wool; and an increase in alanine (6%) and phenylalanine (6%) and a decrease in proline (10%) and tyrosine (15%) in the steely wool.

The normal and steely root sections differ only in serine, glutamic acid, and tyrosine, all of which are less abundant in the normal wool. The normal tip sections, on the other hand, contain more proline, glycine, iso-leucine, leucine, and tyrosine than the steely tips but less threonine, serine, and glutamic acid.

An α-amino content of 0.17% for AT as compared with 0.12% for AR indicates the possibility that peptide chains are hydrolyzed during weathering. The copper-deficient root wool (CR) contains as many α-amino groups as the weathered normal wool tips (AT) and warrants the assumption of shorter chain lengths in the latter case, as was postulated by Burley [3]. The results of Burley have been confirmed by the author through separation of DNP-amino acids on a nylon column.

Summary

1. Weathering of normal good quality wool on the sheep's back results in destruction of cystine and formation, among others, of cysteic acid and probably also of cysteine and lanthionine.

2. This considerable rupturing of the covalent disulfide linkages of cystine leads to increased dye absorption and higher alkali solubility of weathered tips of wools in comparison with the sound root sections.

3. The decrease in urea-bisulfite solubility of wool upon weathering could result from the formation of a small number of lanthionine linkages.

4. Weathering destroys about 20% of the tryptophan present in normal wool, but the tyrosine content increases by about 10% from root to tip.

5. Differences of varying magnitude are encountered in the amino acid composition of sound and weathered wools, the most marked being a 20% increase in glycine content and a decrease of 10% in threonine.

6. Weathering increases the α-amino content of normal wools by about 50%, probably due to peptide hydrolysis.

7. Copper-deficient root wools contain less cystine and more cysteine than normal wools and are regarded as incompletely keratinized. Normal tip wools contain more cystine and tryptophan, but less cysteine, than steely tips.

8. The process of keratinization can continue during aging *in vivo* of the copper-deficient fiber to a limit which is probably dependent on steric factors.

9. The formation of additional disulfide cross-linkages upon further keratinization during aging of steely root wools returns the abnormally high alkali solubility and dye absorption to levels associated with normal weathered wools.

10. Judging by the cysteic acid content, steely wools are more vulnerable to attack by weathering than normal crimped types.

11. Copper-deficient wools have a high α-amino content, probably reflecting the presence of shorter peptide chains than in normal fibers.

12. The over-all amino acid composition of normal and copper-deficient steely root wools is very similar, although the latter contains slightly more serine, tyrosine, and glutamic acid.

Acknowledgment

The author gratefully acknowledges the hospitality and cooperation of Prof. H. Zahn of the German Wool Research Institute, Aachen, and of Prof. E. J. Bigwood of the Department of Biochemistry, University of Brussels, Belgium, with their respective staffs, whose assistance made possible the carrying out of this research project.

Literature Cited

1. Alexander, P. and Hudson, R., "Wool," London, Chapman & Hall, 299 (1954).

2. Burley, R. W., *Nature* **174**, 1019 (1954).
3. Burley, R. W. and De Kock, W. T., *Arch. Biochim. Biophys.* **68**, 21 (1957).
4. Burley, R. W. and Horden, F. W. A., TEXTILE RESEARCH JOURNAL **27**, 615 (1957).
5. Corfield, M. C. and Robson, A., *Biochem. J.* **59**, 62 (1955).
6. Diehl, J. F., *Anal. Chem.* **31**, 1204 (1959).
7. Elöd, E. and Reutter, H., *Melliand Textilber.* **19**, 67 (1938).
8. Fritze, H. and Zahn, H., *Melliand Textilber.* **36**, 1136 (1955).
9. Graham, D. R. and Statham, K. W., *J. Soc. Dyers Colourists* **72**, 434 (1956).
10. Harris, M. and Smith, A., *Am. Dyestuff Reptr.* **25**, 542 (1936).
11. Kainz, G., *Mikrochim. Acta* **4**, 349 (1953).
12. Kainz, G. and Schöller, F., *Biochem. Z.* **327**, 292 (1955).
13. Kendrick, A. B., *J. Biol. Chem.* **117**, 161 (1937); **132**, 739 (1940).
14. Kessler, H. and Zahn, H., TEXTILE RESEARCH JOURNAL **28**, 357 (1958).
15. Kimmel, J. R. et al., *J. Biol. Chem.* **217**, 151 (1955).
16. Lees, K. and Elsworth, F. F., *Proc. Int. Wool Text. Res. Conf. Austr. 1955* **C**, 363 (1956).
17. Louw, D. F., *S. A. Wool Textile Res. Inst. Techn. Rep. No. 12* (1957).
18. Marston, H. R., *Physiol. Revs.* **32**, 86 (1952).
19. Marston, H. R. and Lee, H. J., *Austr. J. Sci. Res., Ser. B* **1**, 376 (1948).
20. Mazingue, G. et al., *Bull. Inst. Text. France* **61**, 37 (1956).
21. Millson, H. E. et al., *Am. Dyestuff Reptr.* **28**, 632 (1939).
22. Moore, S. et al., *Anal. Chem.* **30**, 1185 (1958).
23. Palmer, R. C., *J. Agr. Sci.* **39**, 265 (1949).
24. Race, E. et al., *J. Soc. Dyers Colourists* **54**, 141 (1938).
25. Satlow, G. and Kessler, H., TEXTILE RESEARCH JOURNAL **28**, 359 (1958).
26. Schram, E., Moore, S., and Bigwood, E. J., *Biochem. J.* **57**, 33 (1954).
27. Swan, J. M., TEXTILE RESEARCH JOURNAL **29**, 665 (1959).
28. Van Slyke, D. D., *J. Biol. Chem.* **9**, 185 (1911).
29. Van Wyk, T. P. and Veldsman, D. P., *S. A. Wool Textile Res. Inst. Techn. Rep. No. 10* (1957).
30. Veldsman, D. P., *S. A. Wool Textile Res. Inst. Techn. Rep. No. 11* (1957).
31. Veldsman, D. P., *Chem. and Ind.* **1959**, 878 (1959).
32. Vickerstaff, T., "The Physical Chemistry of Dyeing," London, Oliver & Boyd, 354 (1950).
33. Von Bergen, W., *Melliand Textilber.* **7**, 451 (1926).
34. Zahn, H. and Traumann, K., *Melliand Textilber.* **35**, 1069 (1954).
35. Zahn, H. and Würz, A., *Textil-Praxis* **8**, 971 (1953).
36. Zuber, H. et al., *Proc. Int. Wool Text. Res. Conf. Austr. 1955* **C**, 127 (1956).
37. Zuber, H. et al., *Z. Naturforsch.* **12B**, 531 (1957).

Manuscript received November 23, 1959.

Letters to the Editor

Short communications in the form of Letters to the Editor are intended to provide prompt publication of significant new research results and to permit an exchange of views on papers previously published in the JOURNAL. These communications are not submitted to formal review as are research papers, and the editors do not assume any share of the author's responsibility for the information given or the opinions expressed. When work previously published in the JOURNAL is the subject of critical comment, the authors of the original paper are given an opportunity to submit a reply, which will be published concurrently when possible.

Acid Hydrolysis of Chemically Modified Celluloses

Department of Chemical Technology
University of Bombay
Bombay-19, India
March 1, 1960

To the Editor

TEXTILE RESEARCH JOURNAL

Dear Sir:

As compared with data available in literature on the action of acids on cellulosic fibers, investigations on acid hydrolysis of chemically modified cellulosic fiber substances are comparatively very few. Davidson [5] and Pacsu [7] observed that periodate oxycelluloses resisted the action of cold dilute acids fairly well but they were easily degraded by alkali. Virkola [9], during the studies in the relation between DP values of cellulose determined in alkaline solvents and those determined by nitrate method, found that DP values of periodate oxycelluloses in alkaline solvents were low, whereas DP values of reduced periodate oxycelluloses determined under similar conditions corresponded with each other irrespective of the degree of oxidation. However, the values for nitrate DP of the reduced samples were surprisingly low, indicating that these oxycelluloses were degraded considerably by the nitrating acid. In the present work are given results of preliminary experiments on the action of dilute sulfuric acid on oxycelluloses prepared by the action of potassium metaperiodate and a mixture of potassium dichromate and oxalic acid together with those on their respective reduced forms obtained by sodium borohydride reduction. Further work on the kinetics of hydrolysis of cellulose modified by chemical treatments such as oxidation, reduction, and cross-linking and characterization of the products of hydrolysis with respect to density, swelling, accessibility, etc. is in progress. The results will be published in due course.

Periodate oxycelluloses and dichromate oxalic acid oxycelluloses were prepared from standard cellulose obtained from Indian cotton by the action of 0.01 *M* KIO_4 at pH 5.6 and 30° C. for various lengths of time and with different amounts of 2 *N* $K_2Cr_2O_7$ added to 2 *N* oxalic acid containing suspended cellulose at 30° C. respectively. Reduced forms of these oxycelluloses were obtained by treatment of each of the respective samples with 0.05 *M* $NaBH_4$ at 30° C. for 24 hr. Hydrolysis of standard cellulose, oxycelluloses, and reduced oxycelluloses was carried out using 6 *N* H_2SO_4 at 30 ± 1° C. for different periods, the material:liquor ratio being 1:50. After hydrolysis the samples were washed free of acid with distilled water, air dried, and brought to equilibrium moisture content at 65% RH and 30° C. Copper number of the samples was determined by the modified method of Braidy [3]; the basic DP was calculated from viscometric measurements of standard cuprammonium hydroxide solutions containing the samples by the method suggested by Battista [2]. In case of periodate and dichromate-oxalic acid oxycelluloses, viscometric measurements were carried out after reduction of the original and hydrolyzed samples with $NaBH_4$ because the original oxycelluloses were alkali-sensitive and showed considerably reduced DP due to the strong alkaline action of the solvent. The reduced forms of both periodate and dichromate-oxalic acid oxycelluloses were found to be nonalkali-sensitive and therefore DP of these products before and after hydrolysis could be carried out

TABLE I

Sample	Copper number			DP		
	Original	After hydrolysis for 7 hr.		Original	After hydrolysis for 7 hr.	
Standard cellulose	0.005	0.62		2600	866	
K-metaperiodate (a) oxycelluloses (b)	4.75 7.20	4.91 7.29		1610 1400	1135 1025	
Periodate oxycellulose (a) reduced with $NaBH_4$	0.005	0.20		1610	400	
Periodate oxycellulose (b) reduced with $NaBH_4$	0.005	0.18		1400	380	
		After hydrolysis for 8 hr.	48 hr.		After hydrolysis for 8 hr.	48 hr.
Standard cellulose	0.005	0.75	2.47	2600	758	500
$K_2Cr_2O_7$-oxalic acid (a) oxycelluloses (b) (c)	2.9 6.3 8.0	3.7 7.0 8.77	5.47 — 10.21	1380 1230 970	— 645 —	— — —
$K_2Cr_2O_7$-oxalic acid oxycellulose (a) reduced with $NaBH_4$	0.005	0.74	2.47	1380	685	457
$K_2Cr_2O_7$-oxalic acid oxycellulose (b) reduced with $NaBH_4$	0.005	0.74	—	1230	615	—
$K_2Cr_2O_7$-oxalic acid oxycellulose (c) reduced with $NaBH_4$	0.005	0.74	2.4	970	606	420

directly from viscosity of the respective cuprammonium solutions. Results are given in Table I.

Under identical conditions of hydrolysis, periodate oxycelluloses resist the acid action fairly well as compared with the unoxidized sample; with increasing degree of oxidation, resistance to acid attack increases. For instance, DP of standard cellulose drops from 2600 to 866, while that of periodate oxycellulose with copper number 4.75 decreases from 1610 to 1135 and of oxycellulose with copper number 7.2 reduces from 1400 to 1025. This resistance to acid action can be attributed to the formation of acetal cross-linkages between the aldehyde groups in position 2 and 3 of the glucose unit and the hydroxyl groups of the adjacent cellulose chains in the presence of the acidic hydrolyzing medium. Formation of such linkages in acidic media has been proposed by Rogovin and co-workers [8] and confirmed by Anthoni [1] from the increase in molecular weight of these oxycelluloses after nitration. The cross-linked cellulose structure prevents the access of the hydrolyzing acid to the sites of reaction with the result that these oxycelluloses become resistant to acid hydrolysis. The reduced forms of periodate oxycelluloses are not resistant to acid action, and their DP decreases from 1610 to 400 and 1400 to 380 depending on the extent of oxidation taking place. It is very likely that, during periodate oxidation and subsequent borohydride reduction, the fine structure of cellulose has become more accessible to acid action, with the result that the reduced form of these oxycelluloses are more readily attacked by the hydrolyzing acid as compared with the corresponding oxycelluloses. Although these two reduced forms have been obtained from periodate oxycelluloses with different degrees of oxidation (copper number 4.75 and 7.2 respectively), the final DP obtained as a result of acid action in both cases is nearly the same (400 and 380 respectively), a value which is close enough to the leveling off DP value obtained after hydrolysis of standard cellulose (*viz.*, 370 under identical conditions of acid action [4]). It is interesting to note that, with these reduced forms, although the acid action has brought about considerable reduction in lengths of cellulose chains, the copper numbers of the hydrolyzed products show only a slight increase. Virkola [9] also made similar observations where the reduced periodate oxycellulose on treatment with HCl showed a considerable drop in DP from 1080 to 310 but the copper number of the original and

hydrolyzed samples were 0.1 and 0.04. No satisfactory explanation is yet available for this anomalous behavior but it may be possible that the short chain segments formed during hydrolysis might have been leached out of the samples by the aqueous acidic medium.

In the case of $K_2Cr_2O_7$-oxalic acid oxycelluloses, where most of the oxidizing action has taken place at C atom number 6 of the glucose unit [6], unlike periodate oxycelluloses, acid action results in a decrease in DP from 1230 to 645 while its corresponding reduced form shows a reduction from 1230 to 615. Similarly, other reduced $K_2Cr_2O_7$-oxalic acid oxycelluloses in which oxidation has been carried out to different stages show reduction in DP values depending on the extent of oxidation and duration of hydrolysis. In general, the extent of reduction in DP values of $K_2Cr_2O_7$- oxalic acid oxycellulose and its corresponding reduced form for identical conditions of acid action is nearly the same. In the case of these oxycelluloses and their reduced forms, unlike periodate oxidation and subsequent reduction, the extent of reduction in DP is associated with a corresponding rise in the copper number of the hydrolyzed samples.

Literature Cited

1. Anthoni, B., "Some Aspects of Nitrates of Periodate-Oxidized Cellulose," Dissertation, Meden, Helsinki (1958).
2. Battista, O. A., *Ind. Eng. Chem.* **42**, 502 (1950).
3. Braidy, M. H., *Rev. gen. Mat. Col.* **25**, 35 (1921).
4. Daruwalla, E. H. and Nabar, G. M., *J. Polymer Sci.* **20**, 205 (1956).
5. Davidson, G. F., *J. Textile Inst.* **31**, T81 (1940).
6. Nabar, G. M. and Padmanabhan, C. V., *J. Soc. Dyers Colourists* **69**, 295 (1953).
7. Pacsu, E., TEXTILE RESEARCH JOURNAL **15**, 354 (1945).
8. Rogovin, Z. A., Shorygina, N. N., Yashunskaya, A. G., and Treivas, M. G., *Zuhr. Priklad. Khim.* **22**, 857 (1949).
9. Virkola, N. E., *Paperi ja Puu* **40**, 367 (1958).

E. H. DARUWALLA
P. J. KANGLE
G. M. NABAR

Book Review

Friction in Textiles. H. G. Howell, K. W. Mieszkis, and D. Tabor. New York, Textile Book Publishers, and London, Butterworths, 1959. xii + 263 pages. Price $6.75.

Reviewed by W. James Lyons, Textile Research Institute, Princeton, New Jersey

This monograph, as the authors call it, was written with two types of readership in mind: research workers who are interested in an understanding of the basic phenomena involved in friction in textiles, and textile technologists who are seeking information that can be applied to overcoming problems posed by fiber friction in processing or in the properties of the end-product. To reach this supposedly dichotomous audience, the authors deemed it advisable to divide the book not into two, but into three parts. The division into three parts may have been an implicit recognition that if "black" can indeed be distinguished from "white," there is still a large "grey" area in between, peopled by individuals who have one eye on deeply underlying causes and the other on practical problems.

The first part of the work deals with the laws and relationships pertaining to frictional phenomena and lubrication in general. All three chapters of this part were written by D. Tabor (the authorship of each chapter in the book is indicated). The first chapter, on the general mechanism of friction, leans heavily on metal-to-metal surfaces as the models on which to demonstrate principles. This cannot be avoided, because in most cases there exists no comparable data on other types of materials. In the second chapter, of equal length, the author gets his subject off the ground and takes up the matter of the friction of polymers and fibers. The final chapter in this part is on the mechanism of lubrication. Here the subject-matter deals mostly with fiber-on-fiber and fiber-on-metal situations. Part I could very well serve as a primer on surface friction in general.

The authorships of the chapters of Parts I and II are divided between the other two authors. The

second part is nominally on friction in textile processing. However, the first chapter, which is on wool, consists principally of introductory material on the nature of friction in this fiber, that would seem to belong in Part I. Processing and product performance enter the discussion by little more than allusion. The discussion of the internal structure of the wool fiber fails to mention the *ortho-* and *para-*cortex concept, which has assumed considerable importance since it was introduced by Horio and Kondo in 1953. While the differential frictional effect in wool is an interesting phenomenon, it is questionable, in this reviewer's mind, whether the subject deserves a whole chapter in a work on textiles generally. The authors really get into the processing aspects in the succeeding chapters on the role of friction in spinning, winding, weaving, and knitting. The two brief concluding chapters in this part, on tire-cord and fabrics, pertain to product performance rather than processing.

The third part of the monograph, on test methods, will be of interest to both classes of readers at which the work is aimed. A chapter is devoted to the measurement of the classical coefficient of friction of yarns and fibers. Techniques discussed range from the inclined-plane method (a traditional feature of high-school physics laboratory courses) to the more sophisticated modern-day methods. The two concluding chapters, perhaps by way of lagniappe, deal with two friction-related effects: tension in processing and abrasion resistance. A brief appendix tabulates coefficients of friction and other parameters of various yarns and fibers.

This reviewer finds disconcerting such terms as "the values of friction" which appear in this work. Surface friction is a phenomenon, not a quantity to which a numeric can be attached. "Friction" has no value, any more than "viscosity" (another misused term) or "gravitation" has a value. This comment, however, cannot prevent one from concluding that the book should prove to be very intriguing to anyone interested in the broad field of the trans-surface interaction of textile fibers. Since the word "friction" means but one thing to most people, it may be picayune to remark that a more precise title for this book might have been *Surface Friction in Textiles,* for that is the only type of friction with which it deals. There is, however, another type, internal friction, which is highly important in the performance of fibrous and polymeric materials. As so often happens nowadays in technical and cultural circles, this monograph grew out of a conference, the particular one in this case being the Conference on Fiber Friction held in Belgium in 1954 under the sponsorship of The Textile Institute (Great Britain). While the work is published in association with the Institute, it does not appear to represent the complete proceedings of the Conference. The book is a fine example of the printers' and binders' arts.

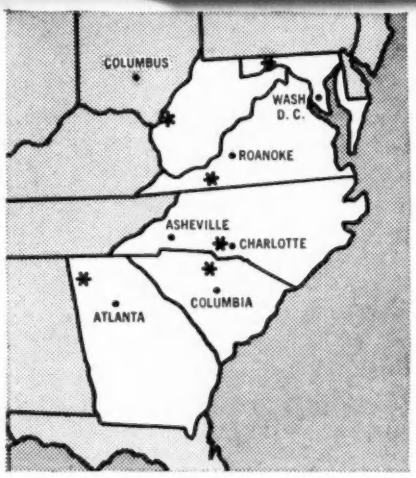

Celanese

FIBERS COMPANY

A division of Celanese Corporation of America

HAS IMMEDIATE OPENINGS

in the Charlotte, N. C. Headquarters and in Plant locations in South Carolina, Virginia, W. Virginia, Georgia & Maryland

These positions provide opportunity to join a company which is diversifying its fiber operations, a multi-product producer of synthetic fibers in the acetate, triacetate, polyester, regenerated cellulose and nytril fields.

Promotional potential is excellent as planned expansion continues. Most positions, therefore, require men capable of rapid advancement, either into positions of greater technical responsibility, into marketing, or into another of the Celanese divisions.

PROCESS DEVELOPMENT

PhD preferred, in ChE, ME or Chemistry with 2 to 10 years experience, preferably in synthetic fibers. To perform process design and economic studies related to new fiber research and development; or to develop and improve methods and equipment and supervise pilot plants tests and trials; or new fiber product development; or process design in extrusion development or chemical processing.

PRODUCT DEVELOPMENT

BS in ChE, Chemistry, Textile Engineering or Physics. 2 to 10 years experience in fibers. To develop new applications for man-made fibers; or to develop industrial fiber products including synthetic fiber papers, non-wovens, woven and knit products; or development and research in cellulose compounds, or development associated with synthetic fiber or textile processing.

QUALITY CONTROL

BS in Chemistry, ChE or Textile Engineering with some experience in quality control, development or related field. To establish and maintain a preventive quality control program in the areas of cellulose compounding, extrusion and textile processing.

DYEING & FINISHING

Polymer Chemist, PhD or MS with 2 to 6 years polymer application experience. For work in chemical modification of textile products.

Colloid Chemist, PhD or MS with 2 to 6 years experience in colloid or surface chemistry.

ANALYTICAL CHEMISTRY

BS in Chemistry or Chemical Engineering with 2 or more years analytical experience. For work in analytical laboratory including development of analytical methods.

PLANT ENGINEERING & MAINTENANCE

BS in ChE, ME or EE with 2 to 7 years experience, preferably in the textile industry. For design and estimation on plant modification or expansion; or design and modification of textile machinery or chemical processing or production equipment; or utilities and maintenance involving control instrumentation, power generation, refrigeration processes.

TECHNICAL SERVICE & SALES

BS with technical textile background and up to 10 years experience in synthetic fibers or related industries.

Please send resume, including salary requirements, to Mr. R. V. Butts.

Celanese **FIBERS COMPANY**

A division of Celanese Corporation of America

P.O. BOX 1414 **CHARLOTTE, NORTH CAROLINA**